DIRECT CURRENT TRANSFORMER FOR MVDC APPLICATIONS

Prof. Dražen Dujić, Renan Pillon Barcelos

École Polytechnique Fédérale de Lausanne (EPFL)
Power Electronics Laboratory (PEL)
Lausanne, Switzerland

INTRODUCTION

Power Electronics Laboratory at EPFL

Prof. Drazen Dujic, Head of the Power Electronics Laboratory at EPFL, Lausanne, Switzerland

Education:

2008	PhD, Liverpoool John Moores University, Liverpool, United Kingdom
2005	M.Sc., University of Novi Sad, Novi Sad, Serbia
2002	Dipl. Ing., University of Novi Sad, Novi Sad, Serbia

Mr. Renan Pillon Barcelos, PhD student with Power Electronics Laboratory at EPFL

Education:

2024	PhD, École Polytechnique Fédérale de Lausanne (EPFL), Lausanne, Switzerland
2021	M.Sc., Universidade Federal de Santa Catarina (UFSC), Florianópolis, Brazil

POWER ELECTRONICS LABORATORY AT EPFL

École Polytechnique Fédérale de Lausanne → **EPFL** — School of Engineering → **STI** — Institute of Electrical and Micro Engineering → **IEM** — **PEL**

- Online since February 2014
- Currently: 10 Ph.D. students, 3 Post Docs, 1 Administrative Assistant
- Funding CH: SNSF, SFOE, Innosuisse
- Funding EU: H2020, S2R JU, ERC CoG
- Funding Industry: OEMs
- `https://www.epfl.ch/labs/pel/`

Competence Centre

▲ PEL Medium Voltage Laboratory

RESEARCH FOCUS

MVDC Technologies and Systems

- System Stability
- Protection Coordination
- Power Electronic Converters

MVDC
ENERGY CONVERSION TECHNOLOGIES AND SYSTEMS

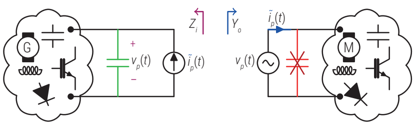

High Power Electronics

- Multilevel Converters
- Solid State Transformers
- Medium Frequency Conversion

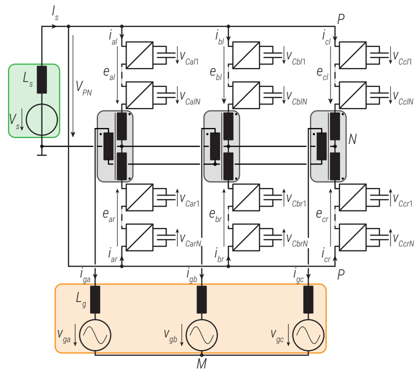

Components

- Semiconductor devices
- Magnetics
- Modeling, Characterization

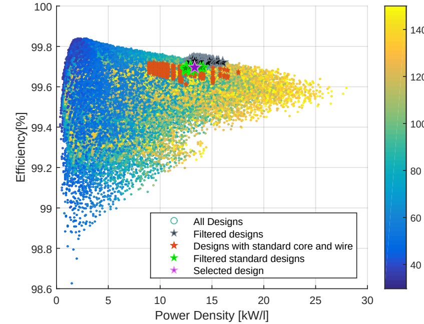

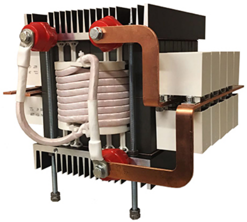

SCHEDULE

Before the coffee break

1) Introduction
- MVDC Applications
- Motivation and Challenges
- Power Electronics Converters

2) Bulk vs Modular Power Conversion
- High Power DC-DC Conversion
- Modular DC-DC Conversion
- Bulk DC-DC Conversion – DC Transformer

3) Resonant Conversion
- Resonant DC-DC Converters
- Modeling
- Control Principles

4) HV Semiconductors
- High Voltage Devices
- IGBT versus IGCT
- Gate Unit for the IGCTs

After the coffee break

5) IGCT HF Operation
- ZVS versus ZCS
- High Frequency Operation
- 1MW DCT prototype

6) MFT Design Optimization
- MW Design Challenges
- Technologies and Materials
- Practical 1MW 5kHz Design Experience

7) Direct Current Transformer Features
- Operating Principles
- Power Reversal Methods
- Practical Examples on LV DCT

8) Summary and Conclusions
- Why MVDC?
- How MVDC?
- When MVDC?

⇒ Tutorial pdf can be downloaded from: *(Source:* `https://www.epfl.ch/labs/pel/publications-2/publications-talks/`*)*

INTRODUCTION

MVDC Applications, Systems and Technologies

WHY DC?

- No reactive power

  Example: @ $cos(\varphi) = 0.95$

  $$\frac{P}{Q} \approx \frac{3}{1}$$

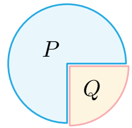

  - No constraints imposed upon transmission distance
  - Transmission capacity increase
  - Lower transmission losses
  - Alleviated stability problems
- No skin effect ($R_\gamma \downarrow \Rightarrow P_\gamma \uparrow$)
- Cheaper solution ("Break-even distance")
- Underwater cable transmission
- No need for synchronization (Marine applications)
- Direct integration of Renewable Energy Sources
- Challenges $\Rightarrow$ DC Transformer/Protection?

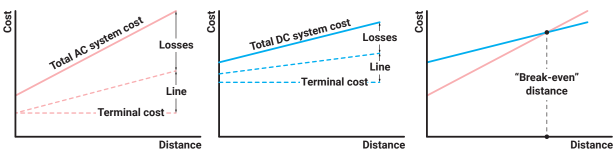

▲ Cost comparison between AC and DC systems

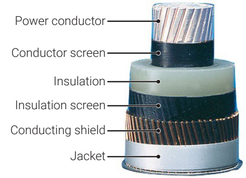

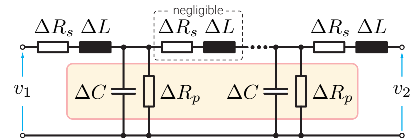

▲ High voltage cable

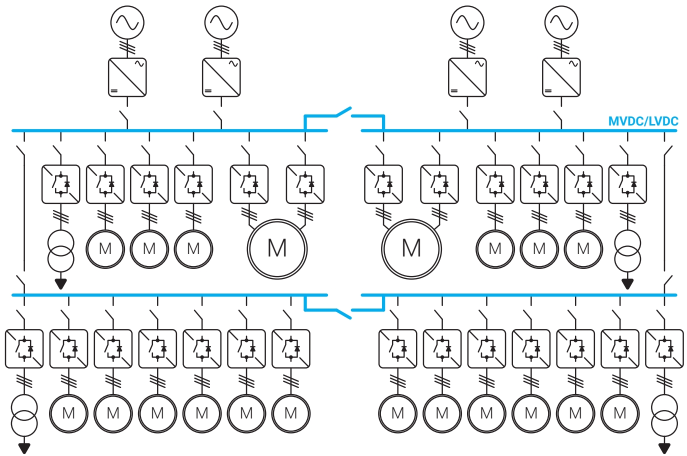

▲ DC Ship distribution system - frequency decoupling through a DC distribution [1]

[1] Uzair Javaid et al. "MVDC supply technologies for marine electrical distribution systems." *CPSS Transactions on Power Electronics and Applications* 3.1 (2018), pp. 65–76

CONVERSION OF AC LINES INTO DC

- Transmission capacity increase
- Employment of the existing conductors
- No change in tower foundations
- Possible tower head adjustment
- Possible isolator assemblies adjustment

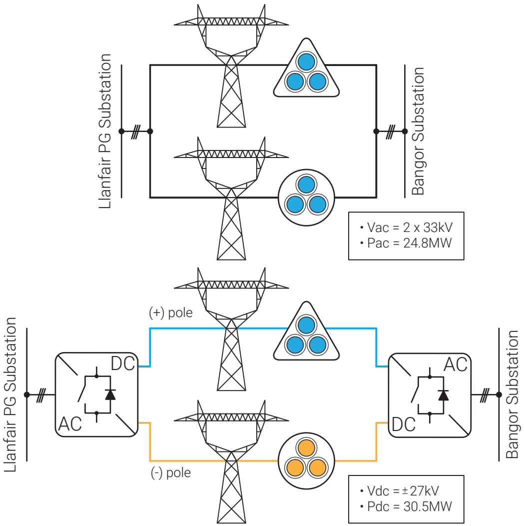

▲ Angle DC Project - UK

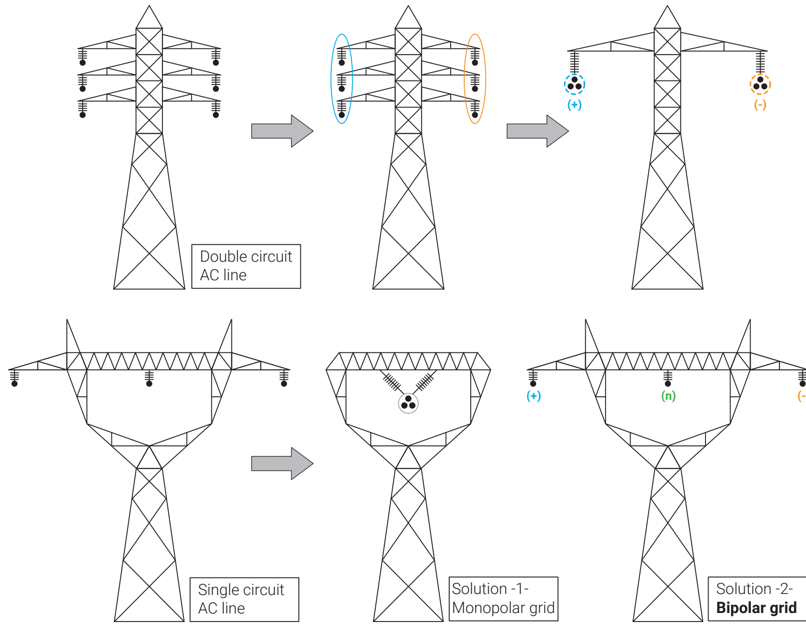

▲ Conversion of two typical AC lines into DC [2], [3], [4], [5]

MVDC POWER DISTRIBUTION NETWORKS

MVDC Power Distribution Networks

- Feasibility (Applications)
- System Level Gains
- Dynamic Stability

Conversion

- Passive and Stable
- Flexible, Modular and Scalable
- Efficient

Protection

- DC Breaker?
- Fault Current Limiting by Converters
- Protection Coordination

▲ Power electronics constituents

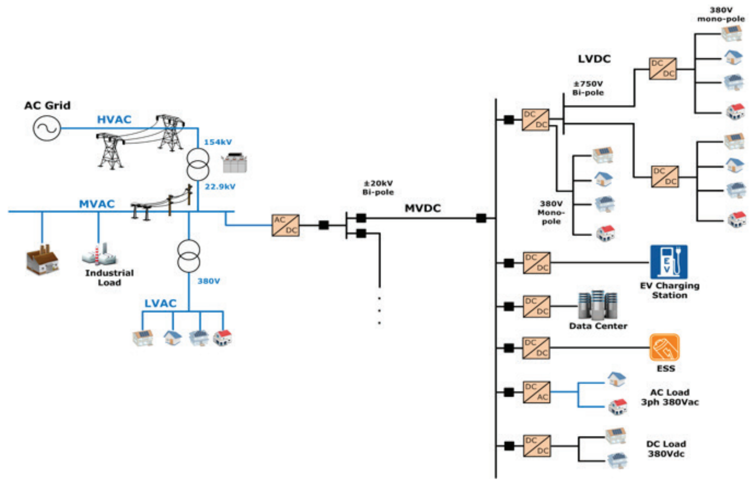

▲ Envisioned future MVDC grids and its links with existing grids

Bulk power transmission

- Break even distance against AC lines
- ~ 50 – 100 km for subsea cables or 600 km for overhead lines
- Long history since 1950s
- Interconnection of asynchronous grids

▲ From mercury arc rectifiers to modern HVDC systems

LVDC ships

- Variable frequency generators ⇒ maximum efficiency of the internal combustion engines
- Commercial products by ABB & Siemens

▲ Specialized vessels with LVDC distribution

Datacenters

- 380 V_{dc}
- DC loads (including UPS)
- Expected efficiency increase

Large PV powerplants

- 1500 V_{dc} PV central inverters
- Higher number of series-connected panels per string

▲ 1500V PV inverter - step towards the MVDC

Open challenges

- DC breaker
- Conversion blocks missing
- Protection coordination
- Business case

A TREND TOWARDS DC

Bulk power transmission

- Break even distance against AC lines
- ~ 50 – 100 km for subsea cables or 600 km for overhead lines
- Long history since 1950s
- Interconnection of asynchronous grids

▲ From mercury arc rectifiers to modern HVDC systems

LVDC ships

- Variable frequency generators ⇒ maximum efficiency of the internal combustion engines
- Commercial products by ABB & Siemens

▲ Specialized vessels with LVDC distribution

Datacenters

- 380 V_{dc}
- DC loads (including UPS)
- Expected efficiency increase

Large PV powerplants

- 1500 V_{dc} PV central inverters
- Higher number of series-connected panels per string

▲ 1500V PV inverter - step towards the MVDC

Open challenges

- DC breaker
- Conversion blocks missing
- Protection coordination
- Business case

⇒ DC is beneficial for medium / high power applications

EMERGING MVDC APPLICATIONS

Installations

- ABB HVDC Light demo: 4.3 km/±9 kV_{dc} [6]
- Tidal power connection: 16 km/10 kV_{dc} (based on MV3000 & MV7000) [7]

- Unidirectional oil platform connection in China: 29.2 km/±15 kV_{dc} [8]

Projects

- Angle DC: conversion of 33 kV MVac line to ±27 kV MVdc [9]

Universities

- Increased number of laboratories active in high power domain
- China, Europe, USA,...

Products

- Siemens MVDC Plus
  - 30 - 150 MW
  - < 200 km
  - < ±50 kV_{dc}

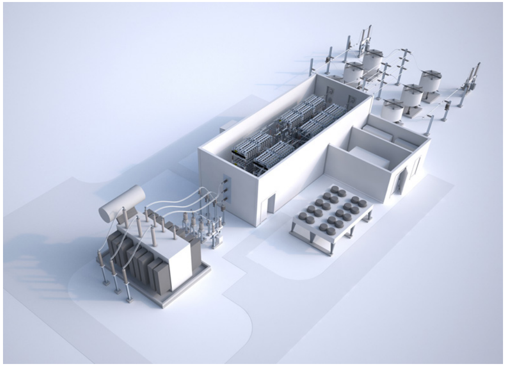

- RXPE Smart VSC-MVDC
  - 1 - 10 MVAr
  - ±5 - ±50 kV_{dc}
  - 40 - 200 km

Installations

- ABB HVDC Light demo: 4.3 km/$\pm$9 kV_{dc} [6]
- Tidal power connection: 16 km/10 kV_{dc} (based on MV3000 & MV7000) [7]

- Unidirectional oil platform connection in China: 29.2 km/$\pm$15 kV_{dc} [8]

Projects

- Angle DC: conversion of 33 kV MVac line to $\pm$27 kV MVdc [9]

Universities

- Increased number of laboratories active in high power domain
- China, Europe, USA,...

Products

- Siemens MVDC Plus
  - 30 - 150 MW
  - < 200 km
  - < $\pm$50 kV_{dc}

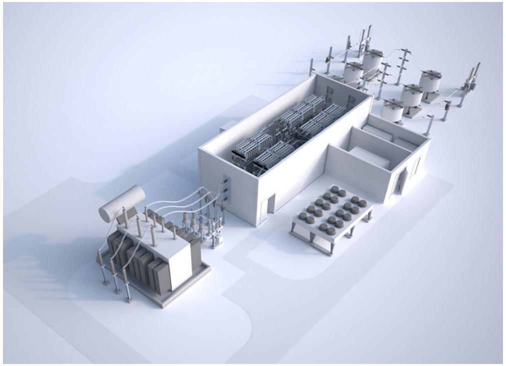

- RXPE Smart VSC-MVDC
  - 1 - 10 MVAr
  - $\pm$5 - $\pm$50 kV_{dc}
  - 40 - 200 km

⇒ MVDC is gaining momentum through early pilot and demonstration projects!

SOLID-STATE TRANSFORMER (SST)

Concept and motivation?

- SST = Switching stages + Isolation
- Firstly envisioned within AC grids
- Power Electronic Building Blocks (PEBBs)
- Conventional transformer vs SST?
- Operating frequency increase **(MFT)**

	Grid Tx	SST
Controlability	No	Yes
Efficiency	$\eta \geq 99\%$	$P_?$
Q compensation	No	Yes
Fault tolerance	No	Yes
Size	Bulky	Compact
Cost	Low	High

Advantages at the expense of cost and reduced efficiency!

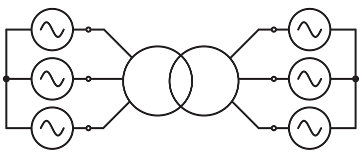

▲ Conventional AC grid transformer

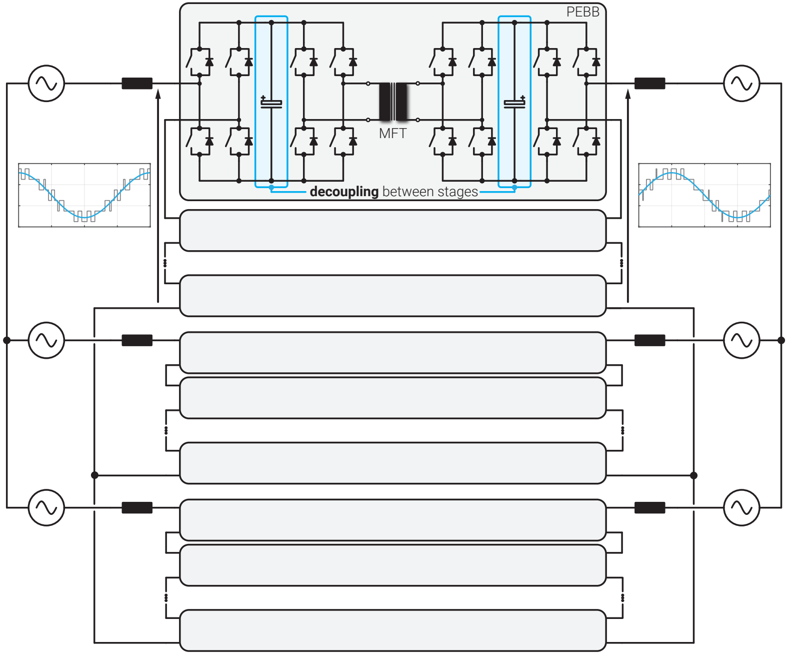

▲ Solid-State Transformer employed with the aim of interfacing two AC systems [10], [11]

SOLID STATE TRANSFORMER FOR TRACTION (ABB - 1.2MW PETT)

Characteristics

- 1-Phase MVAC to MVDC
- Power: 1.2MVA
- Input AC voltage: 15kV, 16.7Hz
- Output DC voltage: 1500 V
- 9 cascaded stages (n + 1)
- input-series output-parallel
- double stage conversion

99 Semiconductor Devices

- HV PEBB: 9 x (6 x 6.5kV IGBT)
- LV PEBB: 9 x (2 x 3.3kV IGBT)
- Bypass: 9 x (2 x 6.5kV IGBT)
- Decoupling: 9 x (1 x 3.3kV Diode)

9 MFTs

- Power: 150kW
- Frequency: 1.75kHz
- Core: Nanocrystalline
- Winding: Litz
- Insulation / Cooling: Oil

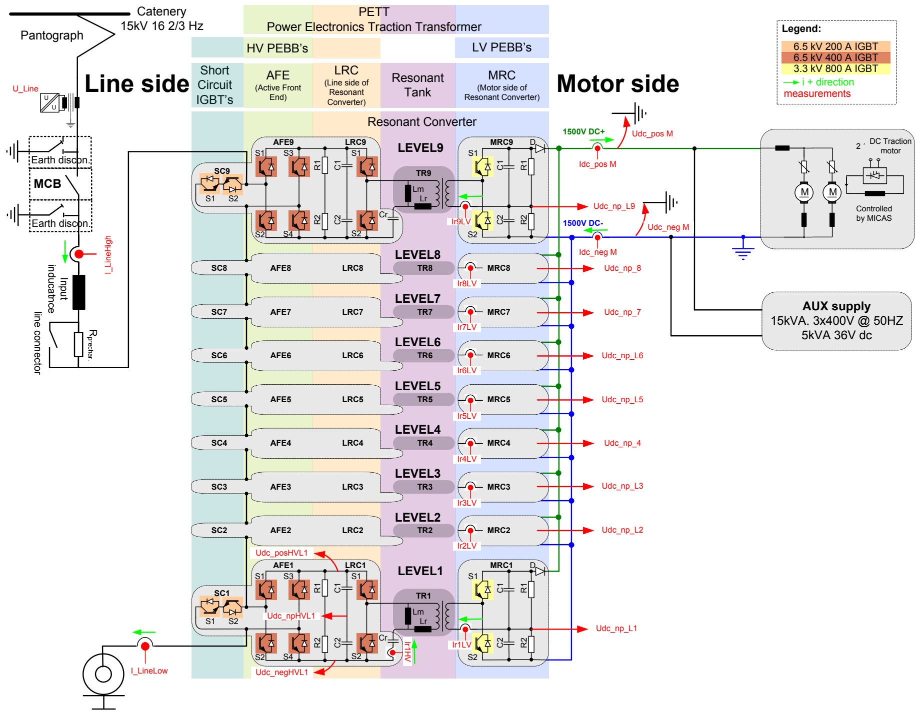

▲ ABB PETT scheme [12], [13]

SOLID STATE TRANSFORMER FOR TRACTION - DESIGN

Retrofitted to shunting locomotive

- Replaced LFT + SCR rectifier
- Propulsion motor - 450kW
- 12 months of field service
- No power electronic failures
- Efficiency around 96%
- Weight: ≈ 4.5 t

Technologies

- Standard 3.3kV and 6.5kV IGBTs
- De-ionized water cooling
- Oil cooling/insulation for MFTs
- n + 1 redundancy
- IGBT used for bypass switch

Displayed at:

- Swiss Museum of Transport
- https://www.verkehrshaus.ch

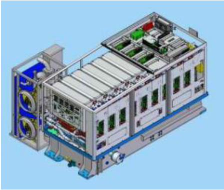



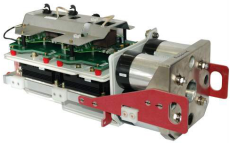
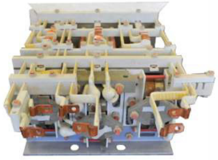
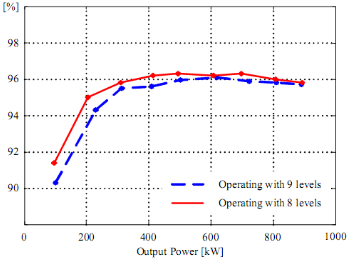

▲ ABB PETT prototype [12], [13]

[12] D. Dujic et al. "Power Electronic Traction Transformer-Low Voltage Prototype." *IEEE Transactions on Power Electronics* 28.12 (Dec. 2013), pp. 5522–5534
[13] C. Zhao et al. "Power Electronic Traction Transformer-Medium Voltage Prototype." *IEEE Transactions on Industrial Electronics* 61.7 (July 2014), pp. 3257–3268

SOLID-STATE TRANSFORMER - OTHER EXAMPLES

UNIFLEX-PM

- Reduced scale prototypes

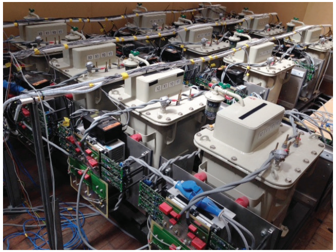

▲ UNIFLEX-PM prototype

FREEDM

- Reduced scale prototypes

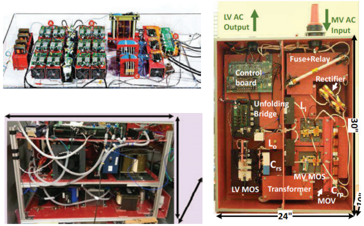

▲ FREEDM SSTs [15]

HEART

- Reduced scale prototypes

▲ HEART project

GE

- Full scale prototype

▲ GE prototype [14]

HUST

- Full scale prototype

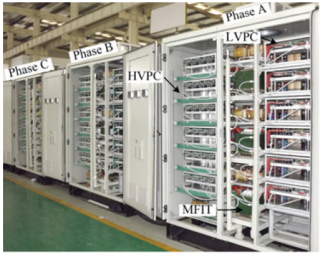

▲ HUST SST [16]

XD Electric Company

- Full scale prototype

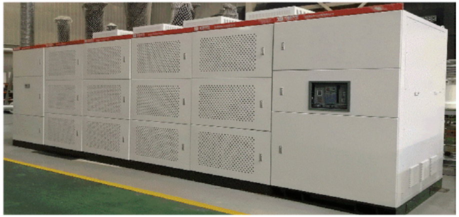

▲ XD Electric Company SST [17]

DC-DC CONVERTERS

- Inherent part of the almost all SST topologies
- Expansion of the existing power system
- Enabling technology for MVDC
- Penetration of renewable energy sources
- Fast / Ultra Fast EV charging
- **Medium Frequency conversion**

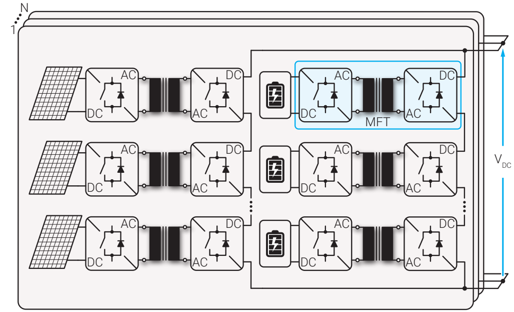

▲ Employment of a DC-DC SST within RES-based systems

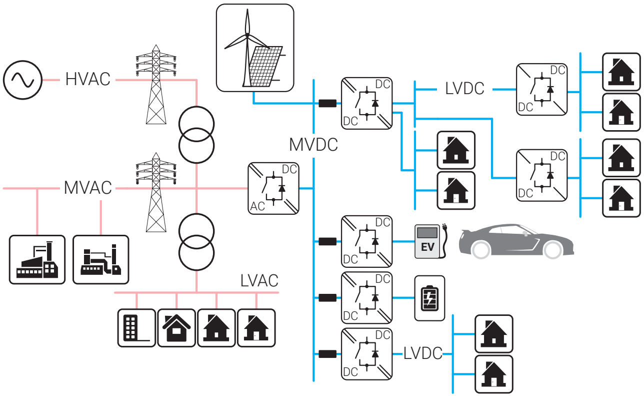

▲ Concept of a modern power system

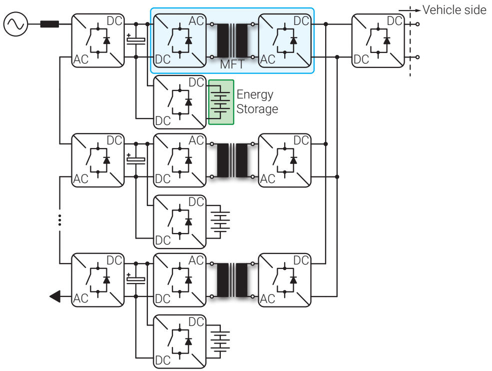

▲ Fast EV charging concept

MEDIUM FREQUENCY TRANSFORMER (MFT) CHALLENGES

- **Skin and proximity effect losses:** impact on efficiency and heating
- **Cooling:** increase of power density ⇒ decrease in size ⇒ less cooling surface ⇒ higher R_{th} ⇒ higher temperature gradients
- **Non-sinusoidal excitation:** impact on core and winding losses and insulation
- **Insulation:** coordination and testing taking into account high $\frac{dV}{dt}$ characteristic for power electronic converters
- **Accurate electric parameter control:** especially in case of resonant converter applications

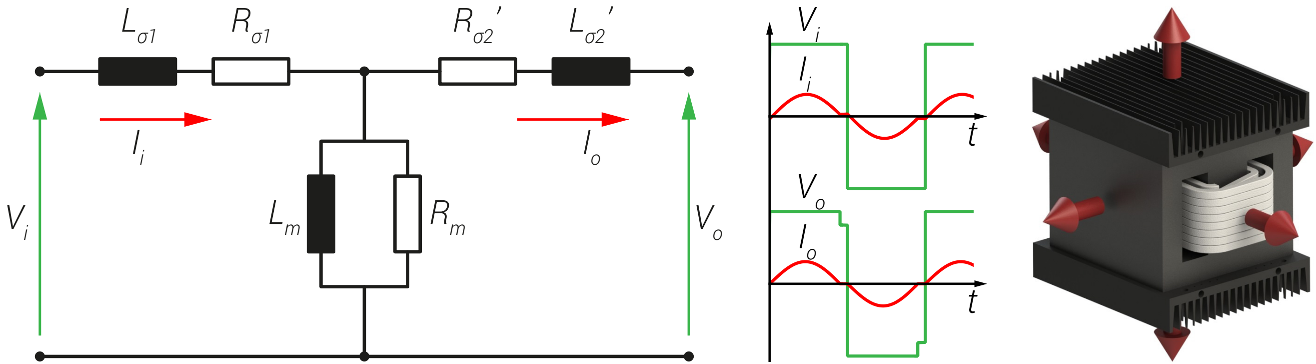

▲ Medium Frequency Transformer challenges

⇒ MFT design is generally challenging and requires multiphysics considerations and multiobjective optimization

MFT NONSINUSOIDAL POWER ELECTRONIC WAVEFORMS

DAB Converter:

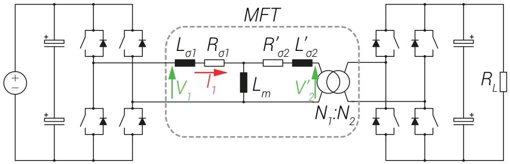

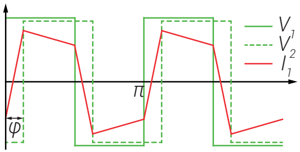

- $V_{1,2}$ square
- I non-sinusoidal

Series Resonant Converter:

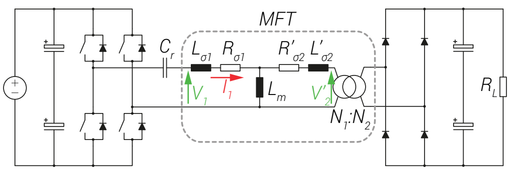

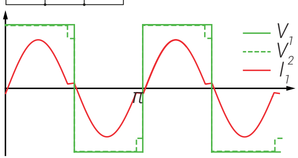

- $V_{1,2}$ square
- I sinusoidal

Core Losses:

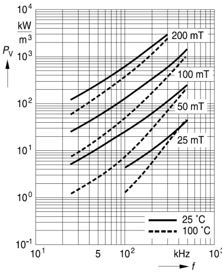

▲ Specific AC core losses

- Data-sheet - sinusoidal excitation
- Steinmetz - sinusoidal excitation losses
- Core is excited with square pulses!
- Losses must be correctly evaluated
- Generalization of Steinmetz model

Winding Losses:

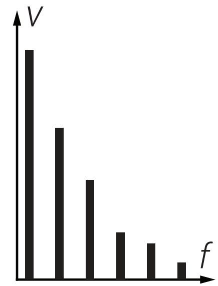

▲ Harmonics impacting winding losses

- Current waveform impacts the winding losses
- Copper is a linear material
- Losses can be evaluated in harmonic basis
- Current harmonic content must be evaluated
- Losses are the sum of the individual harmonic losses

MFT ACCURATE PARAMETERS CONTROL

DAB Converter:

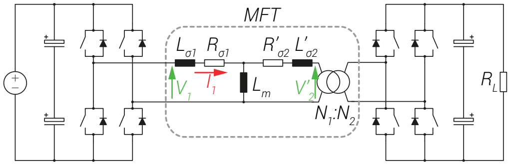

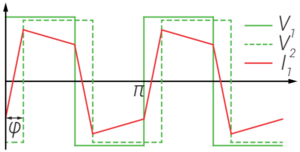

- $V_{1,2}$ square
- I non-sinusoidal

Series Resonant Converter:

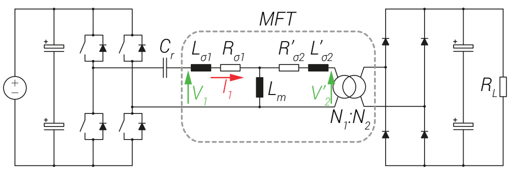

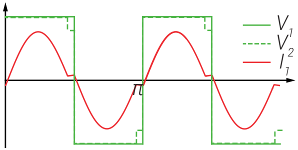

- $V_{1,2}$ square
- I sinusoidal

DAB

- Leakage inductance
- Controllability of the power flow
- Higher than $L_{\sigma.min}$:

$$L_{\sigma.min} = \frac{V_{DC1} V_{DC2} \varphi_{min} (\pi - \varphi_{min})}{2 P_{out} \pi^2 f_s n}$$

- Magnetizing Inductance is normally high

SRC

- Leakage inductance is part of resonant circuit
- Must match the reference:

$$L_{\sigma.ref} = \frac{1}{\omega_0^2 C_r}$$

- Magnetizing inductance is normally high
- Reduced in case of LLC
- Limits the magnetization current to the reference $I_{m.ref}$
- Limits the switch-off current and losses

$$L_m = \frac{n V_{DC2}}{4 f_s I_{m.ref}}$$

- $I_{m.ref}$ has to be sufficiently high to maintain ZVS

MFT VARIETY OF DESIGNS...

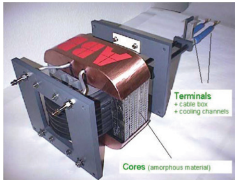

ABB: 350kW, 10kHz

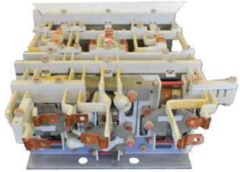
ABB: 3x150kW, 1.8kHz

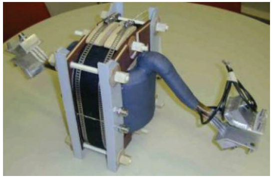
BOMBARDIER: 350kW, 8kHz

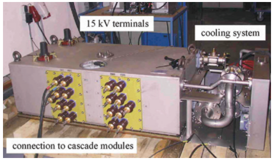

ALSTOM: 1500kW, 5kHz


IKERLAN: 400kW, 5kHz

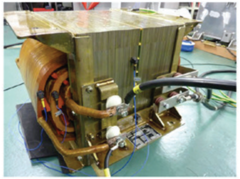
IKERLAN: 400kW, 1kHz

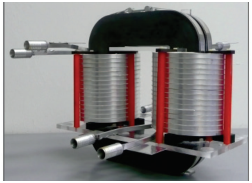
FAU-EN: 450kW, 5.6kHz


CHALMERS: 50kW, 5kHz

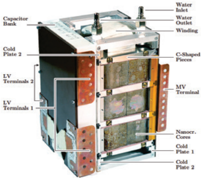

ETHZ: 166kW, 20kHz

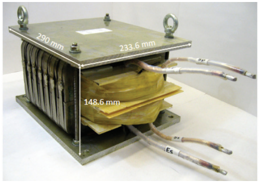

EPFL: 300kW, 2kHz

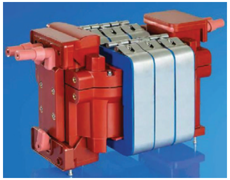
STS: 450kW, 8kHz

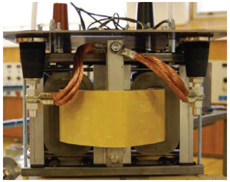
KTH: 170kW, 4kHz

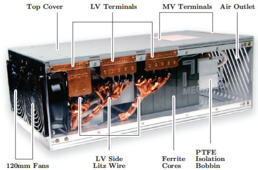

ETHZ: 166kW, 20kHz


EPFL: 100kW, 10kHz

?

ACME: ???kW, ???kHz

ENERGY CONVERSION TECHNOLOGIES AND SYSTEMS

▲ EMPOWER-ing the future energy systems

MVDC Grids

- DC Transformer
- Flexibility
- Stability

DC-DC Conversion

- Resonant principles
- Medium frequency conversion
- Absence of the control loops

DC Protection

- HV semiconductors
- Active protection
- Selectivity

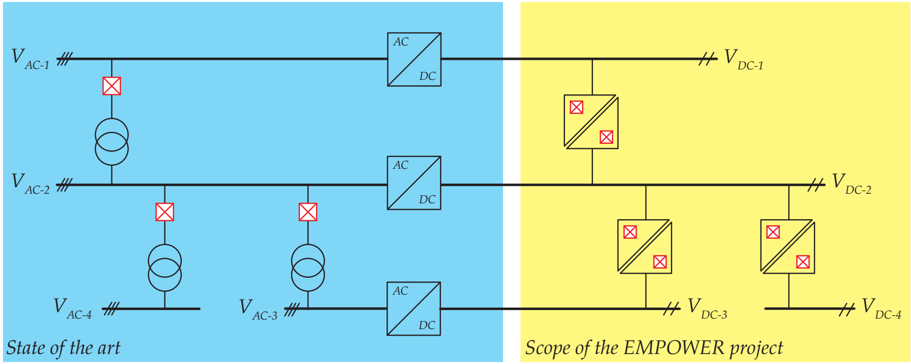

▲ Today's AC and tomorrow's DC power distribution networks enabled by DC Transformers

▲ The EMPOWER - Holistic and Integrated

EMPOWER - A EUROPEAN RESEARCH COUNCIL CONSOLIDATOR GRANT

MVDC
ENERGY CONVERSION TECHNOLOGIES AND SYSTEMS

▲ EMPOWER-ing the future energy systems

MVDC Grids

- DC Transformer
- Flexibility
- Stability

DC-DC Conversion

- Resonant principles
- Medium frequency conversion
- Absence of the control loops

DC Protection

- HV semiconductors
- Active protection
- Selectivity

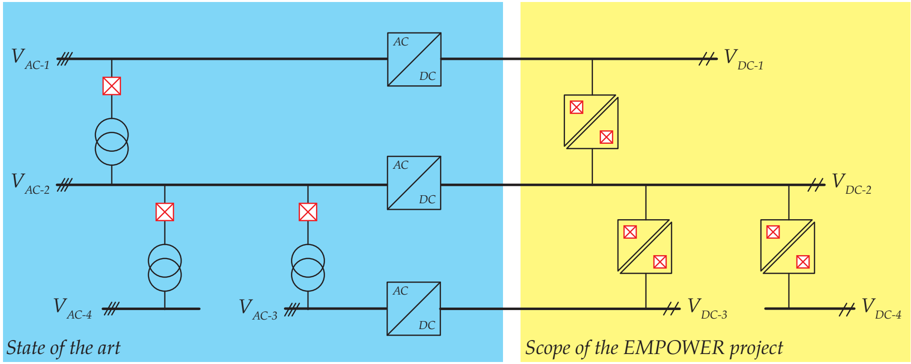

▲ Today's AC and tomorrow's DC power distribution networks enabled by DC Transformers

▲ The EMPOWER - Holistic and Integrated

⇒ Can we make a simple DC Transfomer behaving as much as possible as equivalent AC transformer?

BULK VS. MODULAR POWER CONVERSION

The same conversion function, but many implementation differences

DC-DC SST - BASIC CONCEPTS

Fractional power processing

- Multiple MFTs
- Equal power distribution among PEBBs
- MFT isolation?
- Various PEBB configurations

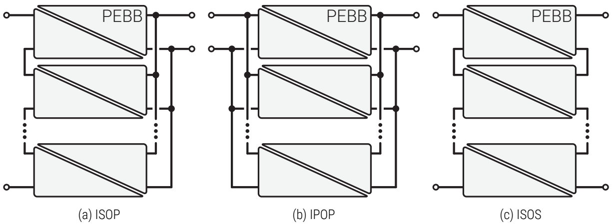

▲ Different structures employed depending upon the voltage level

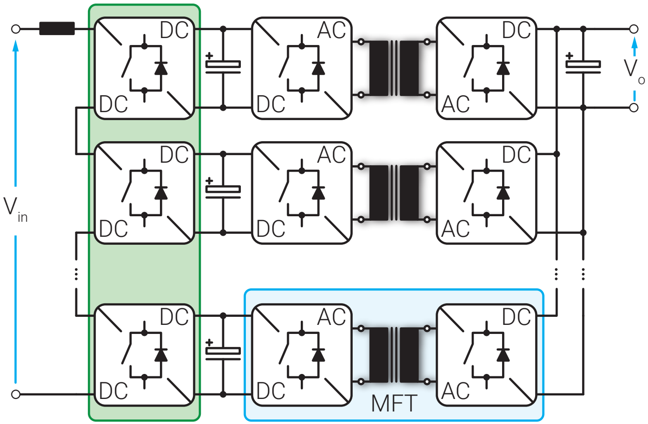

▲ ISOP Structure

Bulk power processing

- Single MFT
- Isolation solved only once
- Various configurations/operating principles

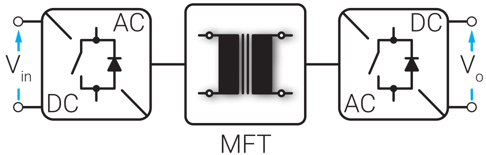

▲ Bulk power processing concept

DC-DC SST - BASIC CONCEPTS

Fractional power processing

- Multiple MFTs
- Equal power distribution among PEBBs
- MFT isolation?
- Various PEBB configurations

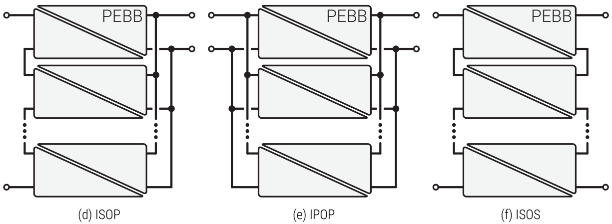

▲ Different structures employed depending upon the voltage level

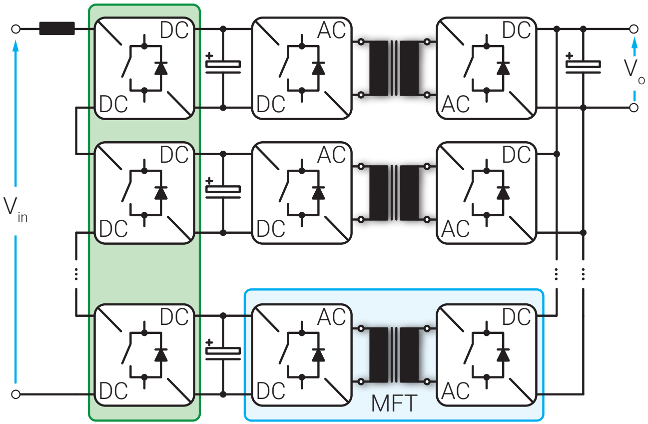

▲ ISOP Structure

Bulk power processing

- Single MFT
- Isolation solved only once
- Various configurations/operating principles

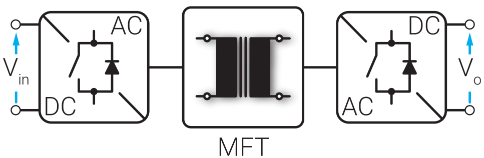

▲ Bulk power processing concept

⇒ Both design approaches are valid, and have their pros and cons! Many factors should be considered!

COMMON PEBB CONFIGURATIONS

Dual-Active Bridge

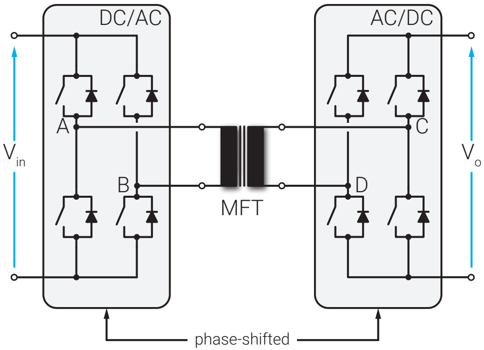

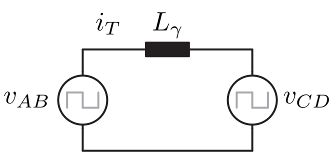

$$P = P(\varphi)$$

▲ Dual Active Bridge [18]

Resonant Converters

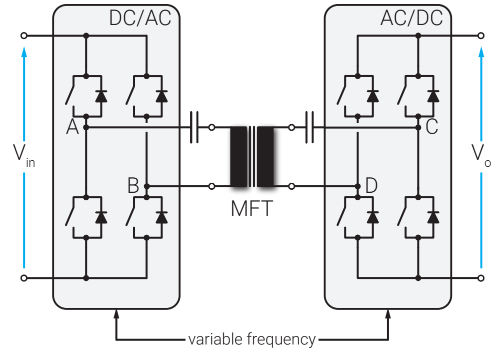

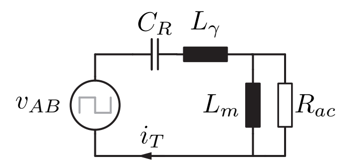

$$f_{r1} = \frac{1}{2\pi\sqrt{C_R L_\gamma}}$$

$$f_{r2} = \frac{1}{2\pi\sqrt{C_R (L_\gamma + L_m)}}$$

$$Q = Q(R_{ac})$$

$$G = G\left(\frac{f_{sw}}{f_{r1}}, \frac{L_m}{L_\gamma}, Q\right)$$

▲ LLC Resonant Converter

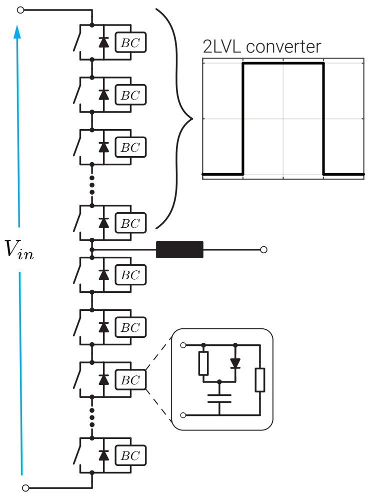

▲ Series connection of switches [19]

- Series connection of switches with snubbers
- Two voltage levels ($n_{LVL} = 2$)
- Two-Level voltage waveforms

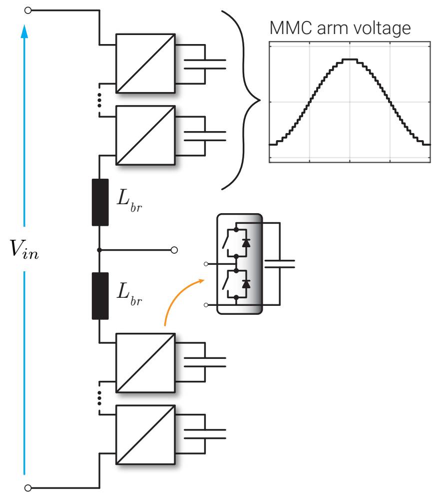

▲ Modular Multilevel Converter (MMC)

- Series connection of Submodules (SM)
- n_{LVL} depending upon number of SMs
- Arbitrary voltage waveform generation

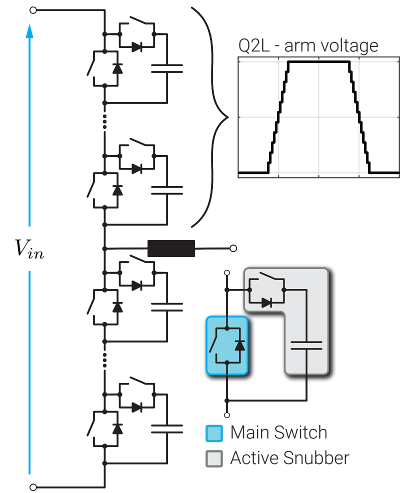

▲ Quasi Two-Level (Q2L) Converter [20], [21]

- Series connection of MMC-alike SMs
- n_{LVL} depending upon number of SMs
- Quasi Two-Level (trapezoidal) voltage waveform

MODULAR MULTILEVEL CONVERTER (MMC)

- Variety of conversion possibilities
- Variety of modulations
- Different types of submodules (SMs)
  - Half-Bridge (HB)
  - Full-Bridge (FB)
  - Others...
- Arbitrary voltage waveform generation

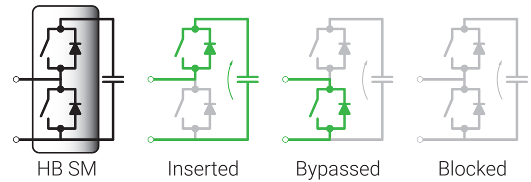

▲ Half-Bridge submodule and its allowed states

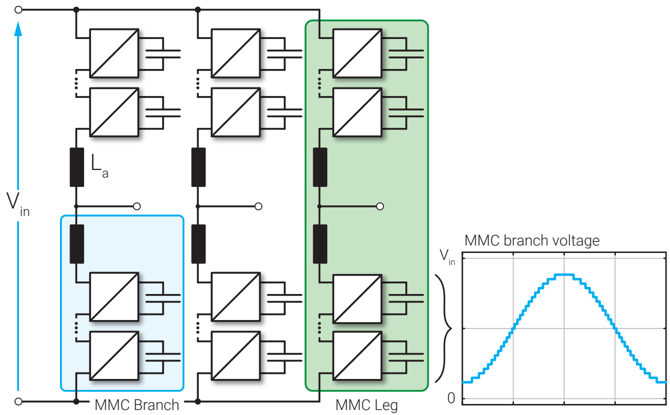

▲ Modular Multilevel Converter (MMC)

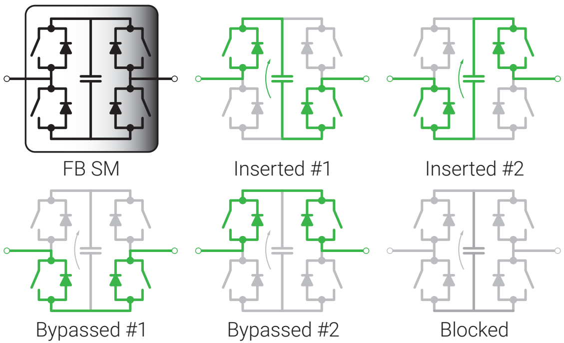

▲ Full-Bridge submodule and its allowed states

Single MMC ratings:

- 3.3kVac
- ±5kV
- 250kW

Single MMC as:

- Voltage source
- Source source

Two MMCs in:

- Series connection
- Parallel connection

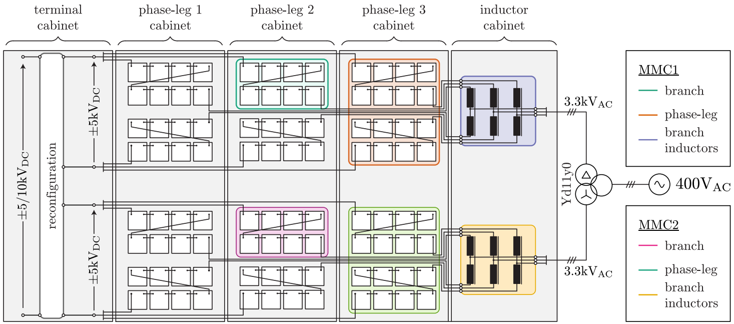

▲ EPFL PEL - Dual MMC-based MVDC source - layout

▲ EPFL PEL - Dual MMC-based MVDC source - realized 2 x 250kW system

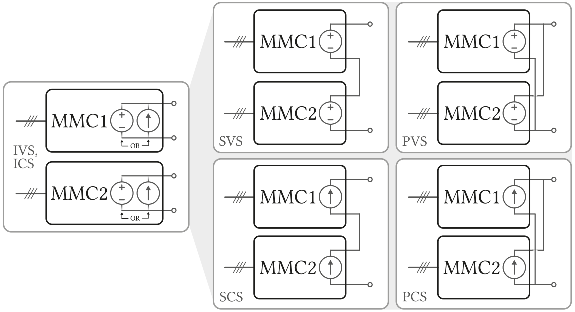

▲ Possible configurations with two MMCs

MMC-BASED DUAL ACTIVE BRIDGE (DAB)

- Basic operation principles are retained
- Easy to comprehend (AC equivalent)

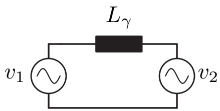

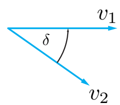

$$P = \frac{V_1 V_2}{\omega L_\gamma} sin(\delta)$$

Challenges?

- Modulation choice (sine, square, etc ... ?)
- System design (N vs V_{grid})
- Energy balancing
- Q2L mode & capacitors sizing
- Engagement within bipolar grids

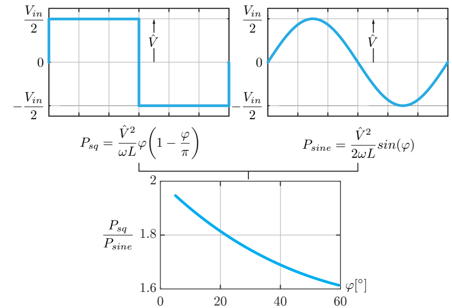

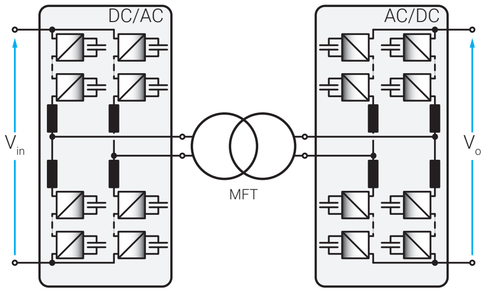

▲ MMC-based 1PH-DAB [22]

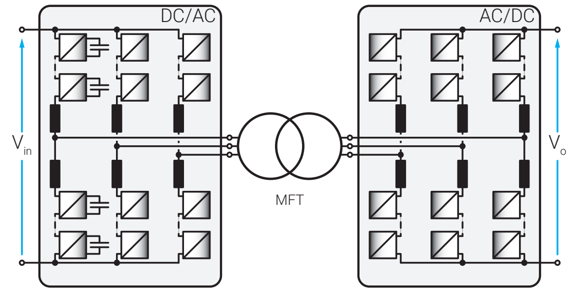

▲ MMC-based 3PH-DAB

[22] Stephan Kenzelmann et al. "Isolated DC/DC structure based on modular multilevel converter." *IEEE Transactions on Power Electronics* 30.1 (2015), pp. 89–98

- Basic operation principles are retained
- Easy to comprehend (AC equivalent)

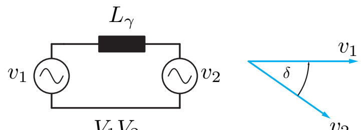

$$P = \frac{V_1 V_2}{\omega L_\gamma} sin(\delta)$$

Challenges?

- Modulation choice (sine, square, etc ... ?)
- System design (N vs V_{grid})
- Energy balancing
- Q2L mode & capacitors sizing
- Engagement within bipolar grids

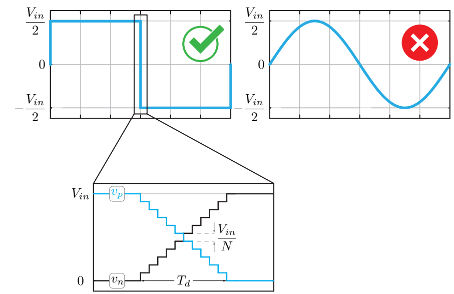

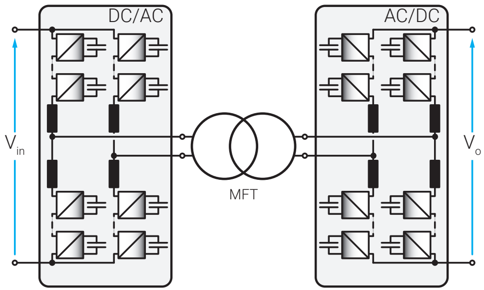

▲ MMC-based 1PH-DAB [22]

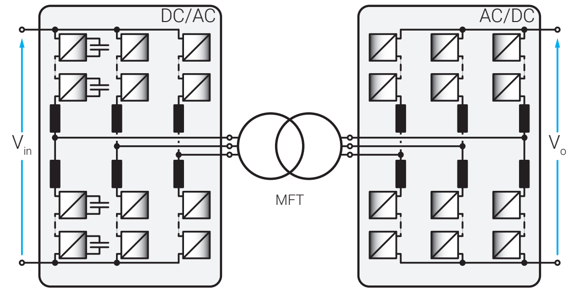

▲ MMC-based 3PH-DAB

[22] Stephan Kenzelmann et al. "Isolated DC/DC structure based on modular multilevel converter." *IEEE Transactions on Power Electronics* 30.1 (2015), pp. 89–98

QUASI TWO-LEVEL (Q2L) CONVERTER

- MMC-alike structure
- Branch inductors removed!
- SM = Main Switch + Active Snubber
- Sequential insertion/bypassing of SMs [23]

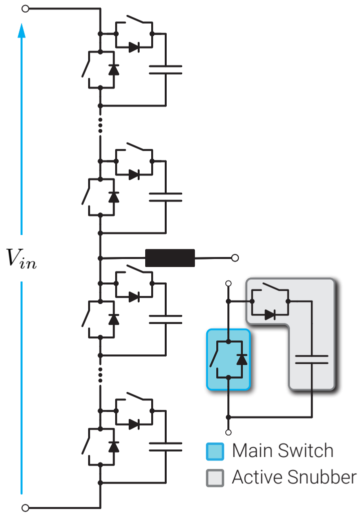

▲ Quasi Two-Level Converter

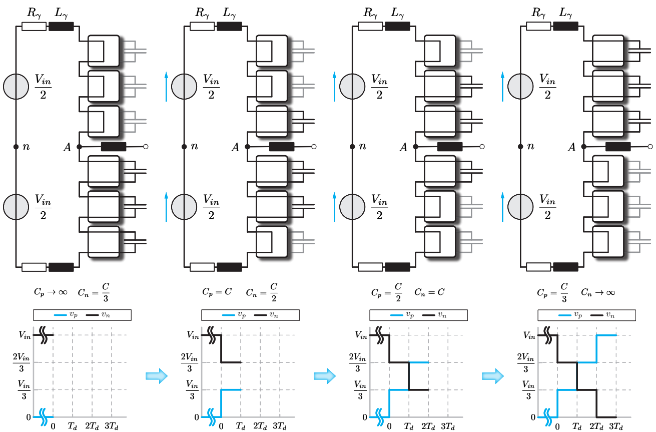

▲ Example of the Q2L Converter transition (N=3)

[23] Stefan Milovanovic and Drazen Dujic. "Comprehensive analysis and design of a quasi two-level converter leg." *CPSS Transactions on Power Electronics and Applications* 4.3 (2019), pp. 181–196

- MMC-alike structure
- Branch inductors removed!
- SM = Main Switch + Active Snubber
- Sequential insertion/bypassing of SMs [23]

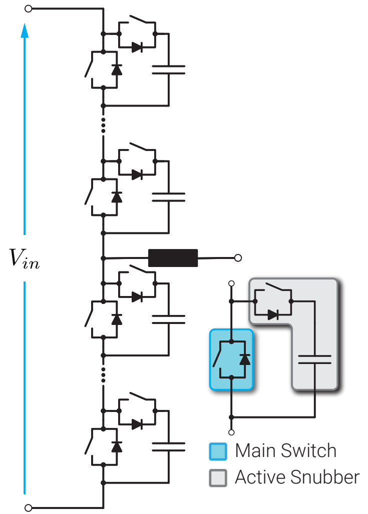

▲ Quasi Two-Level Converter

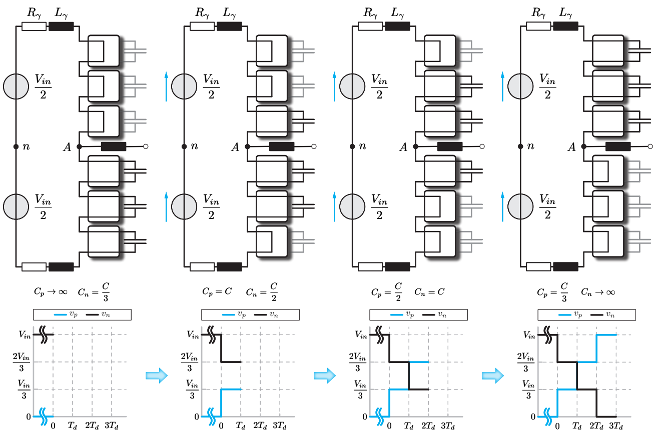

▲ Example of the Q2L Converter transition (N=3)

Every dwell interval introduces new resonant parameters to the circuit!

[23] Stefan Milovanovic and Drazen Dujic. “Comprehensive analysis and design of a quasi two-level converter leg.” *CPSS Transactions on Power Electronics and Applications* 4.3 (2019), pp. 181–196

QUASI TWO-LEVEL (Q2L) CONVERTER

- MMC-alike structure
- Branch inductors removed!
- SM = Main Switch + Active Snubber
- Sequential insertion/bypassing of SMs [23]

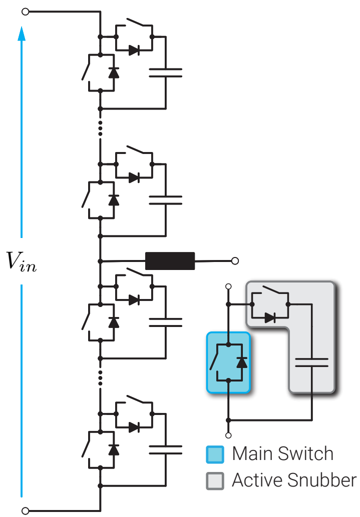

▲ Quasi Two-Level Converter

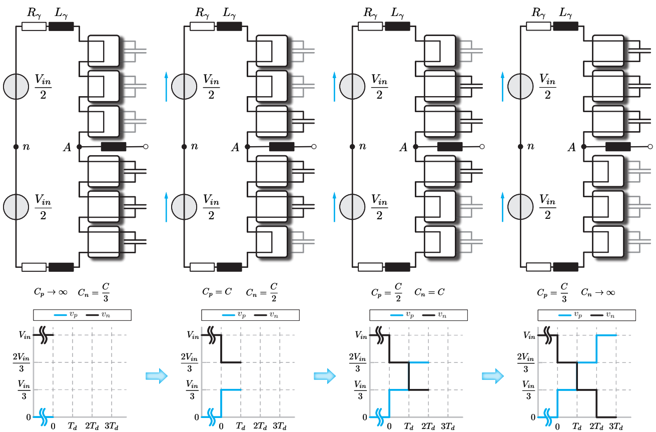

▲ Example of the Q2L Converter transition (N=3)

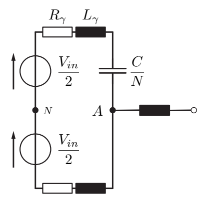

[23] Stefan Milovanovic and Drazen Dujic. “Comprehensive analysis and design of a quasi two-level converter leg.” *CPSS Transactions on Power Electronics and Applications* 4.3 (2019), pp. 181–196

- MMC-alike structure
- Branch inductors removed!
- SM = Main Switch + Active Snubber
- Sequential insertion/bypassing of SMs [23]

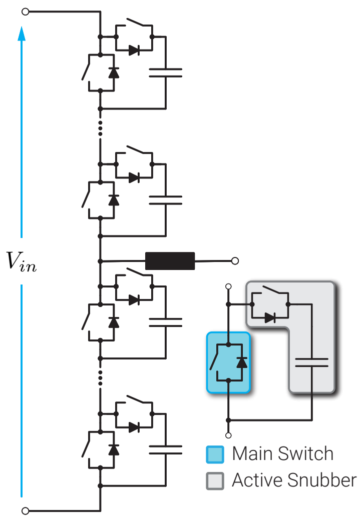

▲ Quasi Two-Level Converter

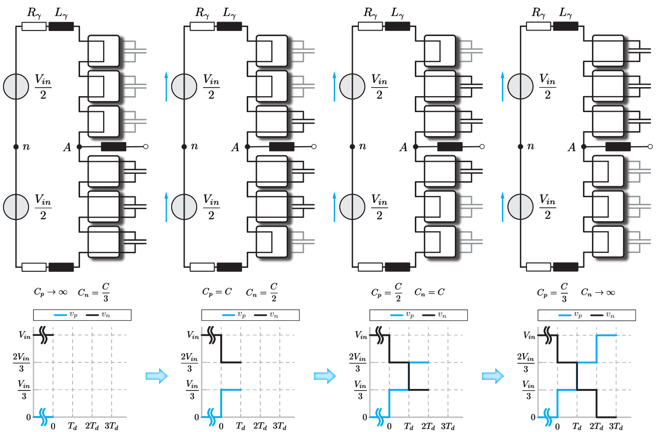

▲ Example of the Q2L Converter transition (N=3)

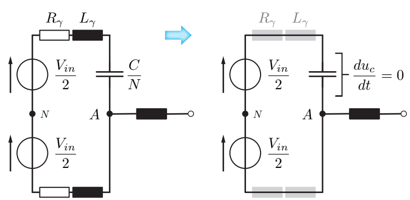

[23] Stefan Milovanovic and Drazen Dujic. "Comprehensive analysis and design of a quasi two-level converter leg." *CPSS Transactions on Power Electronics and Applications* 4.3 (2019), pp. 181–196

- MMC-alike structure
- Branch inductors removed!
- SM = Main Switch + Active Snubber
- Sequential insertion/bypassing of SMs [23]

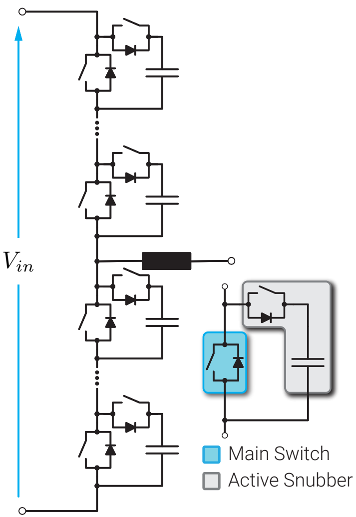

▲ Quasi Two-Level Converter

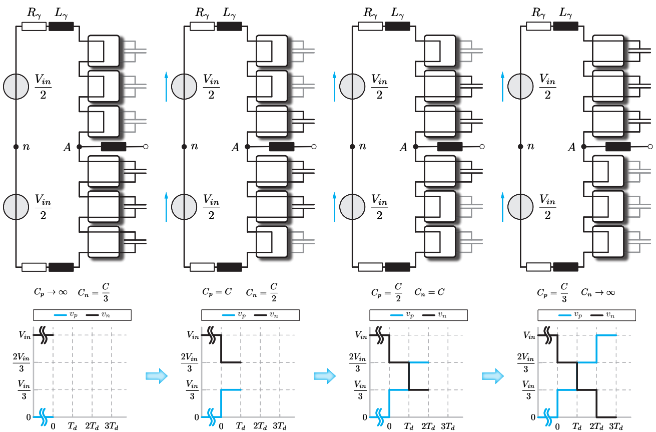

▲ Example of the Q2L Converter transition (N=3)

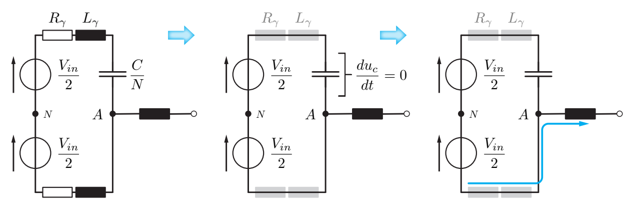

⇒ Output current drifts to a single branch. Common mode current does not exist!

[23] Stefan Milovanovic and Drazen Dujic. "Comprehensive analysis and design of a quasi two-level converter leg." *CPSS Transactions on Power Electronics and Applications* 4.3 (2019), pp. 181–196

Q2L CONVERTER - PROS AND CONS

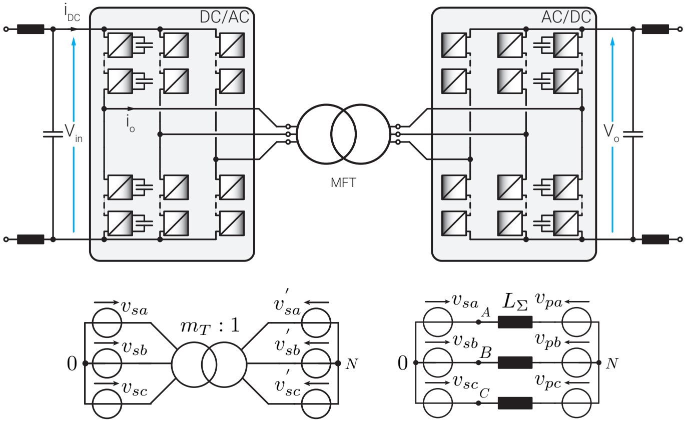

▲ Observed Q2L configuration

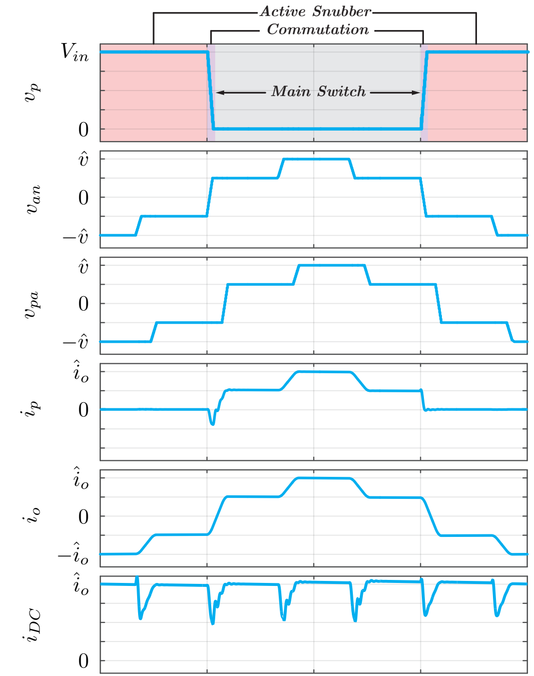

▲ Relevant waveforms of the Q2L converter operating as the 3PH-DAB

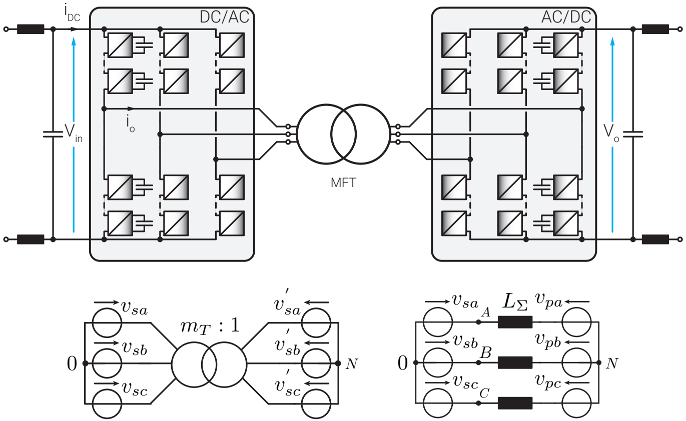

▲ Observed Q2L configuration

⇒ SM capacitor = "short-interval" energy buffer

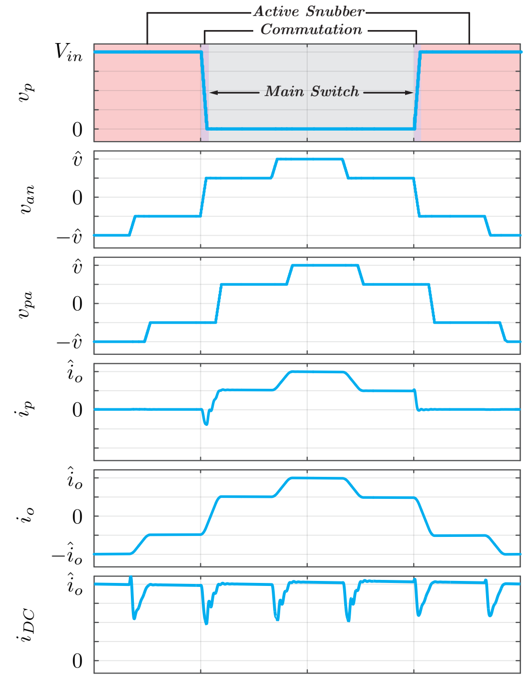

▲ Relevant waveforms of the Q2L converter operating as the 3PH-DAB

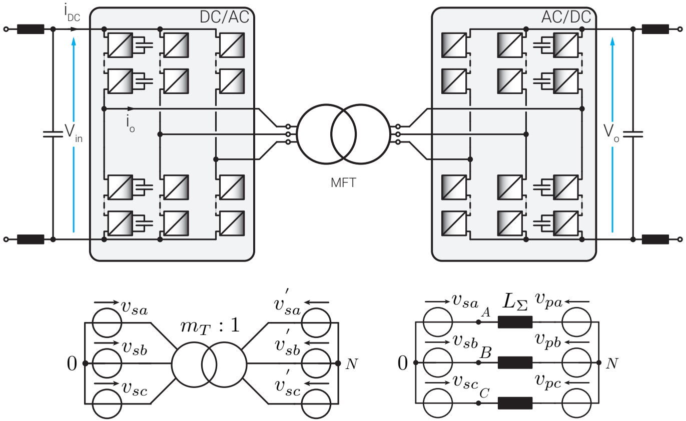

▲ Observed Q2L configuration

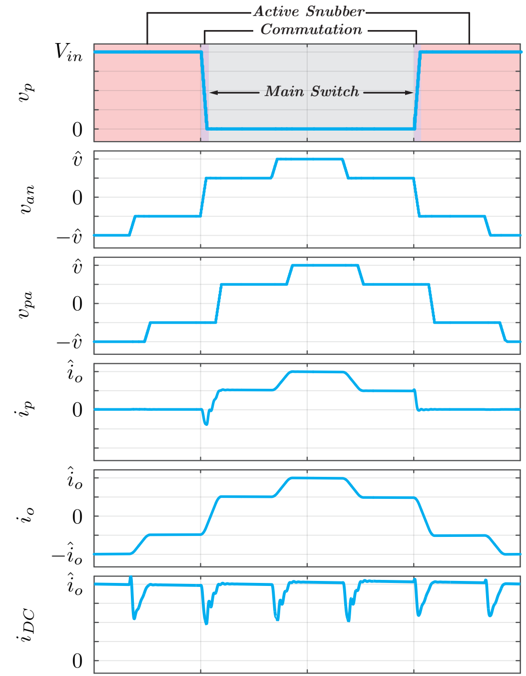

▲ Relevant waveforms of the Q2L converter operating as the 3PH-DAB

Pros

- Significant reduction in submodule capacitance
- Converter size reduction (no branch inductors, small SM capacitance)
- Active snubber switch can be sized for half the rated current

Cons

- Need for HV/MV input/output capacitor
- Complicated analysis of transition process/SM capacitance sizing
- SM capacitance sizing influenced by the branch stray inductance

- Provided ratings

Parameter	Value
Input voltage (V_{in})	$\pm$20kV
Output voltage (V_o)	1.5kV
Rated power (P_{nom})	10MW
Operating frequency (f)	1kHz

- **Redundancy**
- Converter structure considering given grid nature?
  - Topology
  - Operating principles and control
  - Operating frequency
  - Sizing principles considering given ratings
  - Constraints
  - Behavior under faults

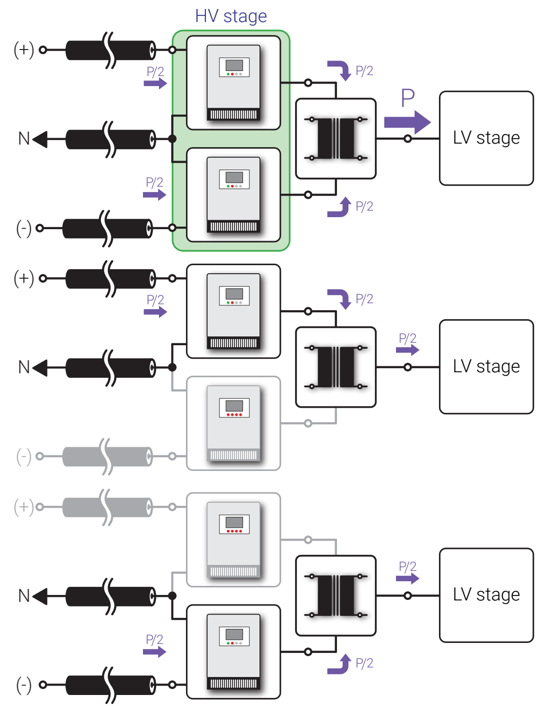

▲ Generic structure of a converter to be employed within a bipolar grid

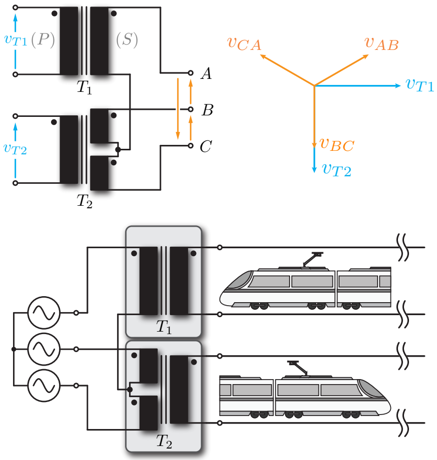

▲ Scott Transformer Connection

- 3PH 3W Tx ⟹ 2 x 1PH Tx
- Number of MMC branches reduction (N_L ↓)
- Ability to operate in a pure rectifier mode
- Medium frequency operation

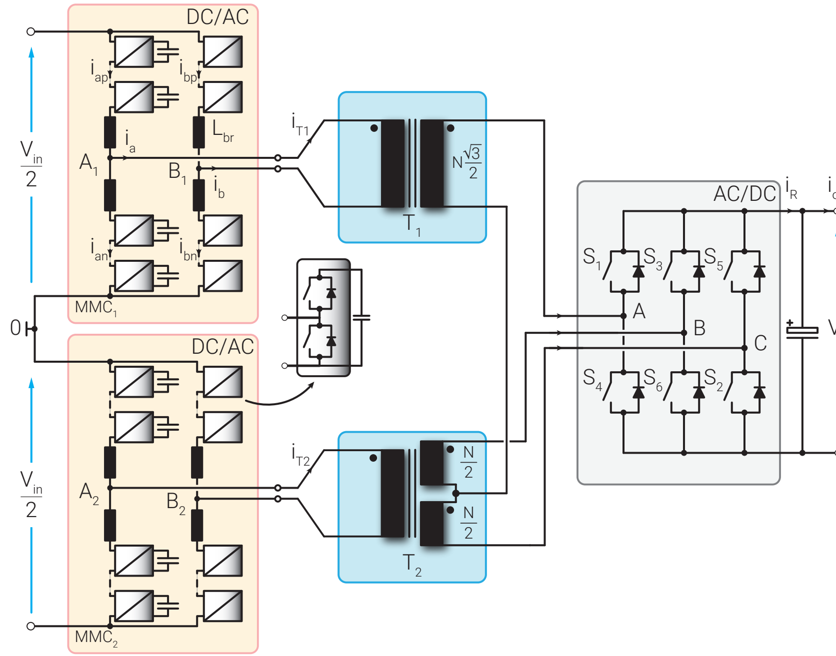

▲ MMC-Based High Power DC-DC Converter Employing Scott Transformer Connection [24]

[24] S. Milovanovic and D. Dujic. "MMC-Based High Power DC-DC Converter Employing Scott Transformer." *PCIM Europe 2018*. June 2018, pp. 1–7

MMC-BASED HIGH POWER UNIDIRECTIONAL DC-DC CONVERTER

- No magnetic coupling between Tx windings
- Parameters mismatch robustness
- Sinusoidal operation mode!

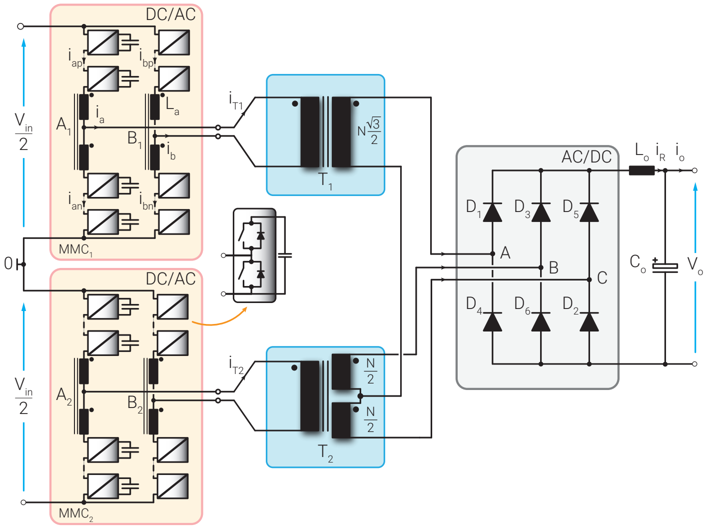

▲ MMC-based High-Power Unidirectional DC-DC Converter

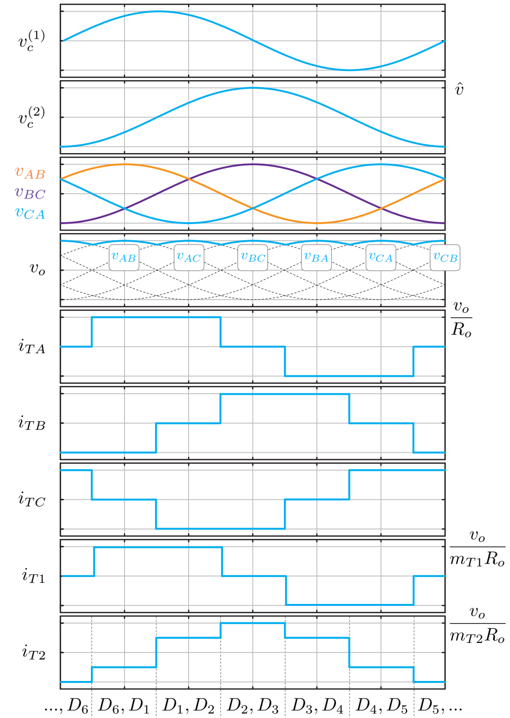

▲ Converter idealized operating waveforms

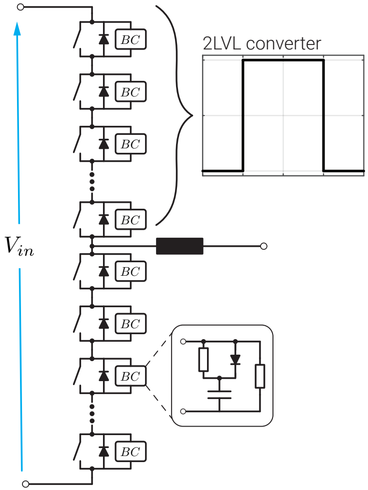

▲ Series connection of switches

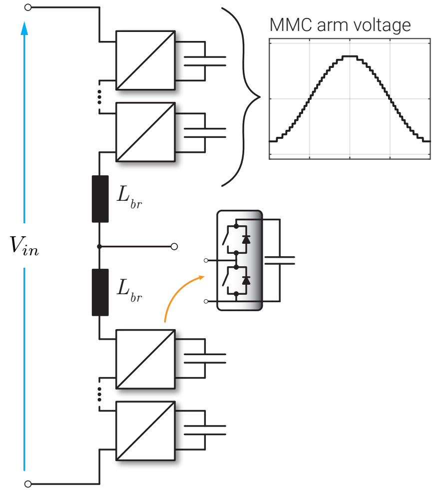

▲ Modular Multilevel Converter (MMC)

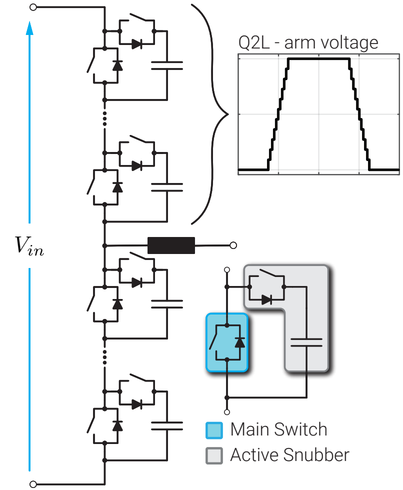

▲ Quasi Two-Level (Q2L) Converter

- Series connection of switches with snubbers
- Two-Level voltage waveforms

- Series connection of Submodules (SM)
- Arbitrary voltage waveform generation

- Series connection of MMC-alike SMs
- Quasi Two-Level (trapezoidal) voltage waveform

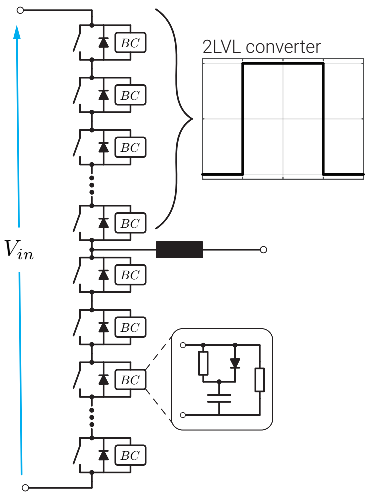

▲ Series connection of switches

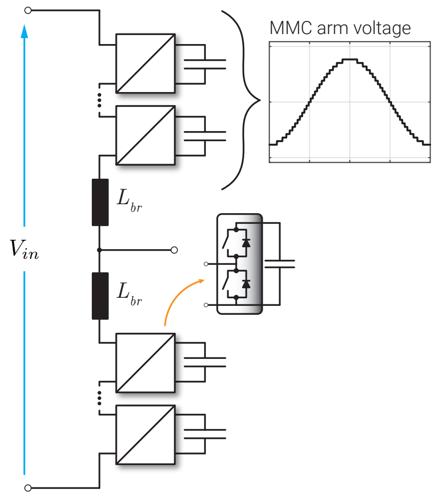

▲ Modular Multilevel Converter (MMC)

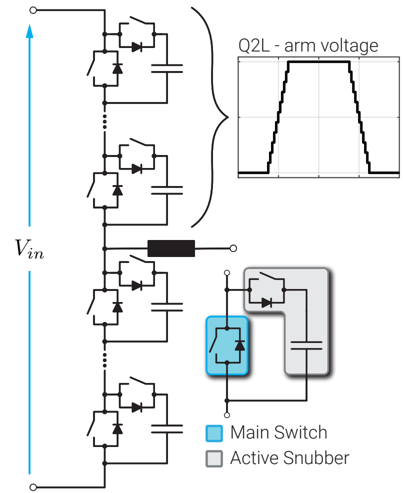

▲ Quasi Two-Level (Q2L) Converter

- Series connection of switches with snubbers
- Two-Level voltage waveforms

- Series connection of Submodules (SM)
- Arbitrary voltage waveform generation

- Series connection of MMC-alike SMs
- Quasi Two-Level (trapezoidal) voltage waveform

⇒ Despite the lack of high voltage semiconductors, we can manage medium/high voltage designs!

RESONANT CONVERSION

DC-DC Converters, Control Principles, Scalability for High Power Applications

General structure

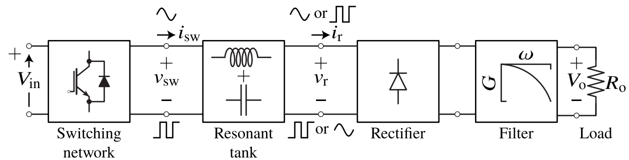

▲ General structure of the resonant converters

$$\hat{V}_{sw}^{(n)} = \begin{cases} \frac{4V_{in}}{\pi n}, & n \text{ is odd} \\ 0, & 0 \text{ is even} \end{cases}$$

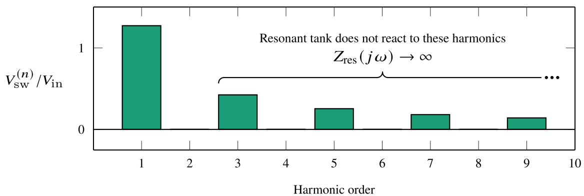

▲ Spectral content of voltage v_{sw} applied to the resonant tank

Resonant converters

- Series resonant
- Parallel resonant
- Series-Parallel resonant (LCC)
- Series-Parallel resonant (LLC)

Switching network

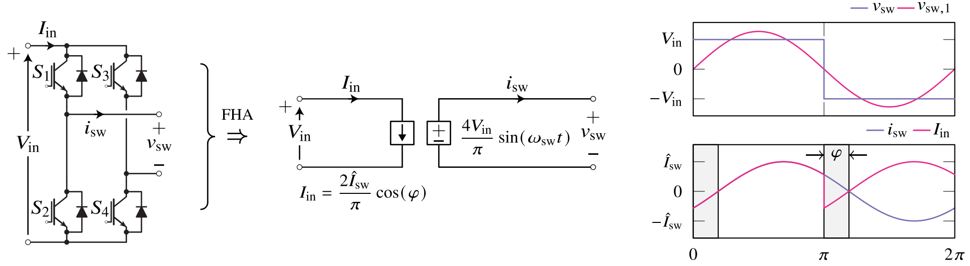

(a) (b) (c)

▲ (a) FB switching network; (b) FHA principle applied to the FB network; (c) Voltage and current waveforms typical for the switching network.

Switching network

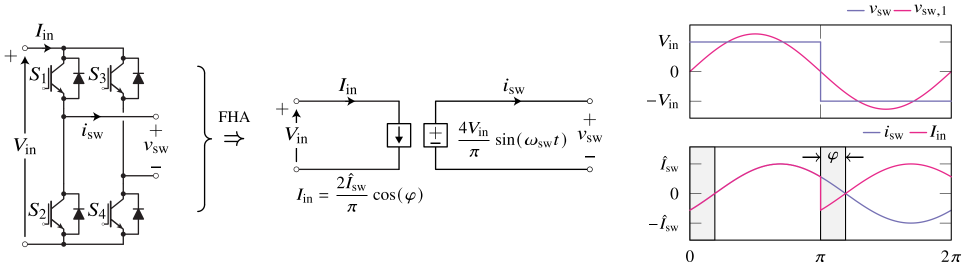

(a) (b) (c)

▲ (a) FB switching network; (b) FHA principle applied to the FB network; (c) Voltage and current waveforms typical for the switching network.

Rectifier and filter

▼ (a) DR with a capacitive filter; (b) DR with an *LC* filter.

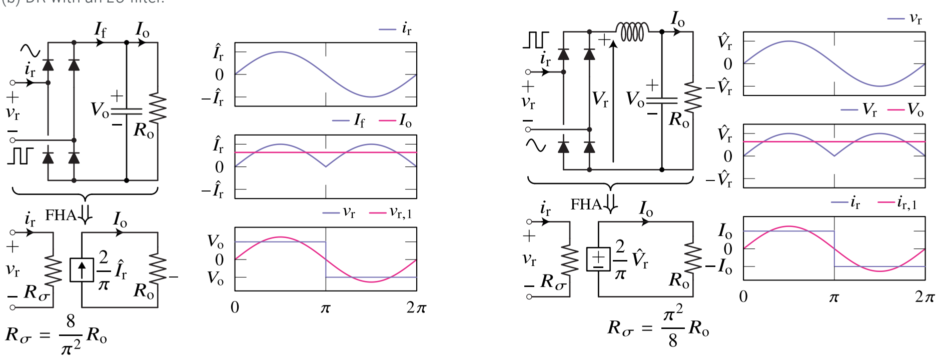

(a) (b)

Averaged Model

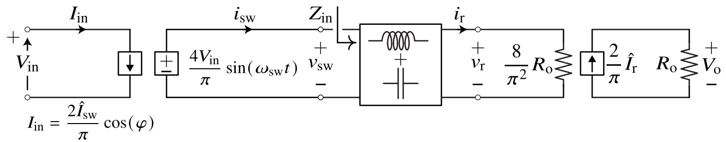

▲ Averaged representation of an arbitrary resonant converter in case rectification stage utilizes purely capacitive filter

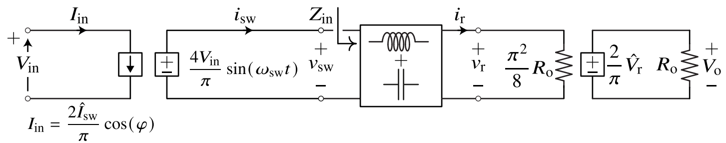

▲ Averaged representation of an arbitrary resonant converter in case rectification stage utilizes an *LC* filter.

Resonant Tank characteristics

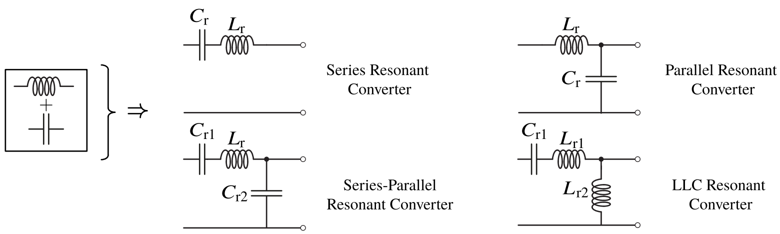

▲ (left) DR with a capacitive filter; (right) DR with an *LC* filter.

Series Resonant Converter

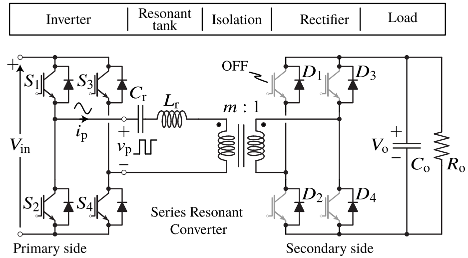

- ▲ Series resonant converter
- ▼ Typical waveforms of an SRC operating at various switching frequencies.

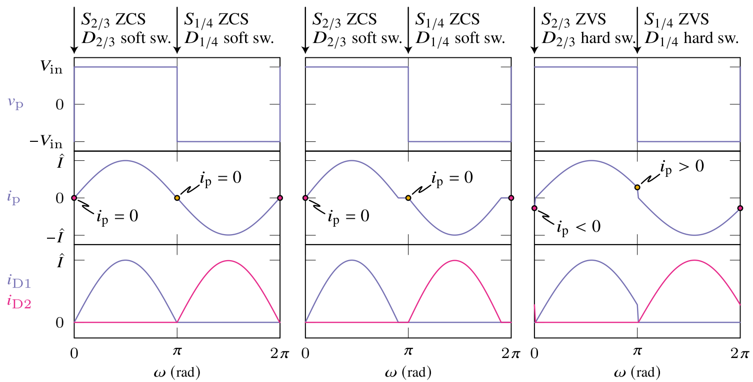

Series Resonant Converter

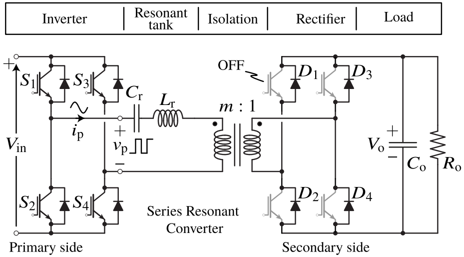

(a)

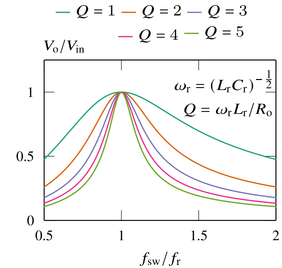

(b)

▲ SRC: (a) Topology; (b) Transfer characteristic derived assuming that $m = 1$;

Series Resonant Converter

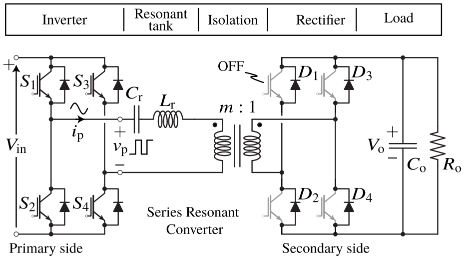

(a)

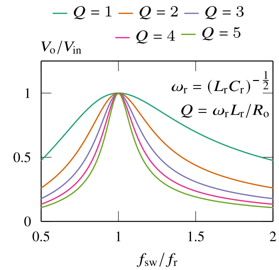

(b)

▲ SRC: (a) Topology; (b) Transfer characteristic derived assuming that $m = 1$;

Parallel Resonant Converter

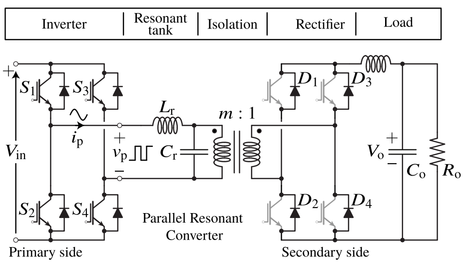

(a)

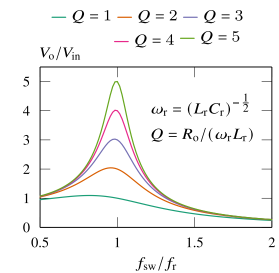

(b)

▲ SRC: (a) Topology; (b) Transfer characteristic derived assuming that $m = 1$;

LCC

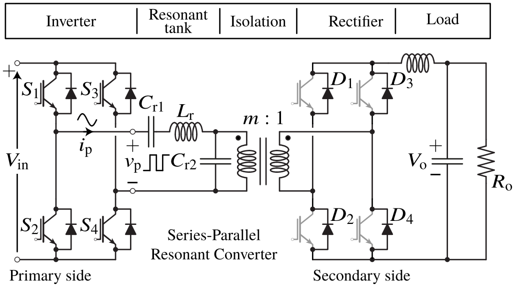

(a)

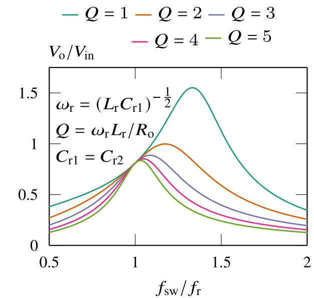

(b)

- ▲ LCC: (a) Topology; (b) Transfer characteristic derived assuming that $m = 1$;

- ▼ FHA equivalent of the *LCC* converter.

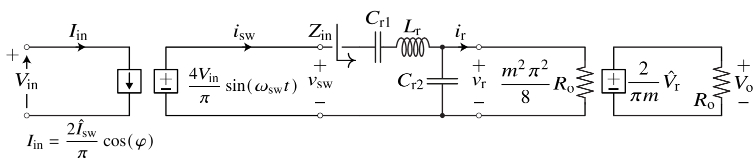

LCC

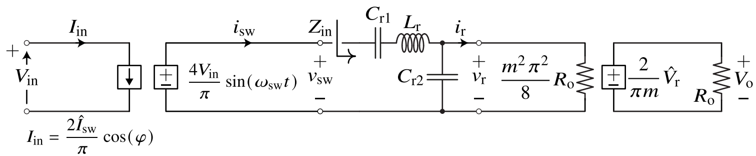

▲ FHA equivalent of the *LCC* converter.

▼ *LCC* converter transfer characteristics for two different ratios of resonant capacitors and different quality factors. Without loss of generality, MFT turns ratio was set as $m = 1$.

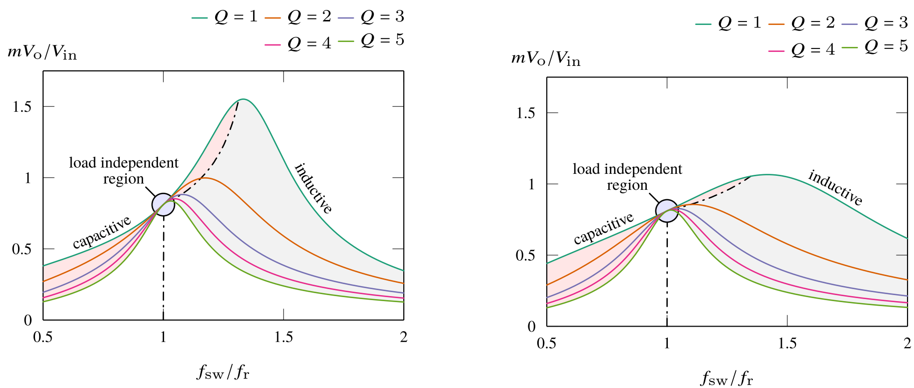

(a)

(b)

LLC

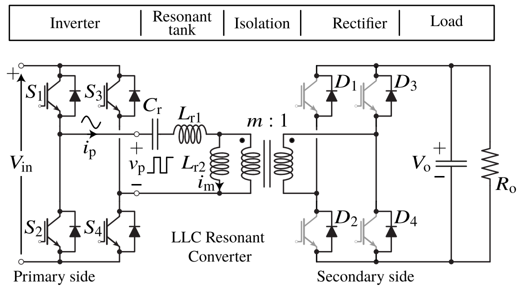

(a)

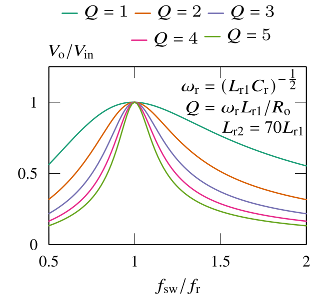

(b)

▲ LLC: (a) Topology; (b) Transfer characteristic derived assuming that $m = 1$;

▼ Typical waveforms of an LLC operating at various switching frequencies

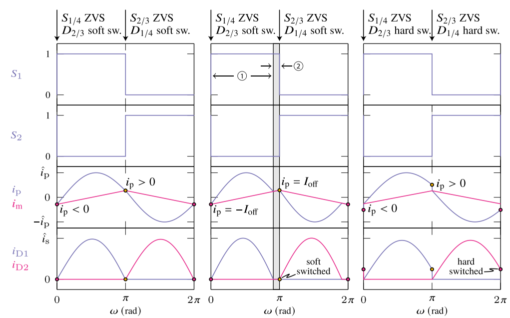

LLC

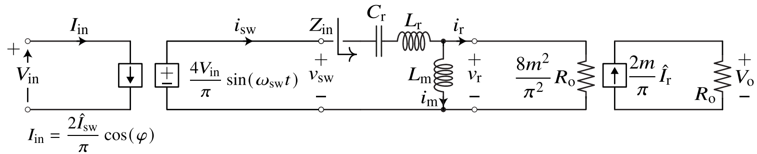

▲ FHA equivalent of the *LLC* converter.

▼ Transfer characteristics of an *LLC* converter for different values of quality factor Q and different ratios of resonant inductors L_r and L_m. Without loss of generality, MFT turns ratio was set as $m = 1$.

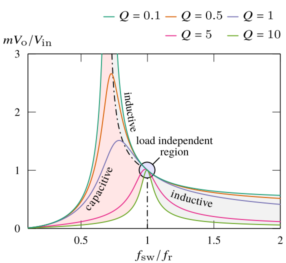

(a) $L_m/L_r = 1$

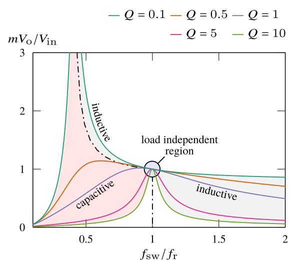

(b) $L_m/L_r = 5$

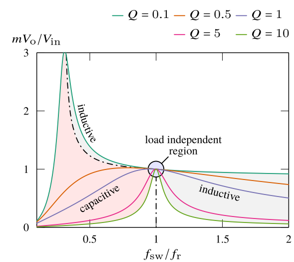

(c) $L_m/L_r = 10$

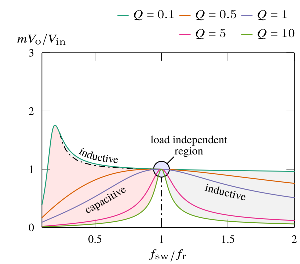

(d) $L_m/L_r = 15$

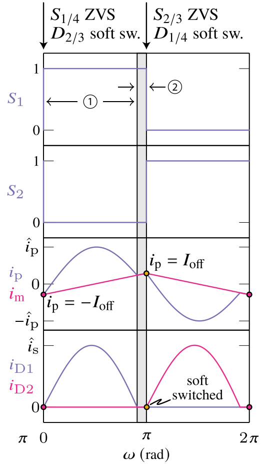

▲ Sub resonant operation

ZVS explained

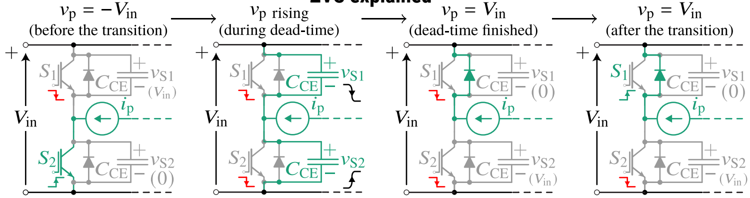

▲ One phase-leg of the switching network during the tank voltage transition

LLC CONVERTER - CONTROL PRINCIPLES (II)

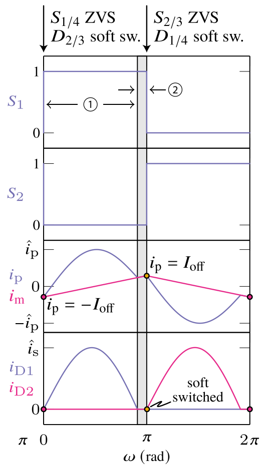

▲ Sub resonant operation

ZVS explained

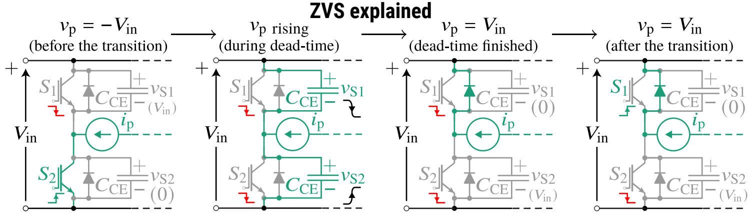

▲ One phase-leg of the switching network during the tank voltage transition

Limit of ZVS

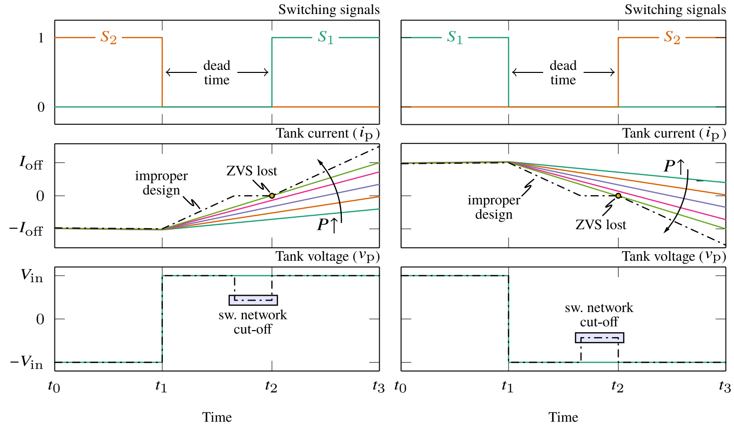

▲ Resonant tank current during dead-time

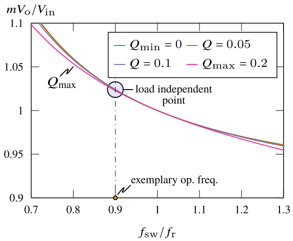

(a) $L_m/L_r = 10$

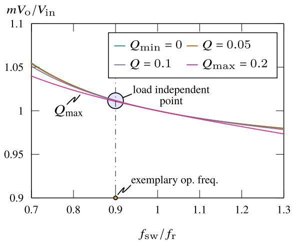

(b) $L_m/L_r = 20$

▲ Converter transfer characteristics zoomed around the resonant frequency for two different values of ratio Lm/Lr

[25] Jakub Kucka and Drazen Dujic. "Smooth Power Direction Transition of a Bidirectional LLC Resonant Converter for DC Transformer Applications." *IEEE Transactions on Power Electronics* 36.6 (2021), pp. 6265–6275

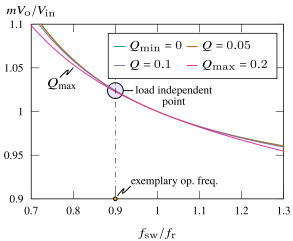

(a) $L_m/L_r = 10$

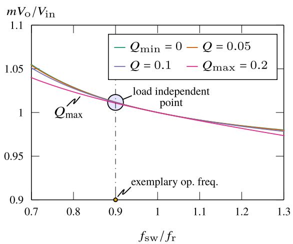

(b) $L_m/L_r = 20$

▲ Converter transfer characteristics zoomed around the resonant frequency for two different values of ratio Lm/Lr

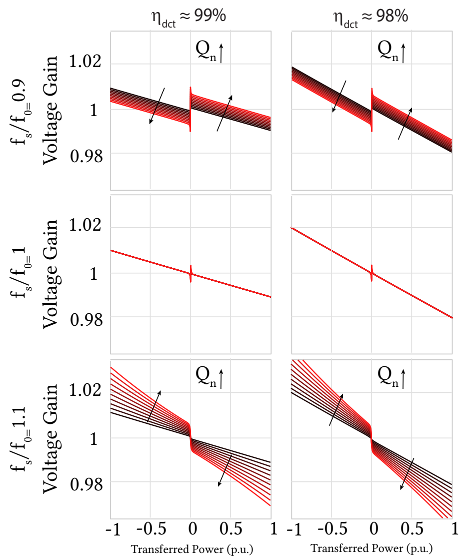

▲ Impact of the switching frequency on the voltage gain for different quality factors ($Q = [0.05, 0.5]$) [25]

[25] Jakub Kucka and Drazen Dujic. "Smooth Power Direction Transition of a Bidirectional LLC Resonant Converter for DC Transformer Applications." *IEEE Transactions on Power Electronics* 36.6 (2021), pp. 6265–6275

LLC CONVERTER - CONTROL PRINCIPLES (III)

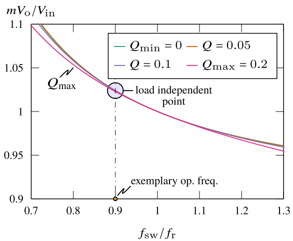

(a) $L_m/L_r = 10$

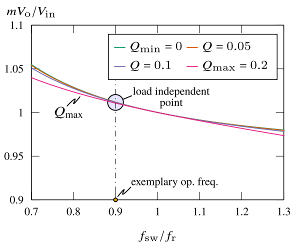

(b) $L_m/L_r = 20$

▲ Converter transfer characteristics zoomed around the resonant frequency for two different values of ratio Lm/Lr

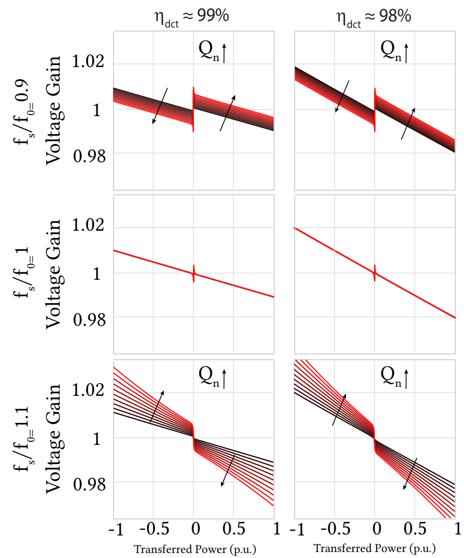

▲ Impact of the switching frequency on the voltage gain for different quality factors ($Q = [0.05, 0.5]$) [25]

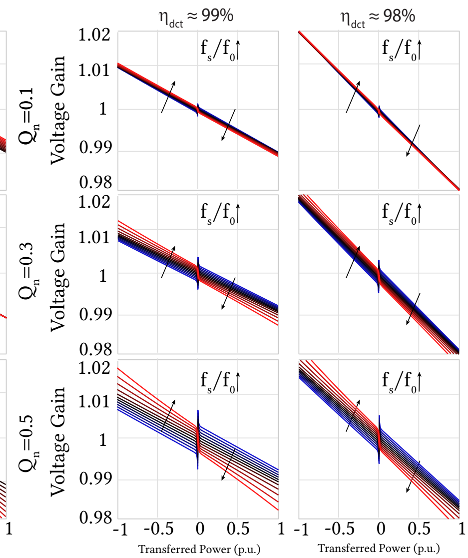

▲ Impact of the quality factor on the voltage gain for different switching frequency ($f_s/f_0 = [0.95, 1.05]$)

[25] Jakub Kucka and Drazen Dujic. "Smooth Power Direction Transition of a Bidirectional LLC Resonant Converter for DC Transformer Applications." *IEEE Transactions on Power Electronics* 36.6 (2021), pp. 6265–6275

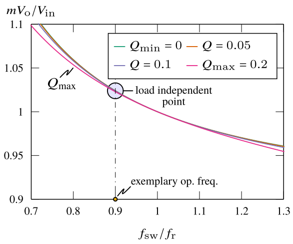

(a) $L_m/L_r = 10$

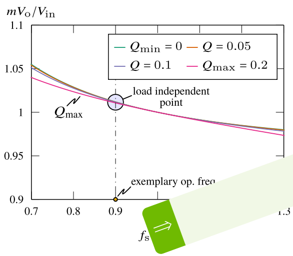

(b) $L_m/L_r = 20$

▲ Converter transfer characteristics zoomed around the resonant frequency for two different values of ratio Lm/Lr

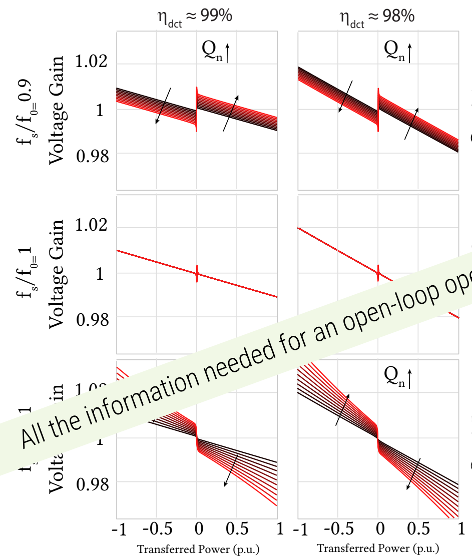

▲ Impact of the switching frequency on the voltage gain for different quality factors ($Q = [0.05, 0.5]$) [25]

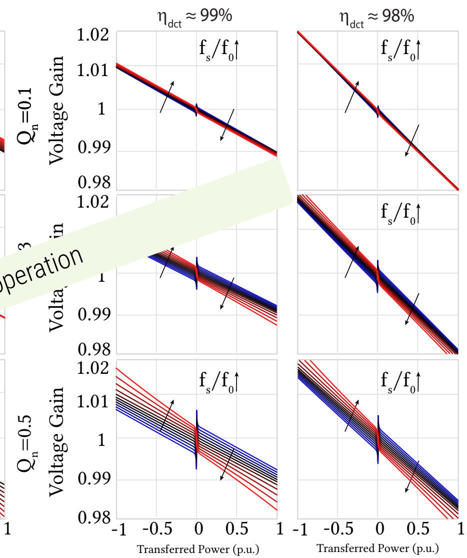

▲ Impact of the quality factor on the voltage gain for different switching frequency ($f_s/f_0 = [0.95, 1.05]$)

⇒ All the information needed for an open-loop operation

[25] Jakub Kucka and Drazen Dujic. "Smooth Power Direction Transition of a Bidirectional LLC Resonant Converter for DC Transformer Applications." *IEEE Transactions on Power Electronics* 36.6 (2021), pp. 6265–6275

HV POWER SEMICONDUCTORS

An abundance of options

POWER SEMICONDUCTORS

Semiconductor devices such as:

- Diodes
- BJTs
- Thyristors
- Triacs
- MOSFETs
- IGBTs
- etc...

Available in:

- Various voltage/current ratings
- Various packages

▲ Power electronics devices exist in a variety of packages and voltage ratings

DEVICES FOR MV APPLICATIONS: FEW MAIN CONTENDERS

Two most used options:

- IGBT
- IGCT
- Thyristors and GTOs are clearly still used

Both devices are:

- Fully controllable
- MV rated

Emerging alternatives:

- HV SiC MOSFETs
- HV SiC IGBTs

Both are slowly emerging, but not mature

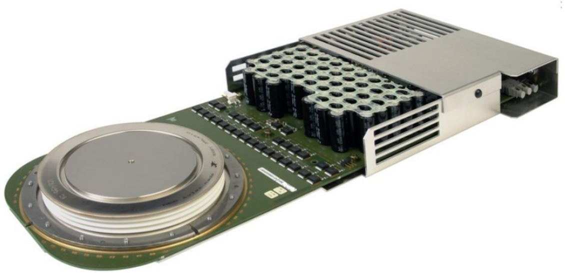

▲ 6.5 kV IGBT module and IGCT

IGBT: CHARACTERISTICS

IGBTs' main characteristics:

- Insulated gate
- Fully controllable
- Voltage controlled
- High power/voltage ratings
- High switching speed
- Simple integration
- Available as module and press-pack

Additional benefits:

- Limitation and turn-off of short circuit current
- Low voltage drop in *ON* state

Device	Voltage Class [kV]	Current Rating [A]	V_{ON} @1kA[V]	V_{ON} @2kA[V]
IGBT/diode	4.5	1600	2.30	3.40
IGBT/diode	4.5	2000	2.55	3.65
IGBT	4.5	2100	1.90	2.70
GTO	4.5	2000	2.20	2.70
Thyristor	4.5	1150	1.35	1.65
IGCT/diode	4.5	2200	2.00	2.50
IGCT	4.5	4000	1.50	1.80

▲ Typical conduction performance of common semiconductor devices

Typical ratings for MV IGBTs:

- 4.5 kV-6.5 kV
- 900 A-1200 A

Commonly available in:

- Modules
- Press-Pack
- StakPak

Switching performance:

- Can be externally affected by Gate Drive Unit
- Offers controllable di/dt with adequate gate resistance values
- Does not require external circuitry for safe operation

▲ IGBT packaging includes modules, press-pack, and StakPak units

IGCTs' main characteristics:

- Thyristor based device
- Lowest conduction loss of fully controllable devices
- Integrated in GDU
- Only available as press-pack
- Snubberless turn-off

Traditional IGCT application:

- Low frequency (<1 kHz)
- Hard switched

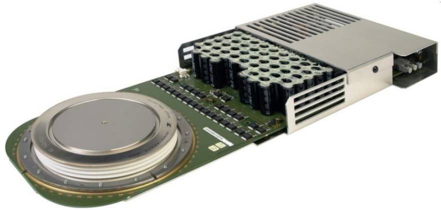

▲ The press-packed GCT is always integrated into the gate driver board to minimise inductance between gate and cathode

IGCT: COMMON TYPES

The main types of IGCTs:

- Asymmetric
- Reverse conducting - RC-IGCT
- Reverse blocking - RB-IGCT

Ratings of the device can be:

- Up to 6.5 kV (engineering samples up to 10 kV)
- Turn-off current higher for asymmetric devices, due to higher thyristor finger surface (up to 6 kA)
- Hard switched

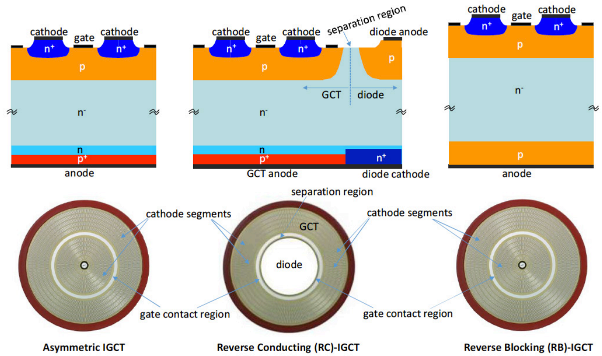

▲ State-of-the-art IGCT device types and their schematic cross sections from top side to bottom side (vertical cross section) [26].

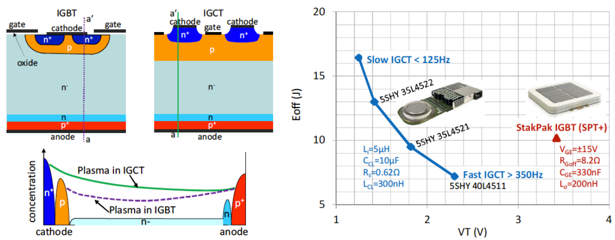

▲ IGCT vs. IGBT. Left: schematic structures of IGCT and IGBT and their plasma distribution during conduction. Right: technology curve comparison between 4.5kV Asymmetric IGCT and StakPak IGBT module at 2.8kV, 2kA, 125°C [26].

IGCT: LIMITATIONS

Compared to the IGBT the IGCT:

- Cannot control turn-on di/dt through GDU
- Requires clamp circuitry
- Cannot turn *OFF* short circuit current
- Has significant GDU power consumption
- Requires bulky GDU capacitors to maintain constant gate-cathode voltage at turn-off

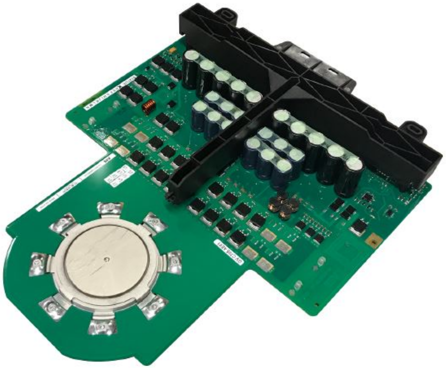

▲ The IGCT GDU allocated a large portion of its surface to capacitors an turn-off MOSFETs

IGCT: CLAMP CIRCUIT

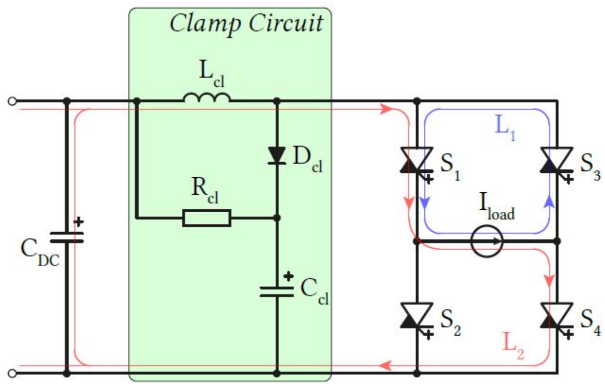

▲ Typical the clamp circuit

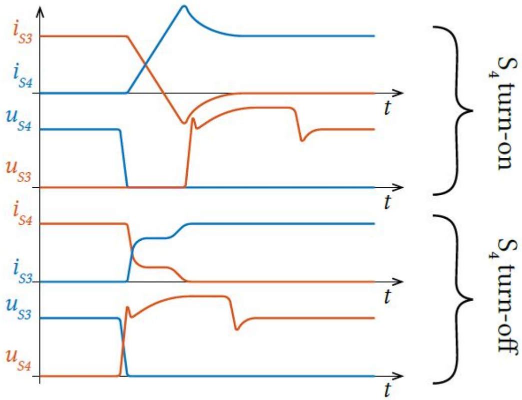

▲ Current and voltage waveforms for the S_3 and S_4 during turn-on and turn-off transients

- IGCT turn-on not fully controlled by GCU action
- Hard IGCT turn-on forces reverse recovery of complementary device antiparallel diode
- Clamp inductor required to limit antiparallel diode reverse recovery di/dt
- RCD snubber limits the overvoltage
- Part of the energy is recovered back to main DC link

IGCT IN RESONANT LLC CONVERTER: HIGH FREQUENCY OPERATION

IGCT frequency limited by:

- Losses and junction temperature
- Gate driver ON/OFF channel capability

Resonant operation implies:

- Lossless turn-on (ZVS or ZCS)
- Low turn-off loss (low turn-off current)
- Limited di/dt

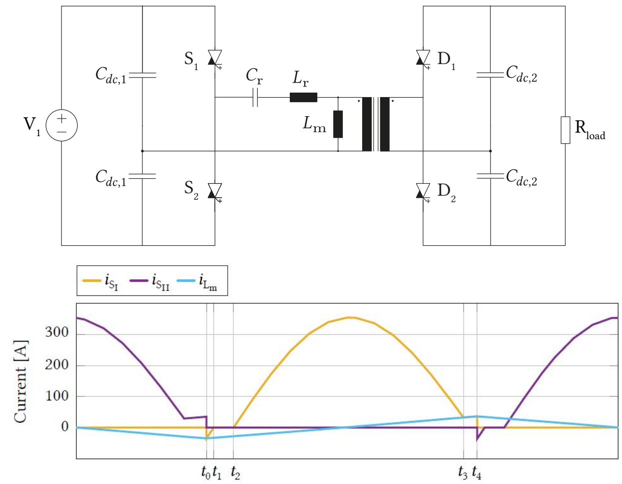

▲ Half-bridge based LLC topology and corresponding current waveforms [27]

[27] Dragan Stamenkovic et al. "Soft Switching Behavior of IGCT for Resonant Conversion." *2019 IEEE Applied Power Electronics Conference and Exposition (APEC)*. 2019, pp. 2714–2719

IGCT IN RESONANT LLC CONVERTER: HIGH FREQUENCY OPERATION

IGCT frequency limited by:

- Losses and junction temperature
- Gate driver ON/OFF channel capability

Resonant operation implies:

- Lossless turn-on (ZVS or ZCS)
- Low turn-off loss (low turn-off current)
- Limited di/dt

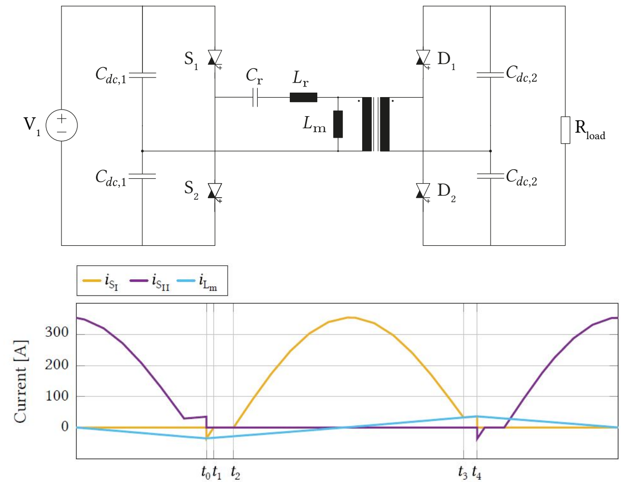

▲ Half-bridge based LLC topology and corresponding current waveforms [27]

⇒ LLC topology can greatly exploit IGCT for high-power designs! High frequency operation must be explored!

[27] Dragan Stamenkovic et al. "Soft Switching Behavior of IGCT for Resonant Conversion." *2019 IEEE Applied Power Electronics Conference and Exposition (APEC)*. 2019, pp. 2714–2719

Hard switched IGCT operation required clamp circuit:

- IGCT turn-on causes reverse recovery of complementary antiparallel diode
- Rate of increase of reverse recovery current must be limited by external means

Soft turn-on removes need for clamp:

- IGCT turn-on occurs while antiparallel diode of the same device is conducting
- Turn-on occurs in ZVS condition
- Current naturally reaches zero in the diode

Removal of clamp circuit is possible for IGCT in LLC topology:

- Significant space saving
- Significant reduction of component count

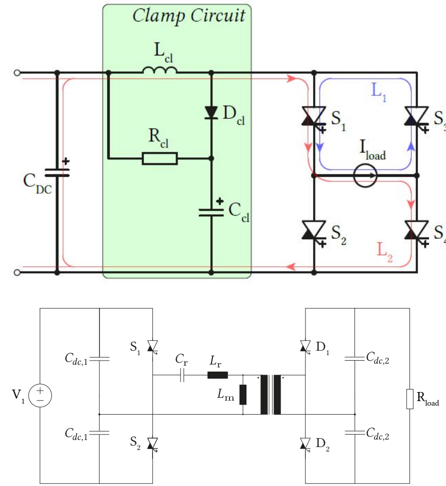

▲ Hard-switched and soft-switched operation differ also by necessity of clamp circuitry [28]

[28] Dragan Stamenković et al. "IGCT Low-Current Switching—TCAD and Experimental Characterization." *IEEE Transactions on Industrial Electronics* 67.8 (2020), pp. 6302–6311

IGCT IN LLC: SERIES CONNECTION IN HARD SWITCHED APPLICATIONS

IGCTs in series connection:

- Dynamic voltage balancing provided by RC or RCD snubbers
- Static voltage balancing provided by passive balancing resistors

Series connection in hard switching:

- Turn-off currents in the kA range
- Snubber capacitance values up to 1 μF

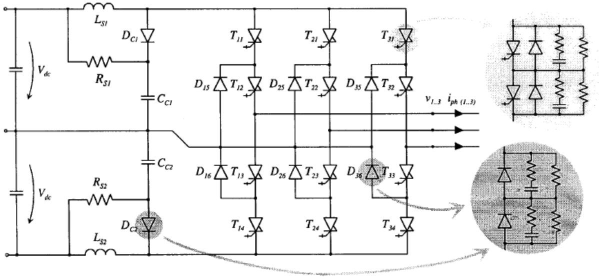

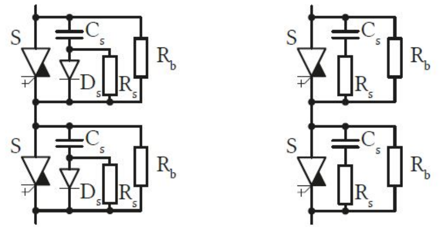

▲ Hard-switched and soft-switched operation differ also by necessity of clamp circuitry

⇒ Large snubber values are needed for hard switched low frequency applications!

Challenges in soft switched series connection:

- Low turn-off current increases transitions times
- Large dynamic voltage balancing capacitors unsuitable

For successful series connection in soft switching:

- Ultra-low values of snubber capacitance (<100 nF)
- Purely capacitive snubbers [29]

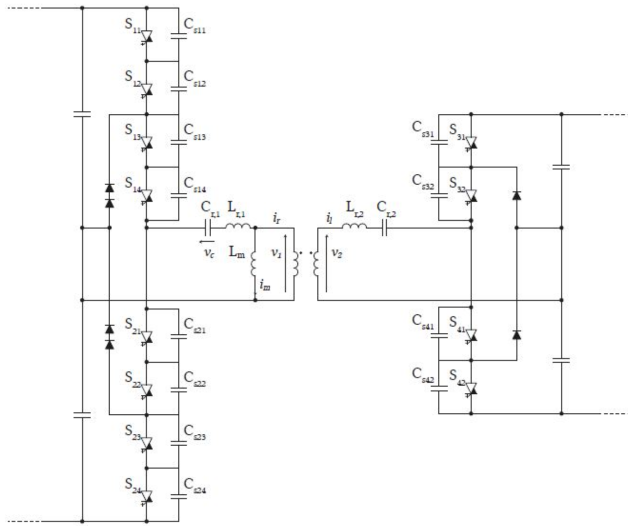

▲ IGCT soft-switching in series connection can employ purely capacitive dynamic voltage sharing snubbers

[29] Gabriele Ulissi et al. "High-Frequency Operation of Series-Connected IGCTs for Resonant Converters." *IEEE Transactions on Power Electronics* 37.5 (2022), pp. 5664–5674

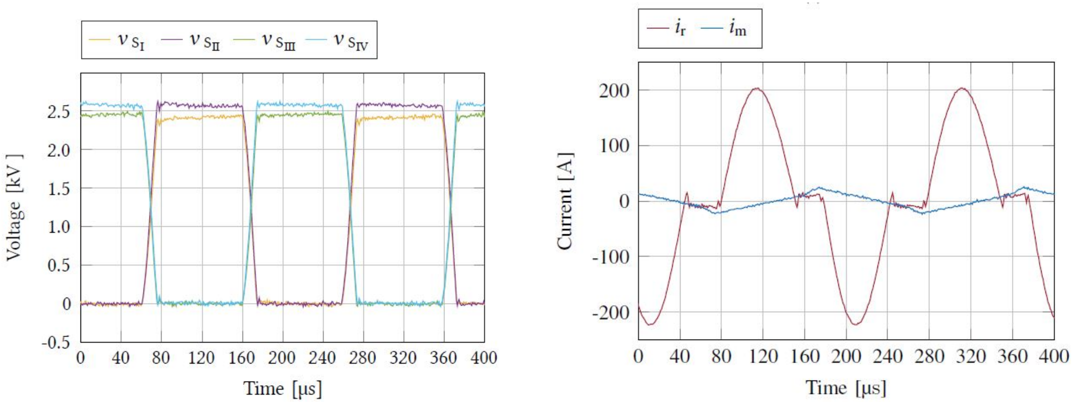

▲ During high-frequency series connected operation the duration of switching transitions is not negligible with respect to the switching period [29]

The duration of switching transitions is significant during high frequency series connected operation due to:

- Presence of snubbers increasing the turn-off an turn-on duration
- Short duration of switching period

Additional factors influencing the switching transition duration are:

- Junction temperature
- Level of current pre-flooding as a result of load level

IGCT GATE UNITS FOR SOFT SWITCHING APPLICATIONS

Design, Soft-switching, and Experience

Gate Commuted Thyristor (GCT)

- Thyristor based technology
- Controlled by current
- Hard driving turn off

Necessary functions of the gate unit: [30]

- Turn ON
- Turn OFF
- Backporch operation
- Negative-voltage backporch operation
- Retrigger

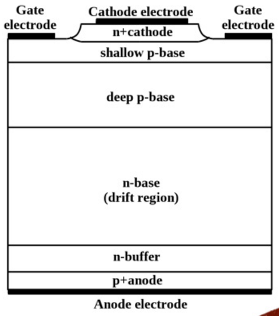

Wikipedia: Integrated gate-commutated thyristor
https://en.wikipedia.org/wiki/Integrated_gate-commutated_thyristor

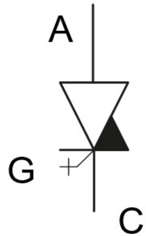

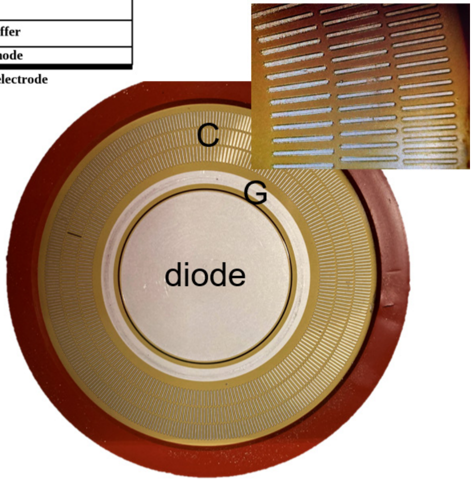

▲ Reverse conducting IGCT structure and symbol

REQUIREMENTS (II)

Turn ON

- Similarly to thyristor the turn on requires steep current into the gate
- The value has to be high enough to turn on all gate cells at once
- Gate current peak is approximately 100 to 300 A
- The device opens practically immediately
- The di/dt is limited only by the external circuit

▲ Simplified illustration of a current pulse applied to the gate

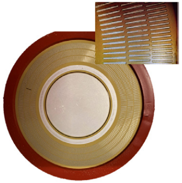

▲ Reverse conducting IGCT structure

Hence:

- The gate unit cannot impact GCT turn-on behavior
- The only task of the high turn-on pulse is to avoid hot-spots
- It ensures fast and equal activation of all GCT fingers

REQUIREMENTS (II)

Turn ON

- Similarly to thyristor the turn on requires steep current into the gate
- The value has to be high enough to turn on all gate cells at once
- Gate current peak is approximately 100 to 300 A
- The device opens practically immediately
- The di/dt is limited only by the external circuit

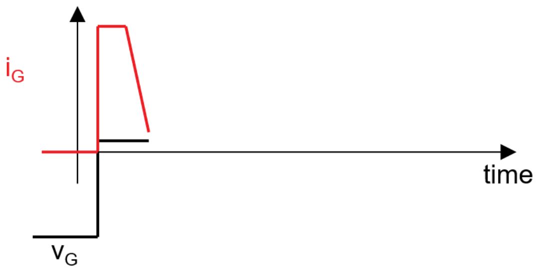

▲ Simplified illustration of a current pulse applied to the gate

Hence:

- The gate unit cannot impact GCT turn-on behavior
- The only task of the high turn-on pulse is to avoid hot-spots
- It ensures fast and equal activation of all GCT fingers

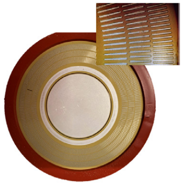

▲ Reverse conducting IGCT structure

Backporch Operation:

- A certain value of gate current is necessary to keep the IGCT on (if the anode current would drop below the latching current value)
- This current is typically regulated in relation to temperature conditions

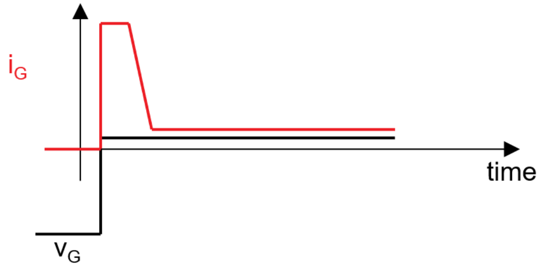

▲ Illustration of backporch current during IGCT conduction

Turn OFF

- Hard-driving the IGCT by clamping the gate voltage to -20 V [31]
- The initial recombination has to happen within a very short time
  → high di/dt of gate current is required
  → low inductance connection of -20 V to gate

- The turn-off dv/dt and di/dt of the switch cannot be impacted by the gate unit
- The lower inductance simply increases the feasible turn-off current

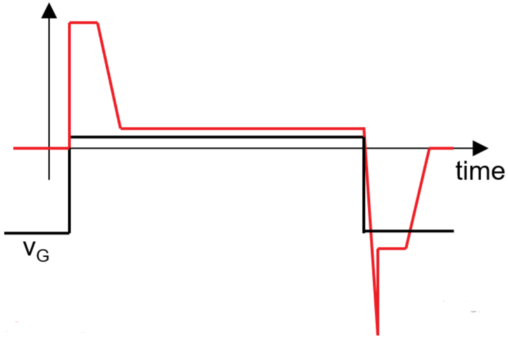

▲ The IGCT turn OFF event - conducted current is commutated to the gate circuitry

- The current plateau equals the anode current
- High power consumption!

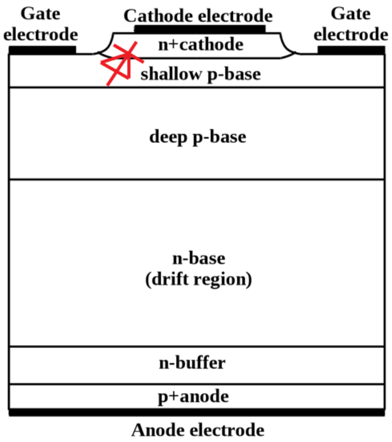

▲ GCT structure

Negative Gate Voltage Backporch operation

- When the antiparallel diode is conducting, a negative voltage drop over GCT is generated
- The PN junction near anode avalanche breaks and the gate-to cathode voltage becomes negative [32], [33], [34]
- The gate unit typically continues supplying backporch current

▲ Gate unit during negative gate voltage

Retrigger Pulse

- Once the anode PN junction closes, a gate current pulse is generated to ensure that all thyristor cells are ready to conduct again
- Problem is eventual high di/dt of the load current
- Retrigger current pulse ensures uniform current take over of the GCT fingers

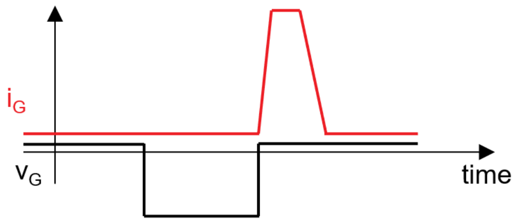

▲ Retrigger pulse applied to the GCT

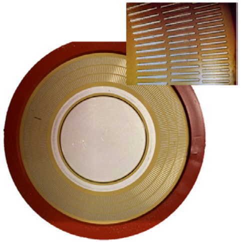

▲ Reverse conducting IGCT structure

Turn OFF Channel

- The solution for the turn off is practically always the same
- A high number of parallel connected MOSFETs connects a high number of capacitors charged to approx. – 20 V to the gate
- High current loading for a very short time
- Parallelization should assure low inductance design
- Covers a large area on a typical gate unit

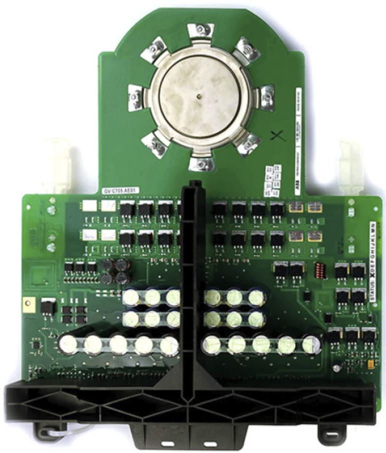

▲ Commercial IGCT - parallel MOSFETs and Capacitors are easily noticable

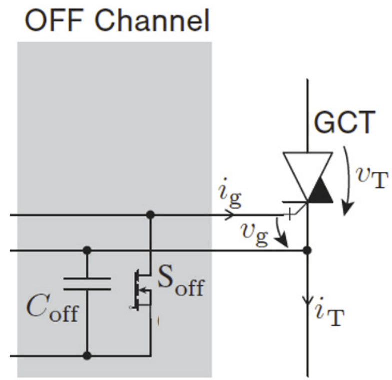

▲ Example of the gate OFF circuit implementation

Turn On & Retrigger Channel

- Typically a single channel for both functions
- High-current inductor with low inductance for current build up
- High current MOSFETs with low switching frequency & a freewheeling diode

Backporch Channel

- A typical solution is a buck converter closed-loop controlling the current at high switching frequency
- The required current is only several Amperes

Negative-Voltage Backporch Channel

- The standard solution is to reduce the backporch current and consume the energy in non-saturated transistors (and resistors) [32], [33]
- Reference [34] provides another solution where the backporch channel utilizes floating power supply

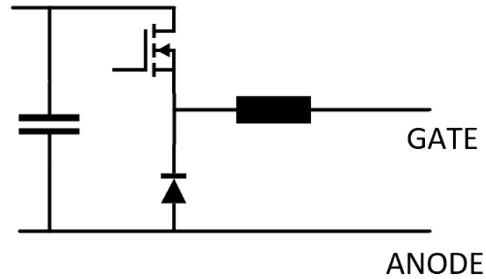

▲ Simplified Gate unit turn ON circuitry

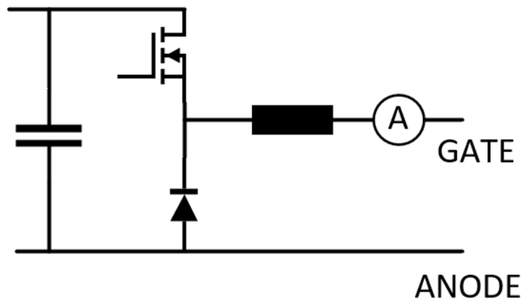

▲ Simplified Gate unit Backporch circuitry

IGCT operating conditions

- Switching at high frequency
- Zero-Voltage turn ON
- Low-Current turn Off
- di/dt during switching is limited by resonant tank

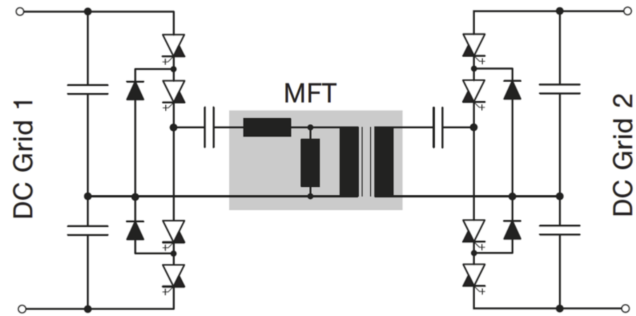

▲ IGCT based DC Transfomer

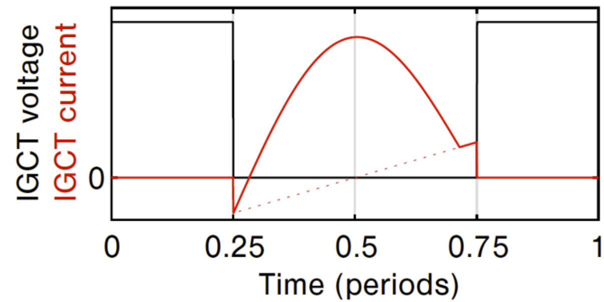

▲ Typical waveforms experienced by IGCT during operation

IGCT operating conditions

- Switching at high frequency
- Zero-Voltage turn ON
- Low-Current turn Off
- di/dt during switching is limited by resonant tank

Gate Unit design

- Low turn-off current
- Lower consumption
- Lower requirements on the turn OFF channel
- Zero-Voltage Turn ON and limited di/dt during retrigger
- The magnitude of turn-on gate current pulse can be reduced

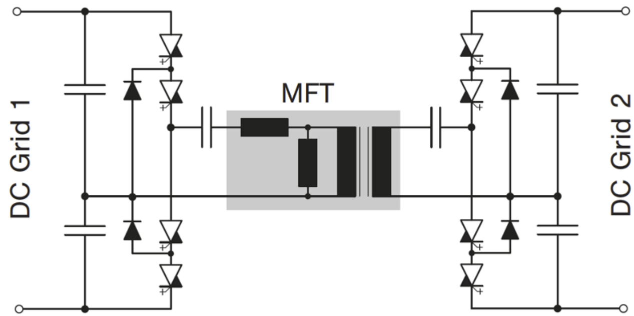

▲ IGCT based DC Transfomer

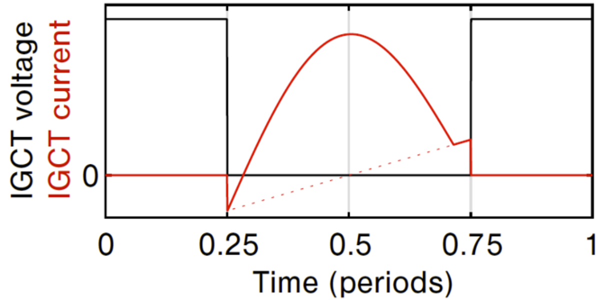

▲ Typical waveforms experienced by IGCT during operation

SOFTGATE IGCT Gate Unit

- Gate unit tailored for soft switching

Integration of multiple functions into a single ON channel:

- Turn-ON function
- Retrigger function
- Backporch function
- Negative-Voltage Backporch functions

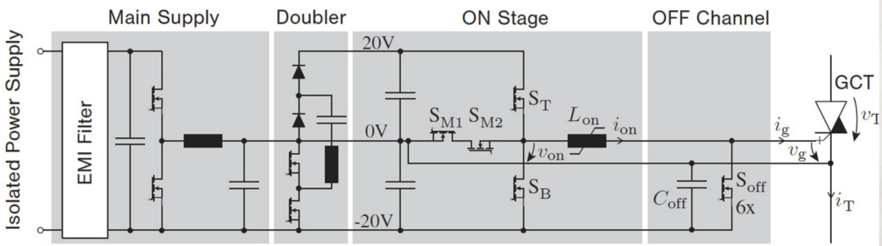

▲ Simplifed SOFTGATE circuitry

▲ Realized SOFTGATE gate unit [35]

[35] Jakub Kucka and Drazen Dujic. "SOFTGATE – An IGCT Gate Unit for Soft Switching." *PCIM Europe 2022; International Exhibition and Conference for Power Electronics, Intelligent Motion, Renewable Energy and Energy Management.* 2022, pp. 1–9

OFF Channel

- Optimized for frequent low-current switching
- Utilizing compact polymer tantalum capacitors and low profile MOSFETs
- Tested up to 1.5 kA emergency turn off

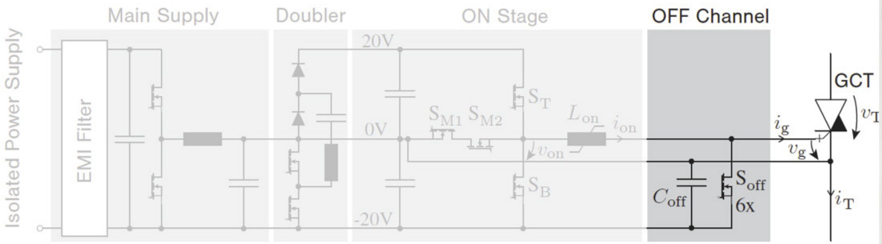

▲ SOFTGATE OFF channel

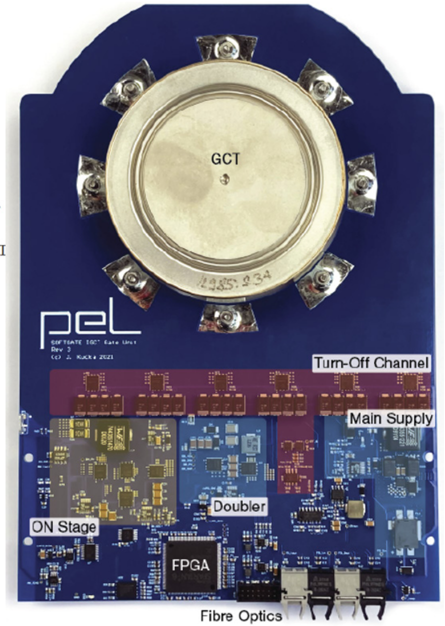

▲ Realized SOFTGATE gate unit

ON Channel

- T-Type NPC topology with nonlinear inductor
- Capable of controlling the gate current by three voltage levels
- Nonlinear inductor enables fast current build-up for turn on and retrigger current pulses

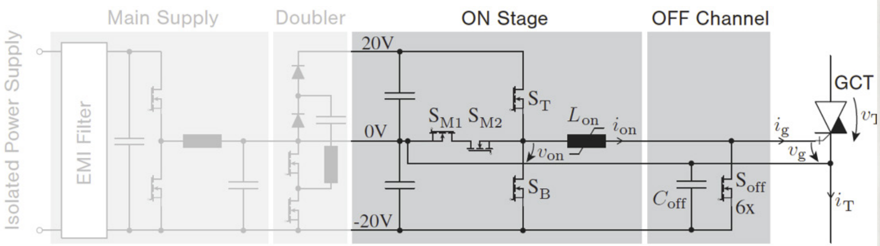

▲ SOFTGATE ON channel

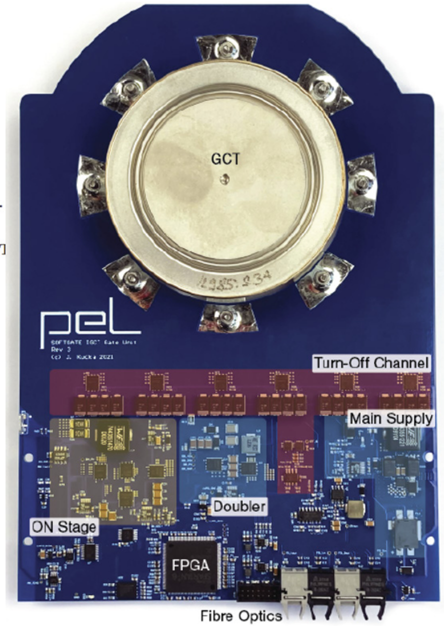

▲ Realized SOFTGATE gate unit

GATE UNIT DESIGN (IV)

ON Channel

- T-Type NPC topology with nonlinear inductor
- Capable of controlling the gate current by three voltage levels
- Nonlinear inductor enables fast current build-up for turn on and retrigger current pulses

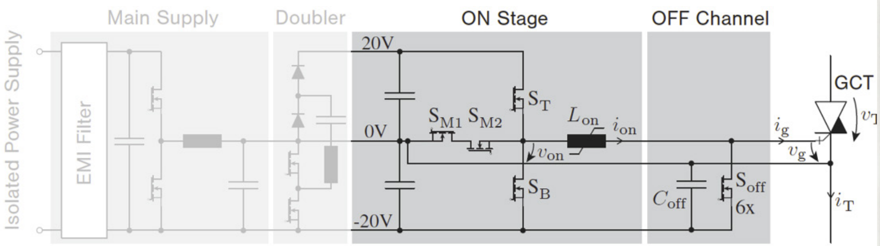

▲ SOFTGATE ON channel

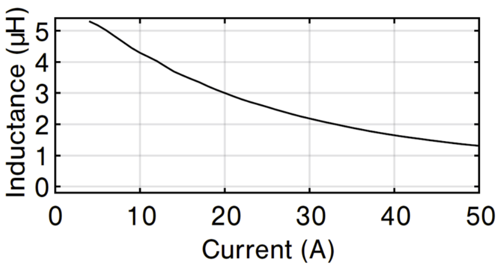

▲ Characteristic of inductor used for the ON channel

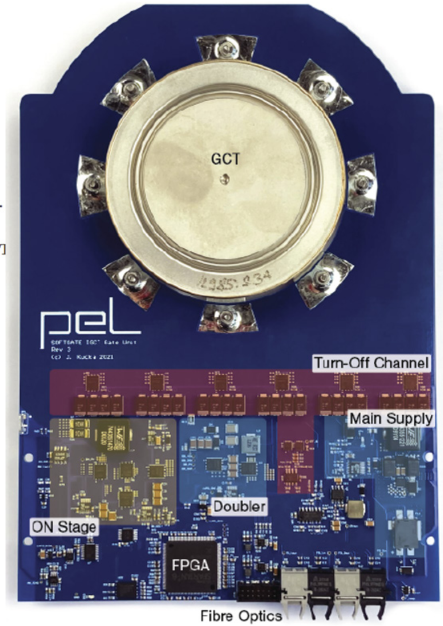

▲ Realized SOFTGATE gate unit

SIZE COMPARISON

⇒ The gate unit size can be greatly optimized and reduced for soft-switching applications!

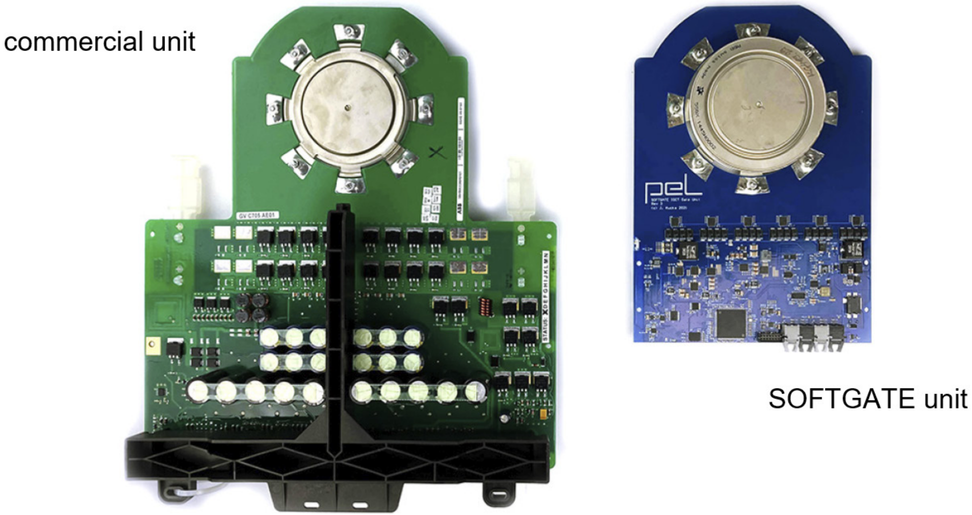

▲ Comparison between commercial and SOFTAGE gate unit [36]

[36] Jakub Kucka and Drazen Dujic. “IGCT Gate Unit for Zero-Voltage-Switching Resonant DC Transformer Applications.” *IEEE Transactions on Industrial Electronics* 69.12 (2022), pp. 13799–13807

1.44kHz Resonant Operation

- Full load operation
- 2.5 kV dc link
- 140 A turn off current
- 750 A peak current

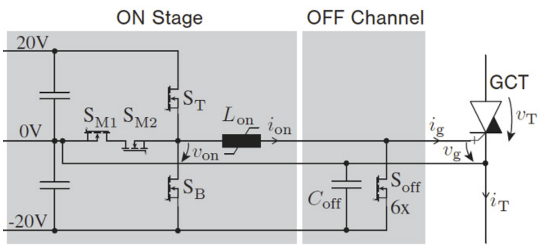

▲ Simplifed SOFTGATE circuitry

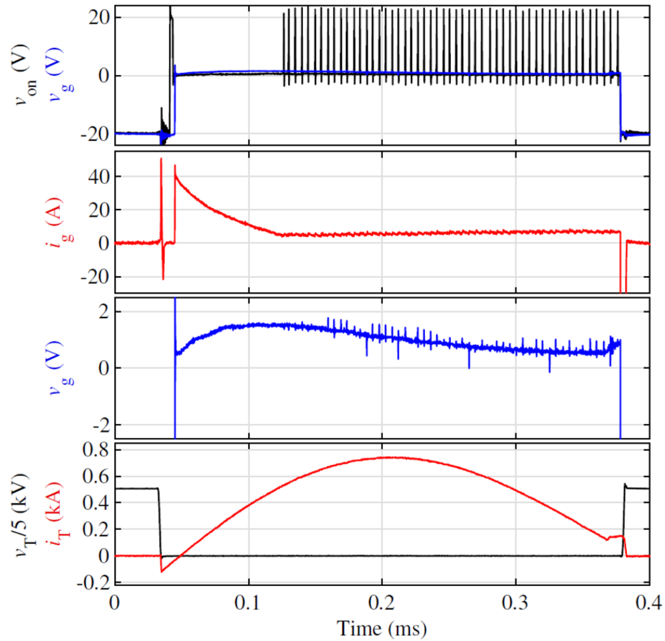

▲ SOFTGATE full load operation

EXPERIMENTAL RESULTS (II)

1.44kHz Resonant Operation

- No load operation
- 2.5 kV dc link
- 140 A turn off current

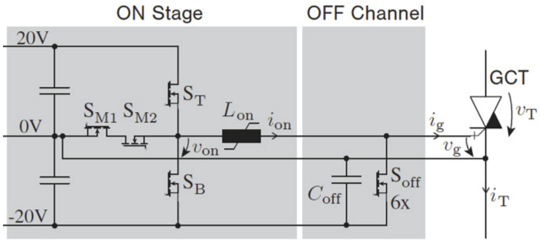

▲ Simplifed SOFTGATE circuitry

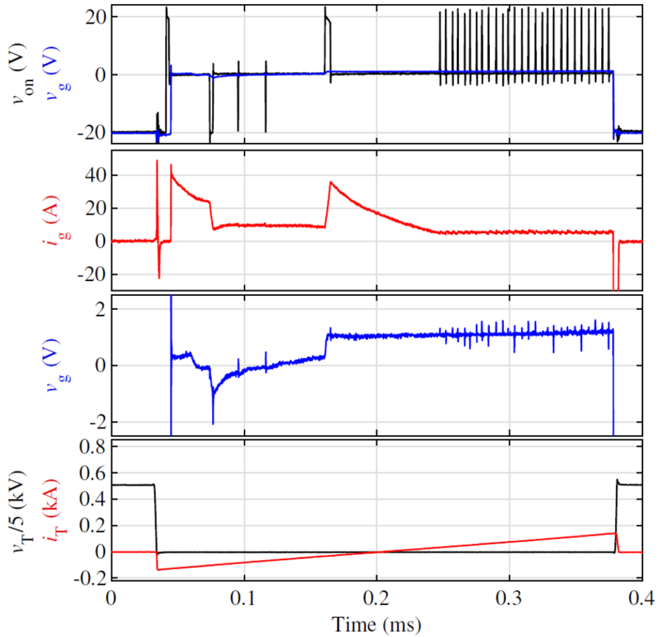

▲ SOFTGATE no load operation

Turn Off Detail

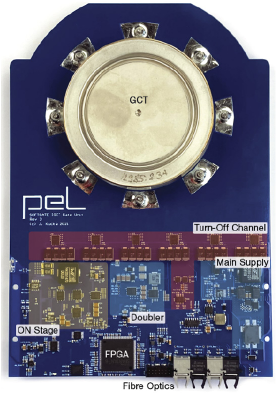

▲ SOFTGATE gate unit

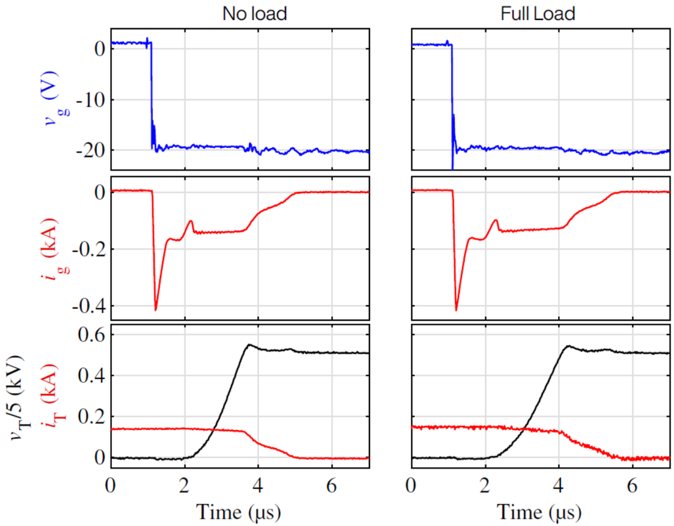

▲ SOFTGATE turn OFF behaviour

High-Current Emergency Turn Off

- 2 kV
- 1.5 kA
- Estimated gate unit turn off inductance: 1.2 nH

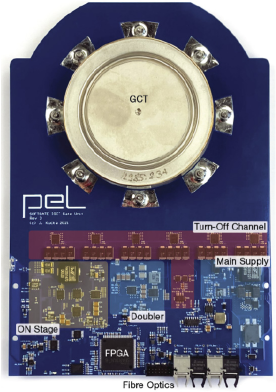

▲ SOFTGATE gate unit

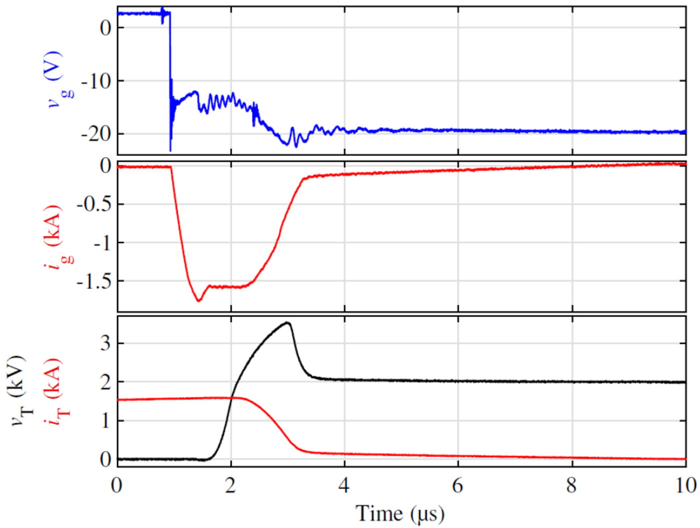

▲ SOFTGATE high current turn OFF

5kHz Resonant Operation

- 2.5 kV dc link
- 16 A turn off current
- 320 A peak current

ϟ Retrigger function had to be disabled!

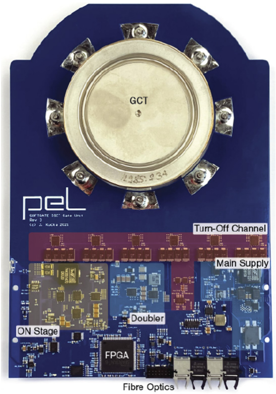

▲ SOFTGATE gate unit

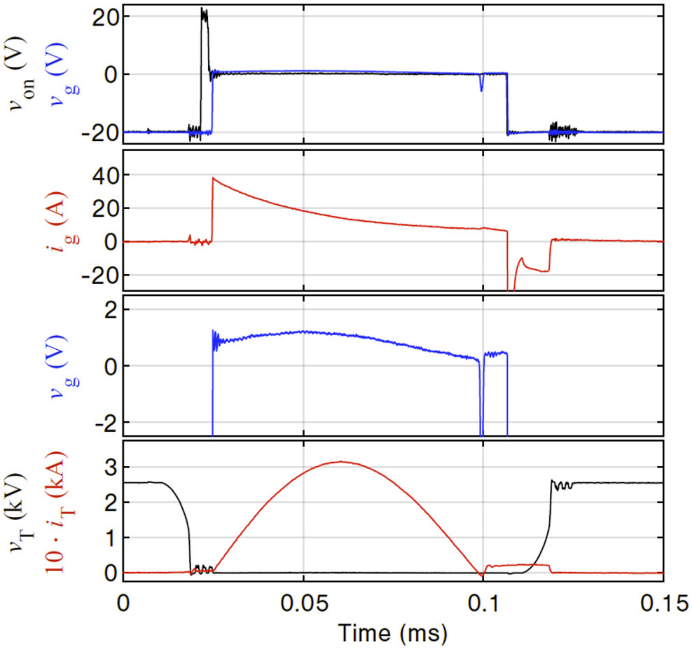

▲ SOFTGATE continuous operation

Consumption

- Only 40 W (compared to commercial 58 W)

Thermal run

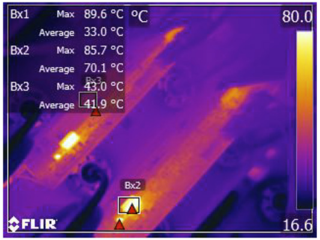

▲ Temperatures in steady state

Turn OFF details

- Long turn off due to low switching current
- Slow voltage build up

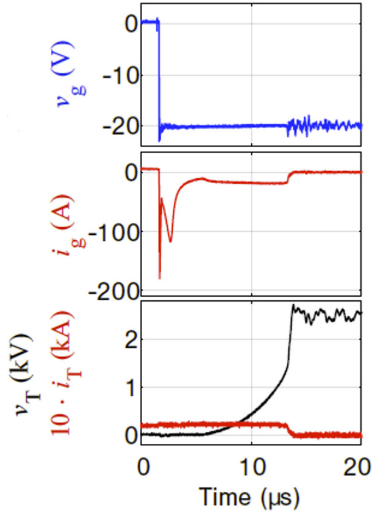

▲ Turn OFF event

Shoot-Through Protection

- Since the application does not require clamping circuit a shoot-through might be fatal
- Idea: measure anode-to-cathode voltage to ensure that the diode is conducting before the turn ON [37]

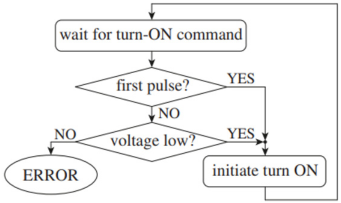

▲ Protection integrated into SOFTGATE

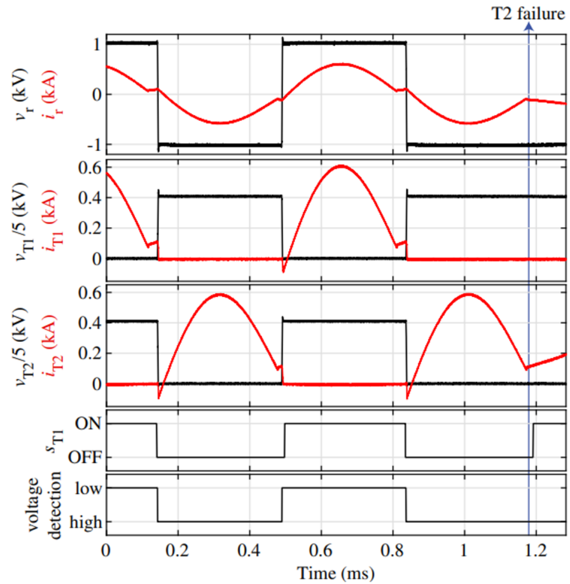

▲ Experimental results

[37] Jakub Kucka and Drazen Dujic. "Shoot-Through Protection for an IGCT-Based ZVS Resonant DC Transformer." *IEEE Transactions on Industrial Electronics* (2022), pp. 1–1

CONCLUSIONS

By tailoring the gate unit for soft-switching:

- The size can be minimized
- The consumption ca be reduced
- 5 kHz resonant operation is feasible with IGCTs...
- ...but a special attention should be paid to details
- IGCT is a preferable switch for a resonant medium-voltage dc transformer

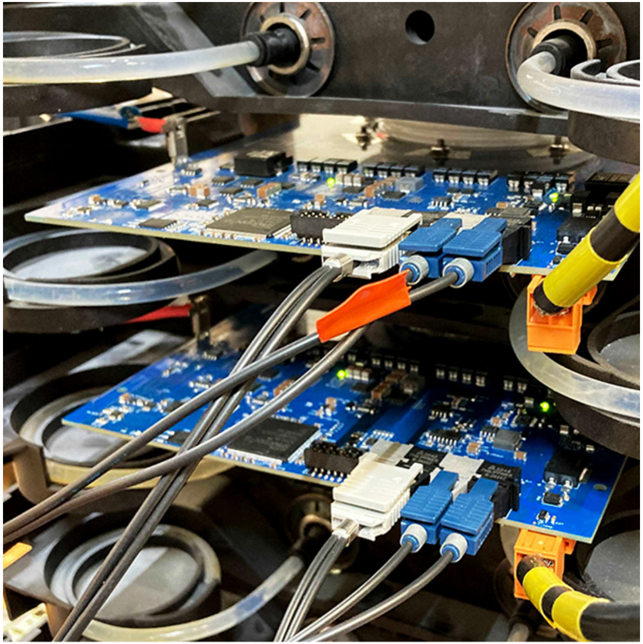

▲ SOFTGATE units inside the IGCT stack

COFFEE BREAK

Well deserved...

IGCT RESONANT SWITCHING

Increasing switching frequency through resonant topology

EXPERIMENTAL IGCT TEST SETUP (II)

Medium Voltage DCT

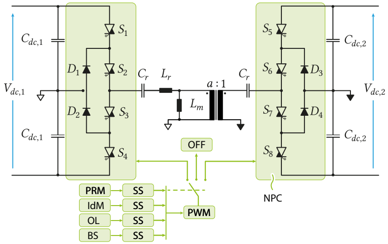

PEL IGCT multifunctional test setup:

- Based on 3L-NPC leg
- Characterization of IGCT during low current turn-off
- Characterization of series connected IGCTs during low current turn-off
- Single pulse tests
- Double pulse tests
- Resonant pulse tests
- Continuous operation with power circulation
- DC link voltage of 2.5 kV-5 kV
- Adjustable resonant frequency

▲ Flexible and reconfigurable IGCT test setup [38]

[38] Dragan Stamenkovic. "IGCT Based Solid State Resonant Conversion." PhD thesis. EPFL, 2020

EXPERIMENTAL IGCT TEST SETUP (II)

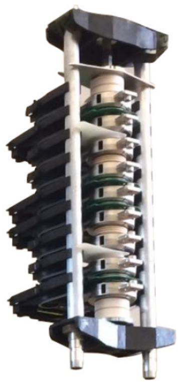

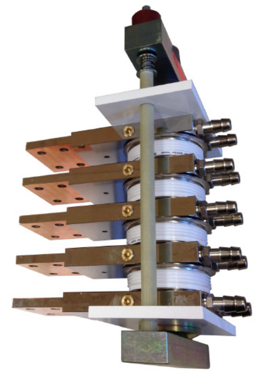

▲ (left) ABB ACS1000 water cooled 3L-NPC IGCT stack (DUT); (middle) Custom-built diodes stack; (right) De-ionised water cooling unit

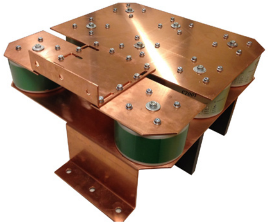

▲ (left) Custom made amorphous alloy core magnetizing inductor; (middle) Configurable array of eight air core resonant inductors; (right) Reconfigurable resonant capacitor bank

Problems to address:

- Minimise total switching energy
- Allow increase of switching frequency
- Ensure safe transitions (dead-time)

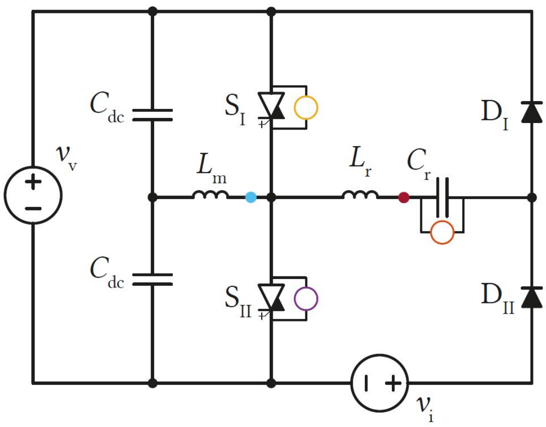

▲ Test setup configuration

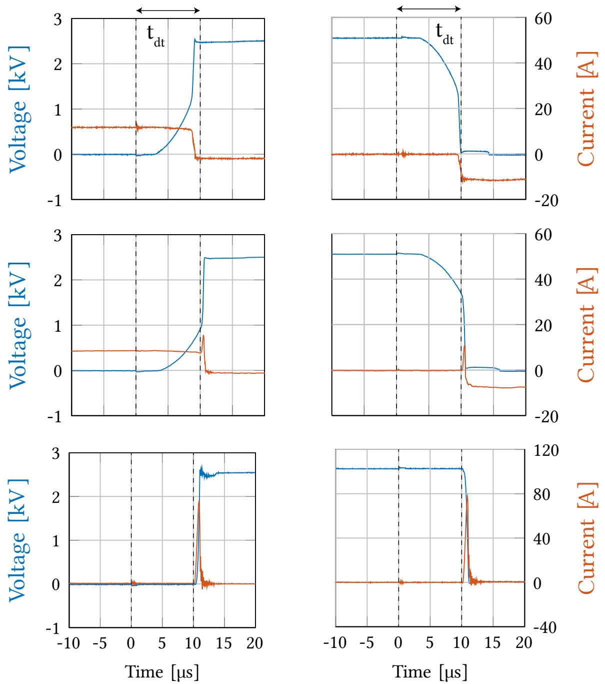

▲ IGCT turn-off and turn-on under (top) ZVS, (middle) non-ZVS, and (bottom) zero-current conditions. The turn-off current values are 17 A, 9 A, and 0 A, respectively. With loss of ZVS partial shoot-though takes place due to incomplete n-base sweep-out.

MINIMISATION OF SWITCHING ENERGY THROUGH ZVS/ZCS (II)

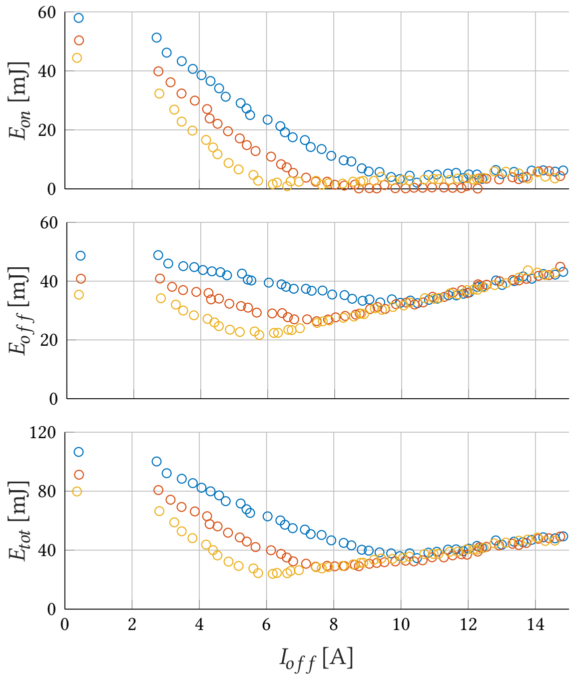

▲ Parametric sweep with different dead-times of o 10 μs, o 12 μs, and o 14 μs, respectively. [39]

Variables:

- Dead-time - from 10 μs to 14 μs
- Turn-off current - from 3 A to 15 A

Temperature has visible effect:

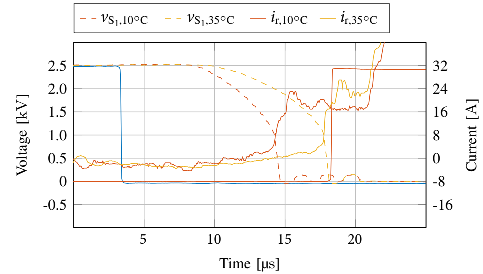

▲ T_j affects and prolongs switching transitions.

[39] Gabriele Ulissi et al. "Resonant IGCT Soft-Switching: Zero-Voltage Switching or Zero-Current Switching?" *IEEE Transactions on Power Electronics* 37.9 (2022), pp. 10775–10783

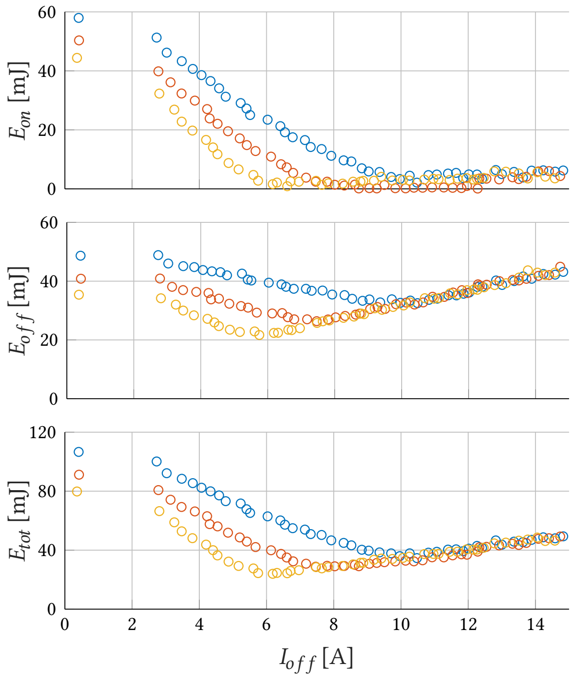

▲ Parametric sweep with different dead-times of o 10 µs, o 12 µs, and o 14 µs, respectively. [39]

Variables:

- Dead-time - from 10 µs to 14 µs
- Turn-off current - from 3 A to 15 A

Temperature has visible effect:

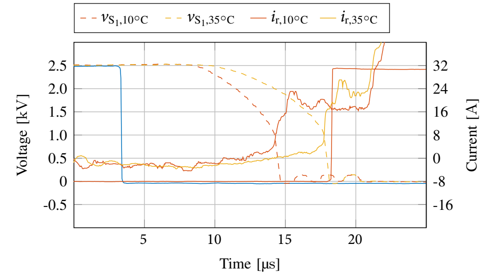

▲ T_j affects and prolongs switching transitions.

Minimum loss

⇒ It is achieved at limit of ZVS conditions!

[39] Gabriele Ulissi et al. “Resonant IGCT Soft-Switching: Zero-Voltage Switching or Zero-Current Switching?” *IEEE Transactions on Power Electronics* 37.9 (2022), pp. 10775–10783

MINIMISATION OF SWITCHING ENERGY THROUGH ZVS/ZCS (III)

3 GCTs devices are tested:

- Standard (5SHX 1445H0001)
- +55% irradiated
- +95% irradiated

Enginering samples are irradiated by HITACHI ENERGY Semiconductors

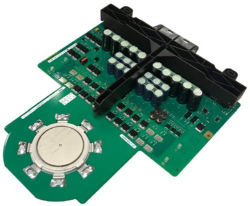

▲ Commercial gate unit is used during testing

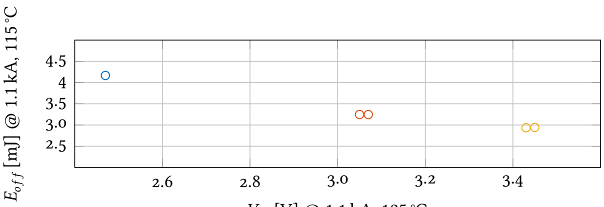

▲ Turn-off energy as a function of on-state voltage under hard switched conditions: o Standard, o +55 % irradiated, and o +95 % irradiated device performance.

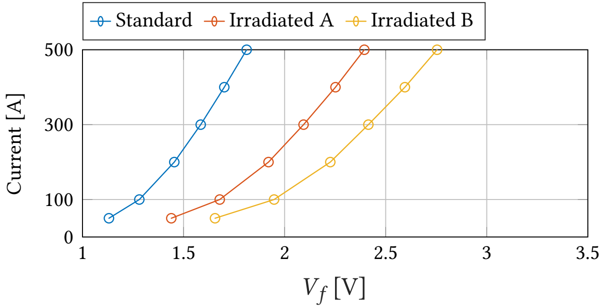

▲ GCT forward voltage

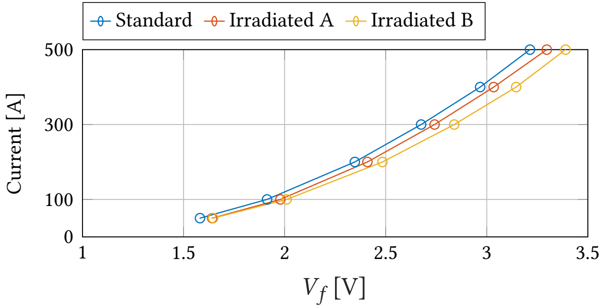

▲ Diode forward voltage

Current pre-flooding:

- How much current resonant peak affects turn OFF event?
- Similar studies have been done for IGBT [40], [41]

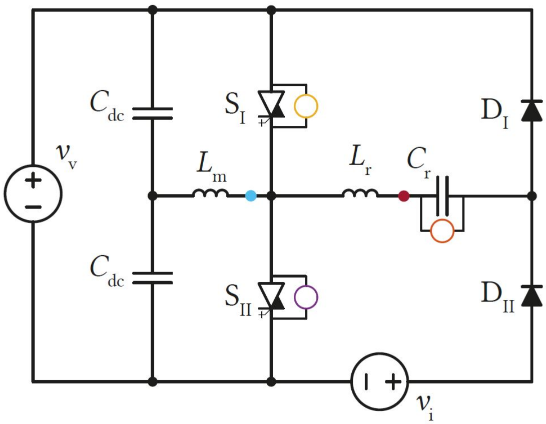

▲ Test setup to evaluate pre-flooding effect

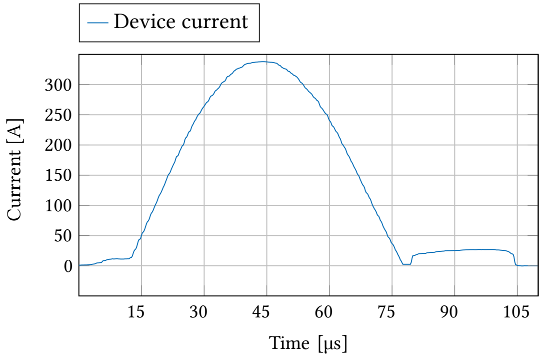

▲ Resonant current pulse

[40] Drazen Dujic et al. "Characterization of 6.5 kV IGBTs for High-Power Medium-Frequency Soft-Switched Applications." *IEEE Transactions on Power Electronics* 29.2 (2014), pp. 906–919

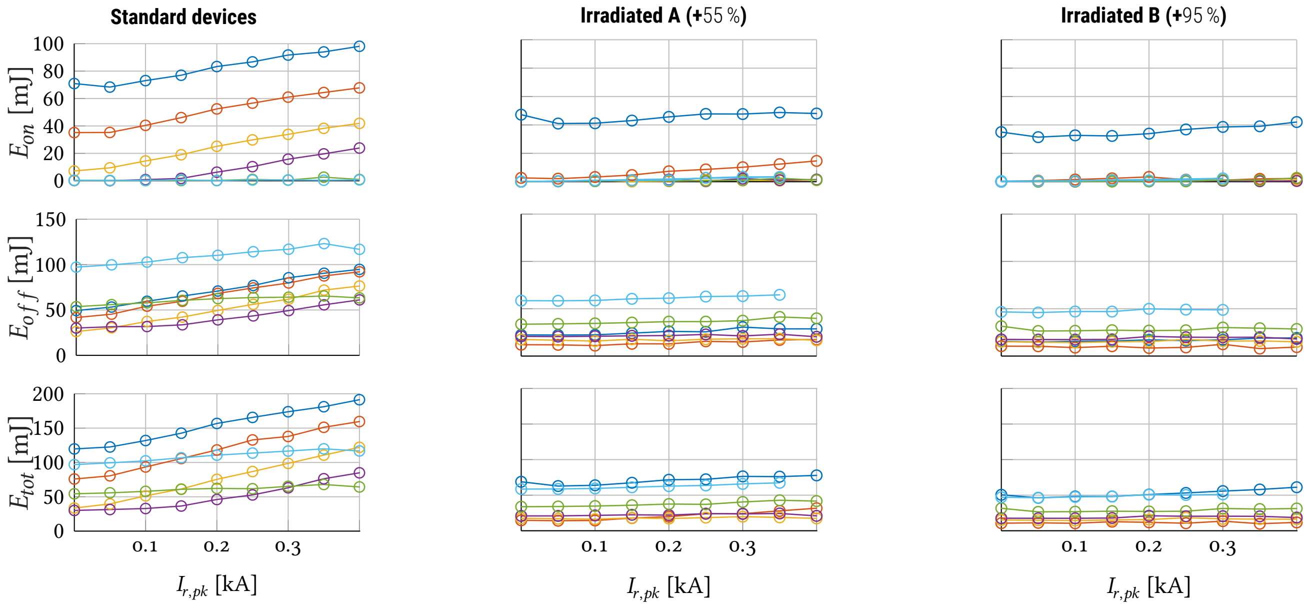

▲ Turn-ON, turn-OFF, and total switching energy for (left) standard commercial RC-IGCTs, (middle) Irradiated A, and (right) Irradiated B devices.

- I_{off} of o 0 A, o 3 A, o 6 A, o 9 A, o 17 A, and o 34 A
- Dead-time of 14 µs

MINIMISATION OF SWITCHING ENERGY THROUGH ZVS/ZCS (V)

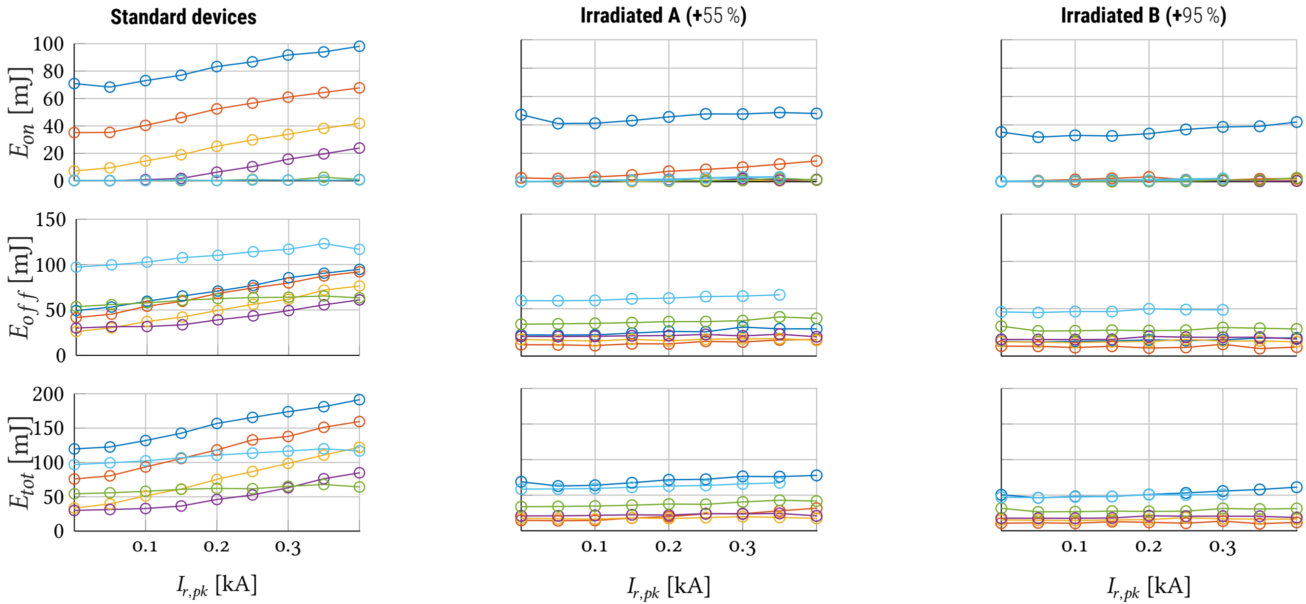

▲ Turn-ON, turn-OFF, and total switching energy for (left) standard commercial RC-IGCTs, (middle) Irradiated A, and (right) Irradiated B devices.

- I_{off} of o 0 A, o 3 A, o 6 A, o 9 A, o 17 A, and o 34 A
- Dead-time of 14 μs

⇒ Compounding benefits with increased irradiation levels!

Objective:

- Push IGCT to 5 kHz switching frequency
- Ensure safe operating conditions
- Estimate total losses

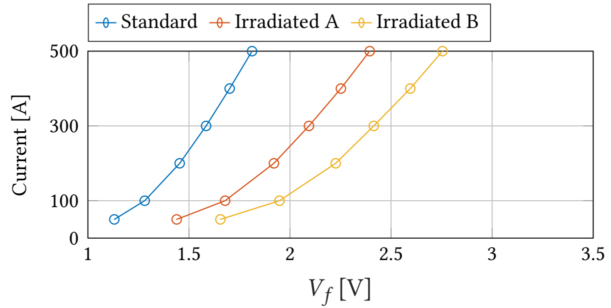

▲ GCT forward voltage

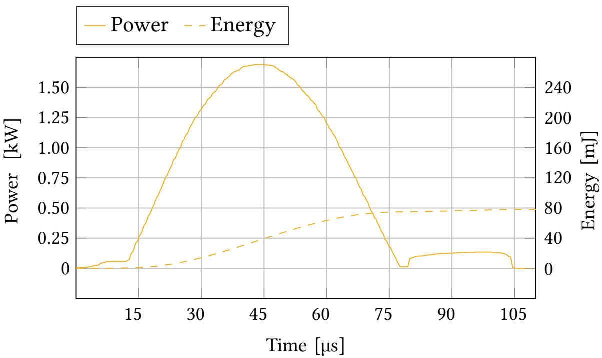

▲ Estimation of losses

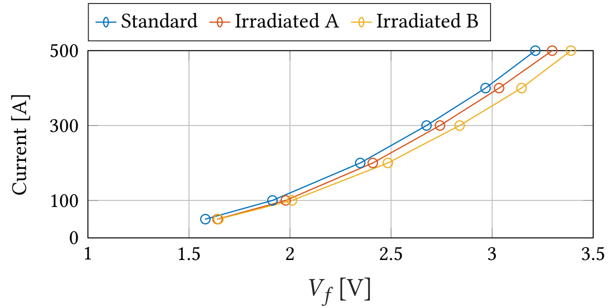

▲ Diode forward voltage

IGCT IN SERIES CONNECTION - HIGH-FREQUENCY OPERATION (I)

Challenges

- Low I_{off}
- Static voltage sharing
- Dynamic voltage sharing
- Snubber capacitance design

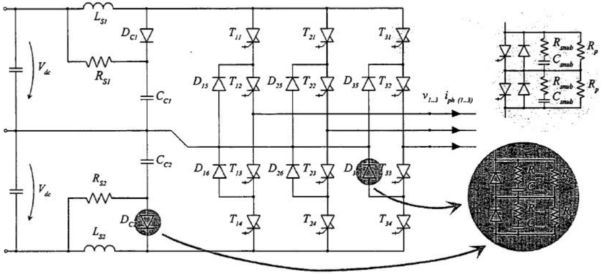

▲ IGCT-based NPC for 6 kV drive [42]

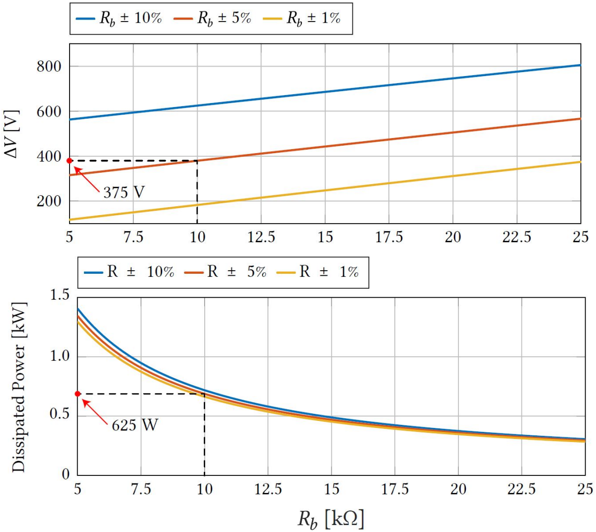

▲ Static balancing determined by max leakage current and accepted voltage difference [42]

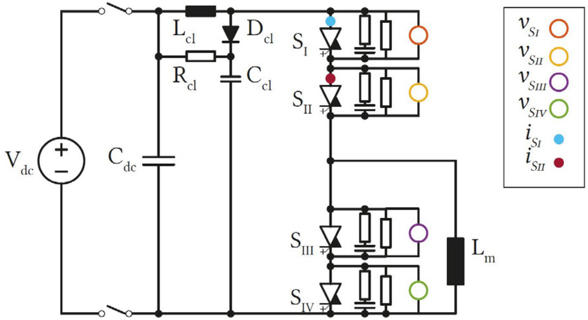

▲ Double Pulse test setup for series-connected IGCT tests

Tested snubber capacitance values:

- 40 nF, 70 nF, and 100 nF

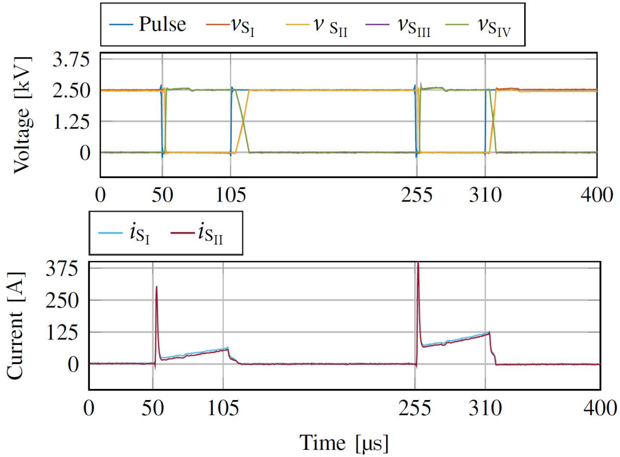

▲ Voltage (top) and current (bottom) waveforms during tests

IGCT IN SERIES CONNECTION - HIGH-FREQUENCY OPERATION (III)

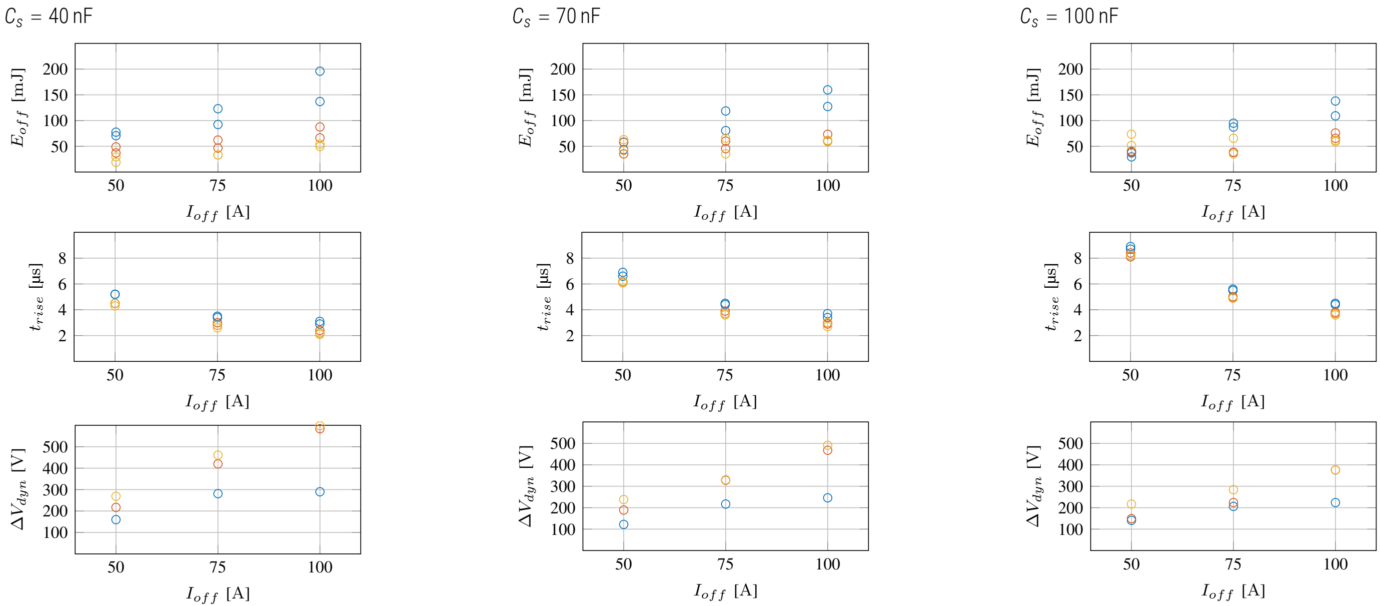

▲ Comparison of switching energy (top), voltage rise time (middle) and ΔV_{dyn} (bottom) during turn-off as a function of I_{off} and for indicated snubber capacitances. o Standard, o +55 % irradiated, and o +95 % irradiated devices

IGCT IN SERIES CONNECTION - HIGH FREQUENCY OPERATION (IV)

Operation at 5 kHz demonstrated:

- With standard devices
- With *C* snubbers only [29]

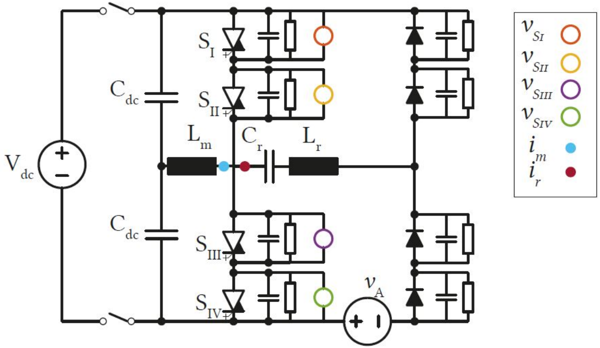

▲ Test setup arrangement for series connected IGCT resonant operation tests

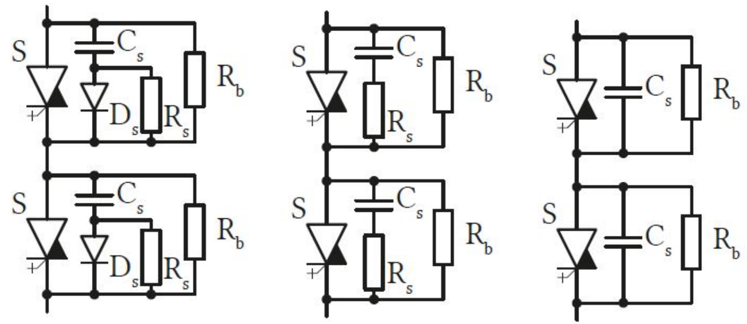

▲ Typical snubber configurations - Only capacitive snubber is used for resonant switching

[29] Gabriele Ulissi et al. "High-Frequency Operation of Series-Connected IGCTs for Resonant Converters." *IEEE Transactions on Power Electronics* 37.5 (2022), pp. 5664–5674

IGCT IN SERIES CONNECTION - HIGH FREQUENCY OPERATION (V)

Operation at 5 kHz demonstrated:

- With standard devices
- With *C* snubbers only [29]

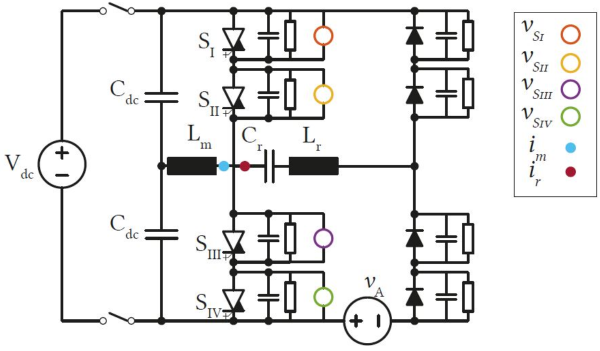

▲ Test setup arrangement for series connected IGCT resonant operation tests

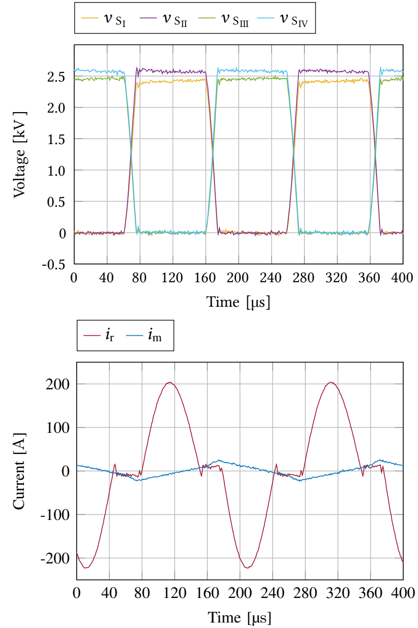

▲ IGCT voltage (top) and resonant current (bottom) during 5 kHz RC-IGCT series-connected resonant operation employing a 17 A turn-off current level and only 20 nF snubber capacitance.

Ongoing work:

- 10 kV IGCT (engineering samples)
- NPC topology modulation

[33] Gabriele Ulissi et al. "High-Frequency Operation of Series-Connected IGCTs for Resonant Converters." *IEEE Transactions on Power Electronics* 37.5 (2022), pp. 5664–5674

MV DCT PROTOTYPE

3L-NPC operating in 2L

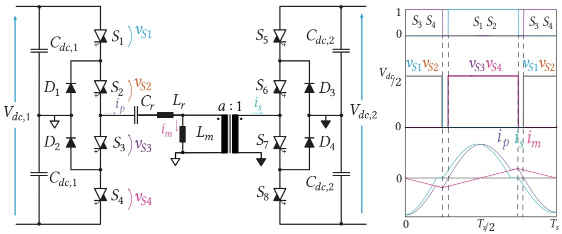

Highlights:

- High switching frequency (up to 5 kHz)
- Ultra-low turn-off current (lower than 25 A)

3L for soft-start

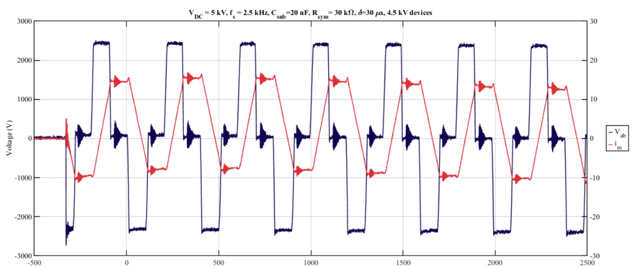

MV 1 MW IGCT-based DCT prototype

▲ Direct Current Transformer demonstrator

Problem

- Not identical leakage currents

Method:

- Simple parallel balancing resistors
- A single symmetrizing resistor

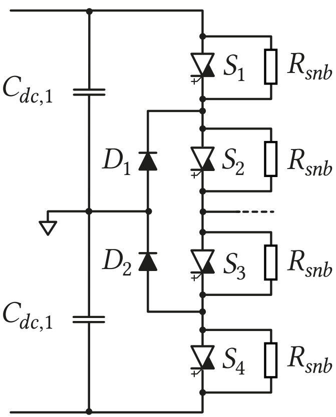

▲ Parallel balancing

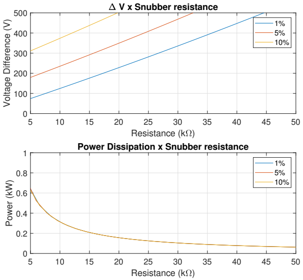

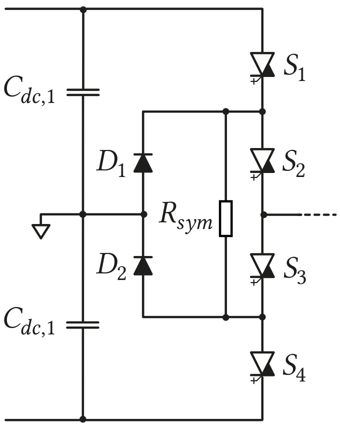

▲ Symmetrizing resistor

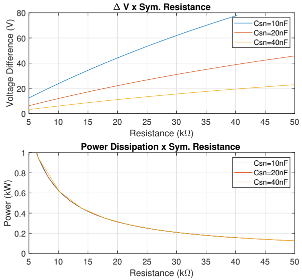

Problem

- Not identical leakage currents

Method:

- Simple parallel balancing resistors
- A single symmetrizing resistor

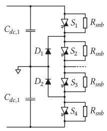

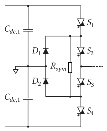

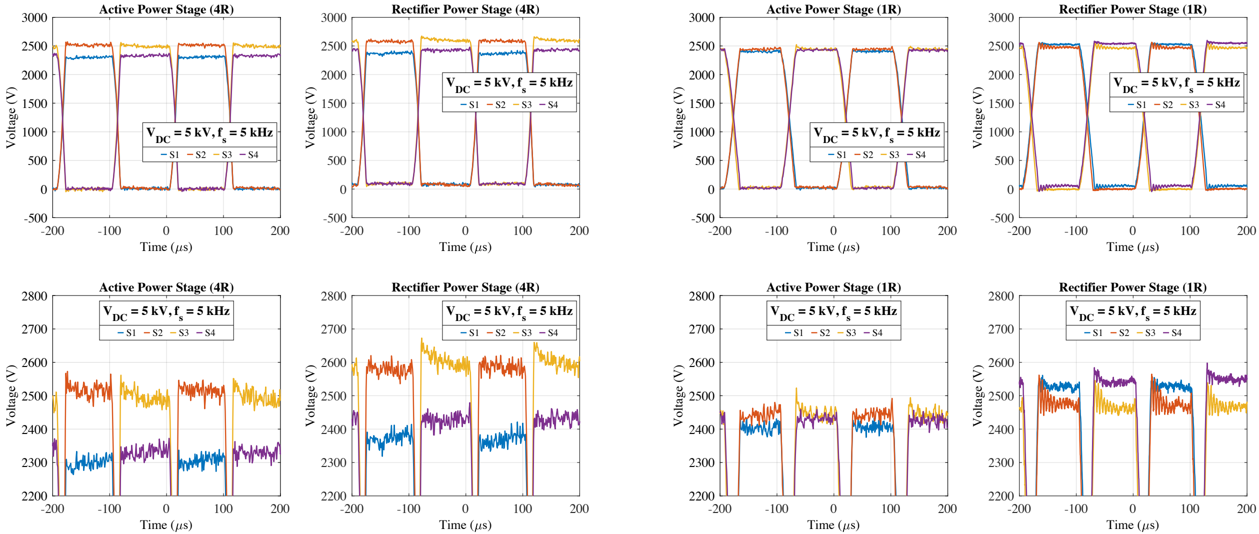

▲ 5 kV and 5 kHz experiments

DYNAMIC VOLTAGE BALANCING (I)

Problem

- Requires fast transition to ensure ZVS
- Maximum dynamic voltage imbalance

Method:

- Only C snubber, thanks to soft-switching

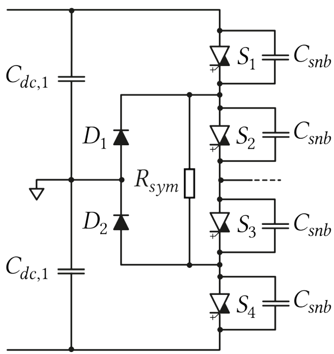

▲ C snubber

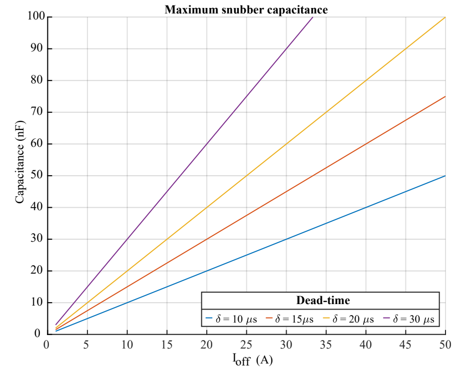

▲ Maximum snubber capacitance vs turn-off current for different dead-time

Problem

- Requires fast transition to ensure ZVS
- Maximum dynamic voltage imbalance

Method:

- Only C snubber, thanks to soft-switching

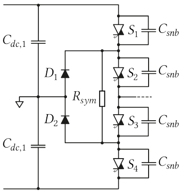

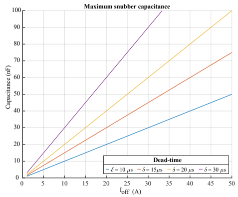

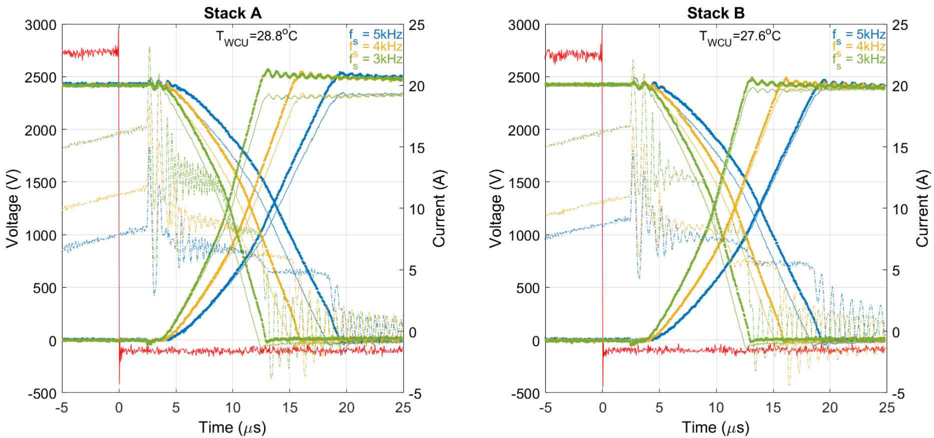

▲ 2L transition details with different switching frequencies

MFT DESIGN SPACE

What are the existing technologies and materials?

Multiphysical optimization problem:

1) Electrical domain:
- Skin and proximity effects due to the increase of the operating frequency
- Accurate electric parameter design

2) Magnetic domain:
- Non-sinusoidal excitation
- Core losses (hysteresis and eddy current losses)

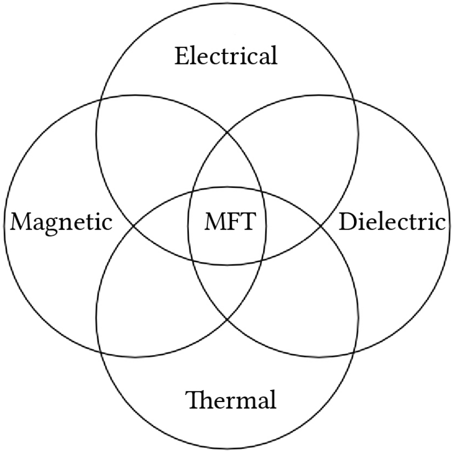

3) Dielectric domain:
- High dV/dt characteristic for the square voltage waveform resulting in over-voltages due to parasitic capacitances
- Insulation coordination

4) Thermal domain:
- Thermal coordination
- Increased hot-spot temperatures
- Thermal anisotropy

⇒ MFT design trade-offs: efficiency vs. power density vs. cost vs. manufacturability vs. ...

DESIGN SPACE EXPLORATION

Construction choices:

- Transformer types:

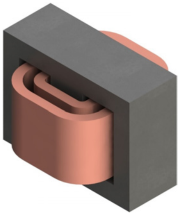

Shell type

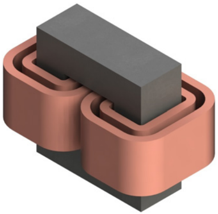

Core type

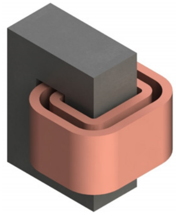

C-type

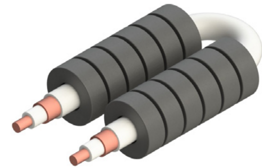

Coaxial type

- Conductor types:

Litz wire

Foil

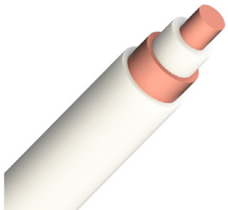

Coaxial

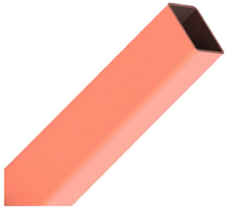

Hollow/Pipes

Materials:

- Core:
  - Silicon steel
  - Amorphous
  - Nanocrystalline
  - Ferrites
- Windings:
  - Copper
  - Aluminum

Technologies:

- Insulation:
  - Air
  - Solid
  - Oil
- Cooling:
  - Air natural/forced
  - Oil natural/forced
  - Deionized water

Composition and applications:

- Ferromagnetic material
- Iron based alloy of Silicon provided as isolated laminations
- Mostly used for line frequency transformers

Advantages:

- Wide initial permeability range
- High saturation flux density
- High Curie-termpature
- Relatively low cost
- Mechanically robust
- Various core shapes available (easy to form)

Disadvantages:

- High hysteresis loss (irreversible magnetisation)
- High eddy current loss (high electric conductivity)
- Acoustic noise (magnetostriction)

Saturation B	Init. permeability	Core loss (10 kHz, 0.5T)	Conductivity
0.8 ~ 2.2 T	$0.6 \sim 100 \cdot 10^3$	50 ~ 250 W/kg	$2 \cdot 10^7 \sim 5 \cdot 10^7$ S/m

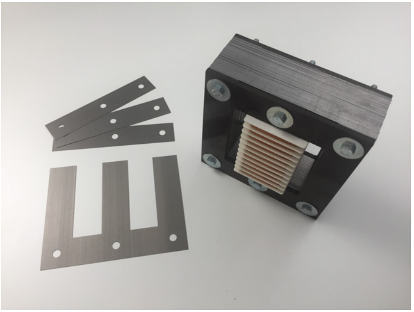

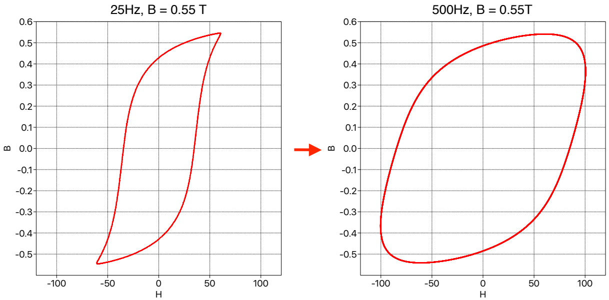

▲ Example: Measured B-H curve of M330-35 laminate.

Composition and applications:

- Ferromagnetic material
- Iron based alloy of Silicon as thin tape without crystal structure
- For both line frequency and switching frequency applications

Advantages:

- High saturation flux density
- Low hysteresis loss
- Low eddy current loss (low electric conductivity)
- High Curie-temperature
- Mechanically robust

Disadvantages:

- Relatively narrow initial permeability range
- Very high acoustic noise (magnetostriction)
- Limited core shapes available (difficult to form)
- Relatively expensive

Saturation B	Init. permeability	Core loss (10kHz, 0.5T)	Conductivity
0.5 ~ 1.6 T	$0.8 \cdot 10^3 \sim 50 \cdot 10^3$	2 ~ 20 W/kg	$< 5 \cdot 10^3$ S/m

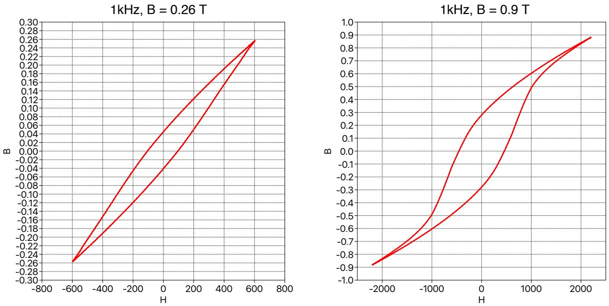

▲ Example: Measured B-H curve of Metglas 2605SA.

Composition and applications:

- Ferromagnetic material
- Iron based alloy of silicon as thin tape with minor portion of crystal structure
- For both line frequency and switching frequency applications

Advantages:

- Relatively narrow initial permeability range
- High saturation flux density
- Low hysteresis loss
- High Curie-temperature
- Low acoustic noise

Disadvantages:

- Eddy current loss (compensated thanks to the thin tape)
- Mechanically fragile
- Limited core shapes available (difficult to form)
- Relatively expensive

Saturation B	Init. permeability	Core loss (10kHz, 0.5T)	Conductivity
1 ~ 1.2 T	$0.5 \cdot 10^3 \sim 100 \cdot 10^3$	< 50 W/kg	$3 \cdot 10^3 \sim 5 \cdot 10^4$ S/m

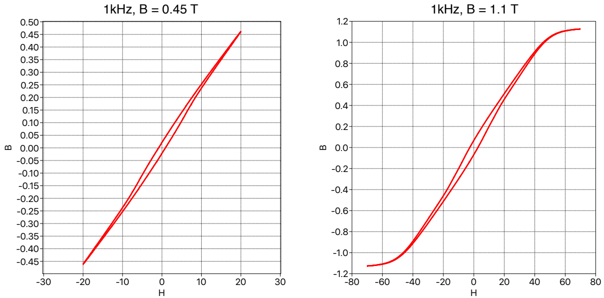

▲ Example: Measured B-H curve of VITROPERM 500F.

Composition and applications:

- Ferrimagnetic material
- Ceramic material made from powder of different oxides and carbons
- For both line frequency and switching frequency applications

Advantages:

- Relatively narrow initial permeability range
- Low hysteresis loss
- Very low eddy current loss
- Low acoustic noise
- Relatively low cost
- Various core shapes available

Disadvantages:

- Low saturation flux density
- Small mechanical size of cores
- Magnetic properties deteriorate with temperature increase
- Mechanically fragile

Saturation B	Init. permeability	Core loss (10kHz, 0.5T)	Conductivity
0.3 ~ 0.5 T	$0.1 \cdot 10^3 \sim 20 \cdot 10^3$	5 ~ 100 W/kg	$< 1 \cdot 10^{-5}$ S/m

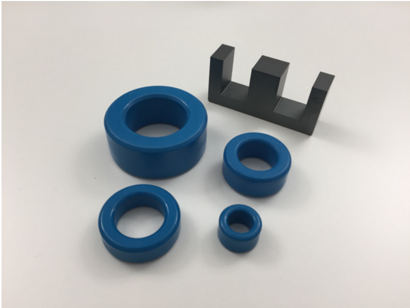

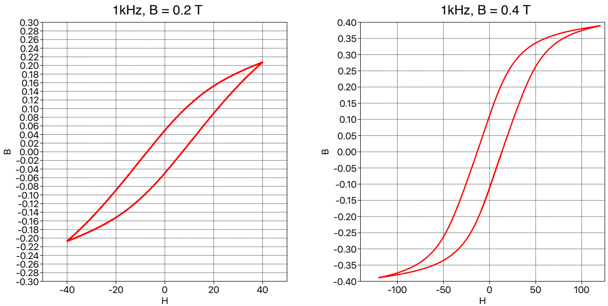

▲ Example: Measured B-H curve of Ferrite N87.

WINDING MATERIALS

Copper winding:

- Flat wire - low frequency, easy to use
- Litz wire - high frequency, limited bending
- Foil - provide flat windings
- Hollow tubes - provide cooling efficiency
- Better conductor
- More expensive
- Better mechanical properties

Aluminium winding:

- Flat wire
- Foil - skin effect differences compared to Copper
- Hollow tubes
- Difficult to interface with copper
- Offer some weight savings
- Cheaper
- Somewhat difficult mechanical manipulations

Copper parameters:

Electrical conductivity	$58.5 \cdot 10^6\ S/m$
Electrical resistivity	$1.7 \cdot 10^{-8}\ \Omega m$
Thermal conductivity	$401\ W/mK$
TEC (from 0° to 100° C)	$17 \cdot 10^{-6}\ K^{-1}$
Density	$8.9\ g/cm^3$
Melting point	$1083\ ^\circ C$

Aluminum parameters:

Electrical conductivity	$36.9 \cdot 10^6\ S/m$
Electrical resistivity	$2.7 \cdot 10^{-8}\ \Omega m$
Thermal conductivity	$237\ W/mK$
TEC (from 0° to 100° C)	$23.5 \cdot 10^{-6}\ K^{-1}$
Density	$2.7\ g/cm^3$
Melting point	$660\ ^\circ C$

INSULATION

Multiple influencing factors:

- Operating voltage levels
- Over-voltage category
- Environment - IP class
- Temperature
- Moisture
- Cooling implications
- Ageing (self-healing?)
- Manufacturing complexity
- Partial Discharge, BIL
- Cost

Dielectric properties:

- Breakdown voltage (dielectric strength)
- Permittivity
- Conductivity
- Loss angle

Dielectric material	Dielectric strength (kV/mm)	Dielectric constant
Air	3	1
Oil	5 - 20	2 - 5
Mica tape	60 - 230	5 - 9
NOMEX 410	18 - 27	1.6 - 3.7
PTFE	60 - 170	2.1
Mylar	80 - 600	3.1
Paper	16	3.85
PE	35 - 50	2.3
XLPE	35 - 50	2.3
KAPTON	118 - 236	3.9

▲ Variety of choices available.

Heat dissipation through heat transfer mechanisms on core and winding surfaces

Three main cooling methods/media for effective dissipation:

Air:

- Natural convection - inefficient for high power designs
- Forced convection - requires a fan
- Increased complexity, reduced reliability
- For both core and windings
- 2 A mm^{-2} current density

Oil:

- Various mineral oils exist - very efficient
- Forced convection, heat exchangers necessary
- Increased cost, complexity
- High power distribution transformers
- For both core and windings
- 4 A mm^{-2} current density

Water:

- Forced convection - very efficient
- Hollow conductors for winding cooling
- Ducts/panels for core cooling
- Traction applications
- Indirect water cooling
- 6-7 A mm^{-2} current density

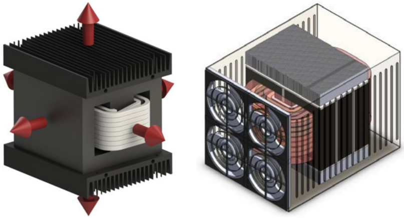

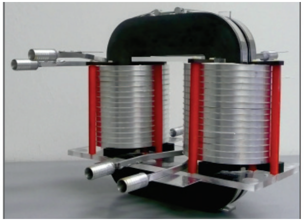

Every cooling method requires modeling, trade-off between accuracy and computational cost

MFT DESIGN DIVERSITY

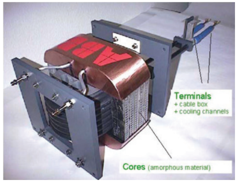

ABB: 350kW, 10kHz

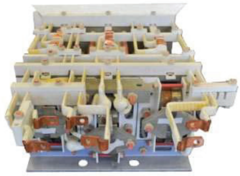
ABB: 3x150kW, 1.8kHz

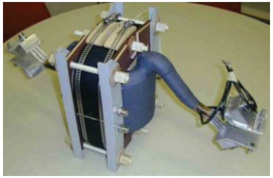
BOMBARDIER: 350kW, 8kHz


CHALMERS: 50kW, 5kHz


IKERLAN: 400kW, 5kHz

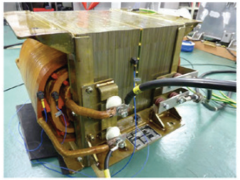
IKERLAN: 400kW, 1kHz

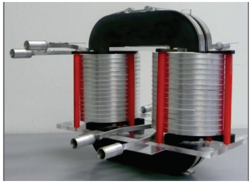
FAU-EN: 450kW, 5.6kHz

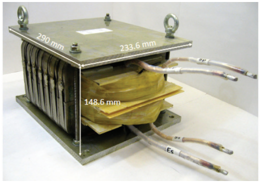

EPFL: 300kW, 2kHz

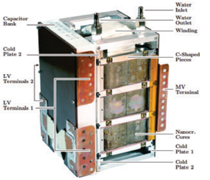

ETHZ: 166kW, 20kHz

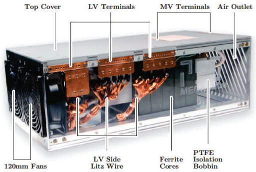

ETHZ: 166kW, 20kHz

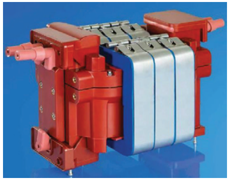
STS: 450kW, 8kHz

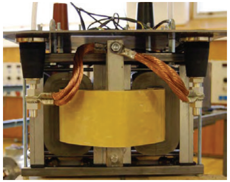
KTH: 170kW, 4kHz


EPFL: 100kW, 10kHz

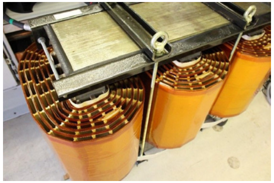
SCHAFFNER: 5000kW, 1kHz

?

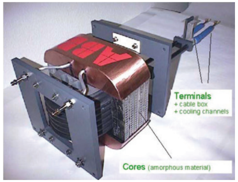

ABB: 350kW, 10kHz

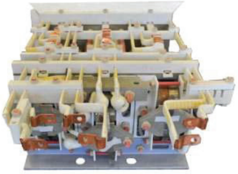

ABB: 3x150kW, 1.8kHz

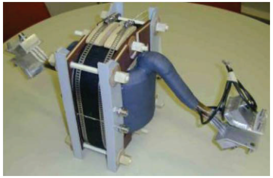

BOMBARDIER: 350kW, 8kHz

CHALMERS: 50kW, 5kHz

IKERLAN: 400kW, 5kHz

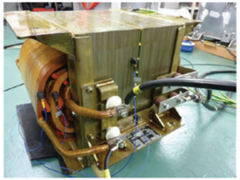

IKERLAN: 400kW, 1kHz

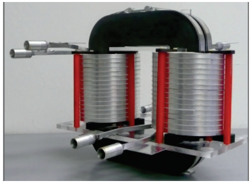

FAU-EN: 450kW, 5.6kHz

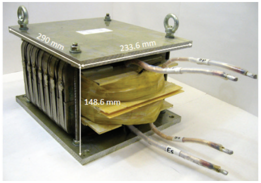

EPFL: 300kW, 2kHz

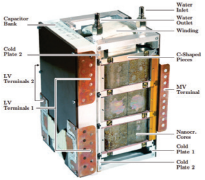

ETHZ: 166kW, 20kHz

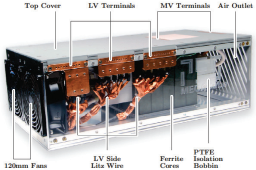

ETHZ: 166kW, 20kHz

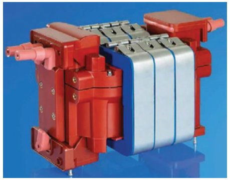

STS: 450kW, 8kHz

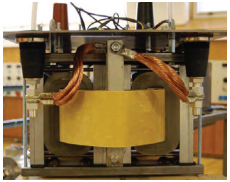

KTH: 170kW, 4kHz

EPFL: 100kW, 10kHz

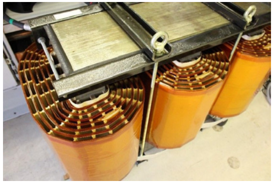

SCHAFFNER: 5000kW, 1kHz

?

⇒ Large number of MFT designs has been reported, relying on various combinations of technologies!

MFT DESIGN EXAMPLES

Variety of technological combinations

TECHNOLOGIES, MATERIALS, DESIGNS

Construction Choices:

- MFT Types

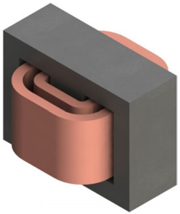

Shell Type

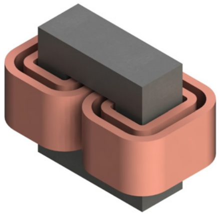

Core Type

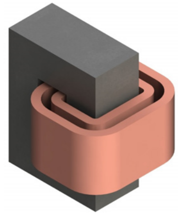

C-Type

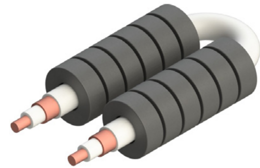

Coaxial Type

- Winding Types

Litz Wire

Foil

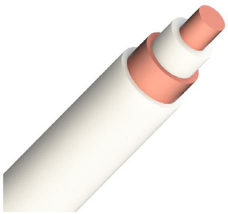

Coaxial

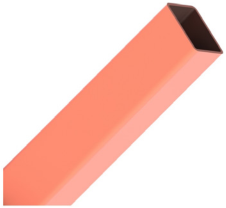

Hollow/Pipes

Materials:

- Magnetic Materials
  - Silicon Steel
  - Amorphous
  - Nanocrystalline
  - Ferrites
- Windings
  - Copper
  - Aluminum
- Insulation
  - Air
  - Solid
  - Oil
- Cooling
  - Air natural/forced
  - Oil natural/forced
  - Water

MFT HALL OF FAME

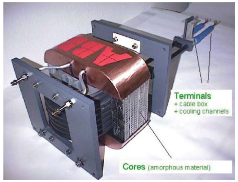

ABB: 350kW, 10kHz

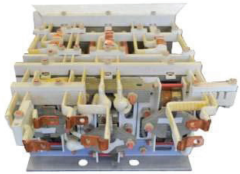

ABB: 3x150kW, 1.8kHz

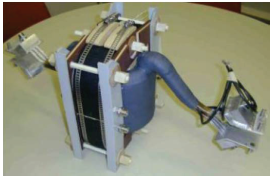

BOMBARDIER: 350kW, 8kHz

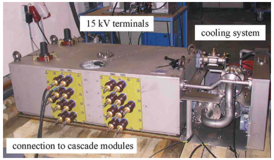

ALSTOM: 1500kW, 5kHz

IKERLAN: 400kW, 6kHz

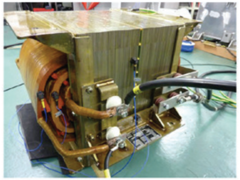

IKERLAN: 400kW, 600Hz

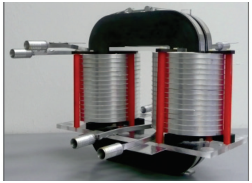

FAU-EN: 450kW, 5.6kHz

CHALMERS: 50kW, 5kHz

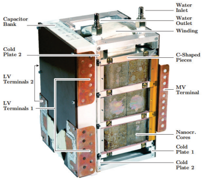

ETHZ: 166kW, 20kHz

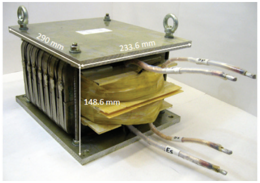

EPFL: 300kW, 2kHz

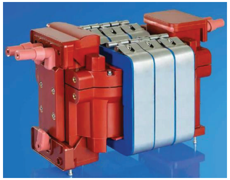

STS: 450kW, 8kHz

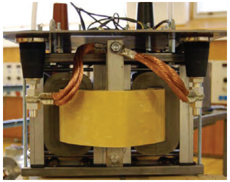

KTH: 170kW, 4kHz

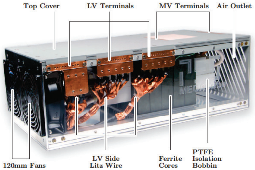

ETHZ: 166kW, 20kHz

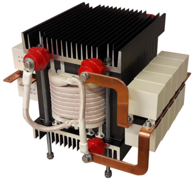

EPFL: 100kW, 10kHz

?

ACME: ???kW, ???kHz

ABB MFT - 2002

Construction
- Shell Type
- Coaxial winding

Electrical Ratings
- Power: 350kW
- Frequency: 10kHz
- Input Voltage: $\pm 3000V$
- Output Voltage: $\pm 3000V$

Core Material
- VAC Vitroperm 500F
- U cores

Windings
- Coaxial (Al inside, Cu outside)

Cooling
- Winding - De-ionized water
- Core - Air

Insulation
- Solid

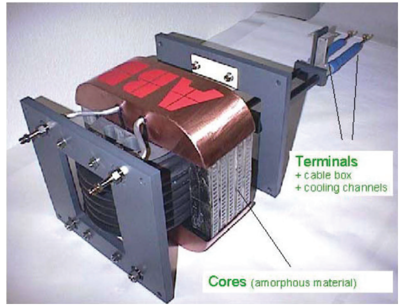

▲ 350kW MFT by ABB [43]

MFT dimensions
- Volume: ≈ 37 l
- V-Density: ≈ 9.5 kW/l
- Weight: < 50 kg
- W-Density: ≈ 7 kW/kg

Insulation Tests
- PD: 38kV, 50Hz, 1 min
- BIL: 95 kV (peak), 10 shots

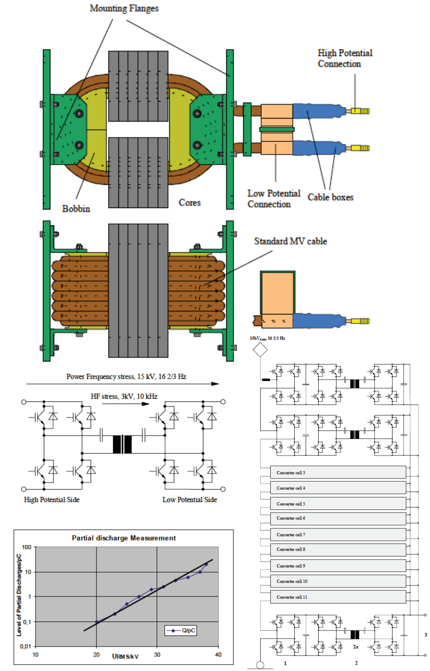

▲ Multilevel line side converter by ABB (2002)

Construction

- Single core with multiple windings

Electrical Ratings

- Power: 1.5MW
- Frequency: 5kHz
- Input Voltage: $\pm 1800V$
- Output Voltage: $\pm 1650V$

Core Material

- Ferrite
- Size and shape unclear

Windings

- Litz wire

Cooling

- Oil (MIDEL)
- Common with power electronics

Insulation

- Oil (MIDEL)
- Immersed

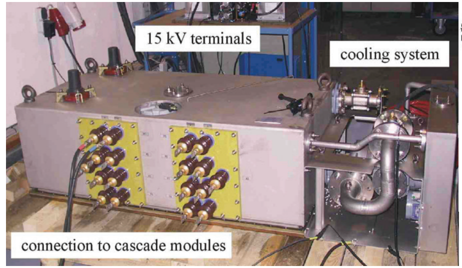

▲ 1.5MW MFT by ALSTOM

MFT dimensions

- Volume: 0.72 m^3 (2.0 x 0.73 x 0.49) m
- V-Density: 2.1 kW/l
- Weight: < 1 t (estimation)
- W-Density: < 1.5 kW / kg (estimation)

e-Transformer dimensions

- (2.1 x 2.62 x 0.58) m
- Volume: 3.22 m^3
- Weight: 3.1 t (50% less)

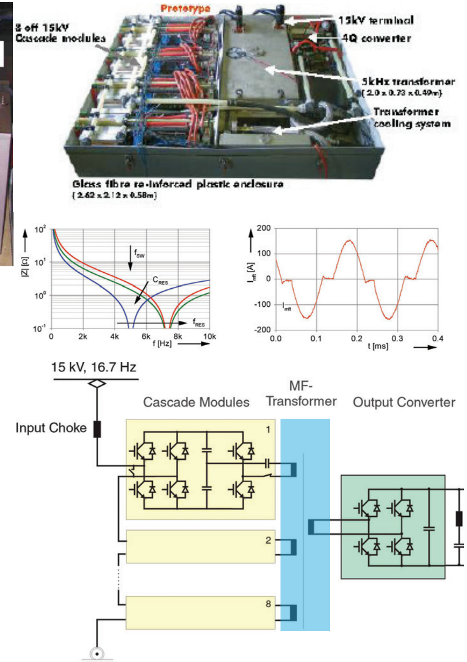

▲ e-Transformer by ALSTOM [44], [45]

ABB MFT - 2007

Construction

- C-type

Electrical Ratings

- Power: 75kW (x16)
- Frequency: 400Hz
- Input Voltage: $\pm 1800V$
- Output Voltage: $\pm 1800V$

Core Material

- SiFe
- Custom made sheets

Windings

- Bar wire

Cooling

- Oil
- Common with power electronics

Insulation

- Oil
- Immersed

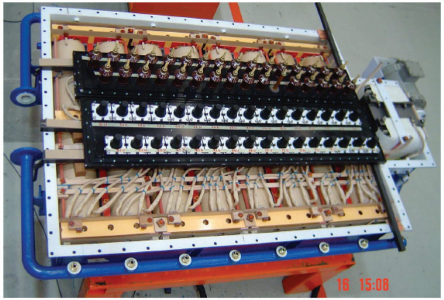

▲ Enclosure with 16 MFTs by ABB

MFT dimensions

- Volume: not reported
- V-Density: ? kW/l
- Weight: not reported
- W-Density: ? kW/kg

PETT dimensions

- Volume: 20% less
- Weight: 50% less
- Efficiency: 3% increase

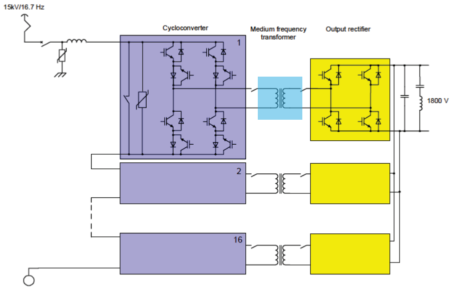

▲ PETT by ABB [46]

BOMBARDIER MFT - 2007

Construction

- Core Type
- Hollow conductors

Electrical Ratings

- Power: 350kW (500kW peak)
- Frequency: 8kHz
- Input Voltage: $\pm 1000V$
- Output Voltage: $\pm 1000V$

Core Material

- Nanocrystalline
- U cores

Windings

- Hollow tubes

Cooling

- Winding - De-ionized water
- Core - Water cooled heatsink

Insulation

- Solid

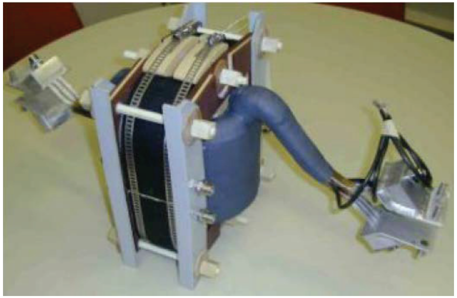

▲ 350kW MFT by Bombardier [47]

MFT dimensions

- Volume: not reported
- V-Density: ? kW/l
- Weight: 18 kg
- Density: ≈ 7 kW/kg

Insulation Tests

- PD: 33kV, 50Hz
- BIL: 100 kV (1.2/50)

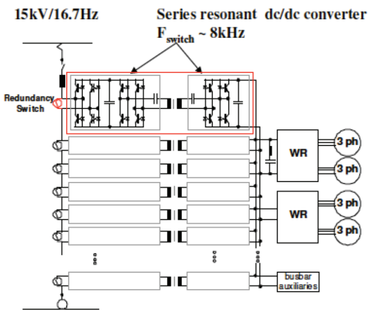

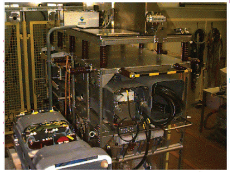

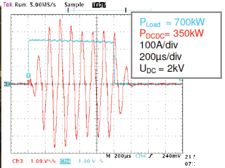

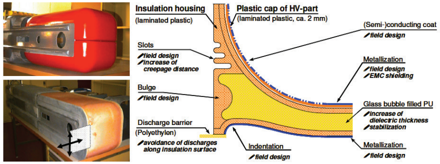

▲ Medium frequency topology by Bombardier

ABB MFT - 2011

Construction
- C-core
- Assembly with 3 MFTs

Electrical Ratings
- Power: 150kW
- Frequency: 1.75kHz
- Input Voltage: $\pm 1800V$
- Output Voltage: $\pm 750V$

Core Material
- Nanocrystalline
- C-cut cores

Windings
- Bar wire

Cooling
- Oil

Insulation
- Oil
- Immersed

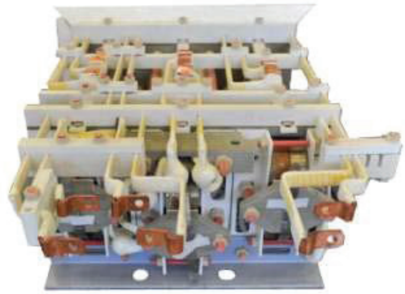

▲ 3 x 150kW MFT by ABB

MFT dimensions
- Volume: ≈ 80 l
- V-Density: ≈ 2.4 kW/l
- Weight: ≈ 170 kg
- W-Density: ≈ 1.1 kW/kg

PETT dimensions
- Weight: 4.5 t

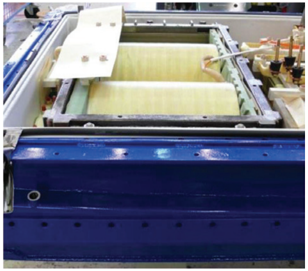

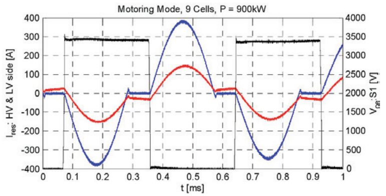

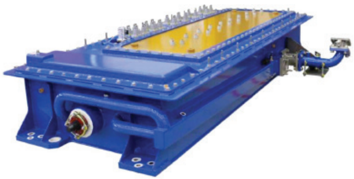

▲ PETT tank with magnetics by ABB [12], [13]

Construction
- Core Type

Electrical Ratings
- Power: 450kW
- Frequency: 5.6kHz
- Input Voltage: $\pm 3600V$
- Output Voltage: $\pm 3600V$

Core Material
- Nanocrystalline VITROPERM 500F
- U cores

Windings
- Aluminum
- Hollow profiles

Cooling
- Winding - de-ionized water
- Core - Oil

Insulation
- Oil - Immersed (primary to secondary)
- NOMEX - between turns

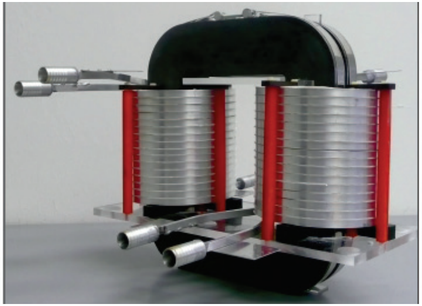

▲ 450kW MFT by UEN [48], [49], [50]

MFT dimensions
- Volume: not reported
- V-Density: ? kW/l
- Weight: 24 - 38.2 kg
- W-Density: ≈ 18.8 - 11.8 kW/kg

Insulation Tests
- Designed for 25kV railway lines
- PD, BIL: not reported

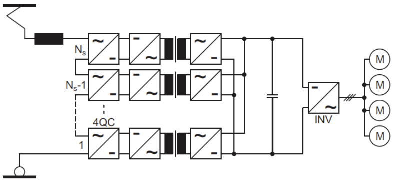

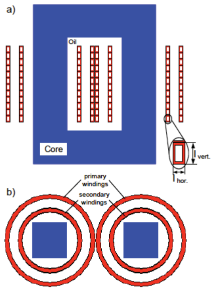

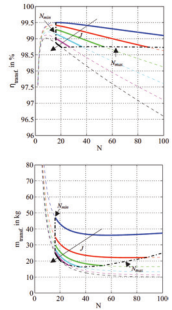

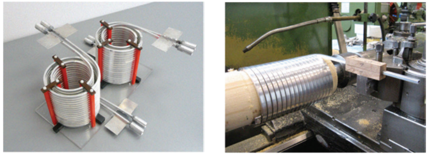

▲ MFT by UEN

Construction
- Shell Type
- for the use with HC-DCM-SRC

Electrical Ratings
- Power: 166kW
- Frequency: 20kHz
- Input Voltage: $\pm 1000V$
- Output Voltage: $\pm 400V$

Core Material
- Nanocrystalline Vitroperm 500F
- C-cores

Windings
- Square Litz Wire

Cooling
- Water-cooled heat sinks

Insulation
- Solid
- Mica tape

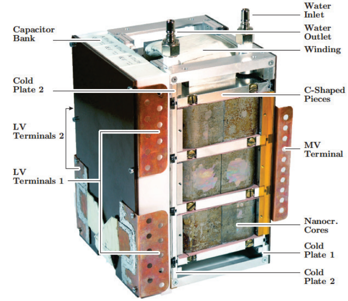

▲ 166kW MFT by ETH [51], [52], [53]

MFT dimensions
- Volume: ≈ 5 l
- V-Density: ≈ 32.7 kW/l
- Weight: ≈ 10 kg
- W-Density: ≈ 16.6 kW/kg

Insulation Tests
- No details provided

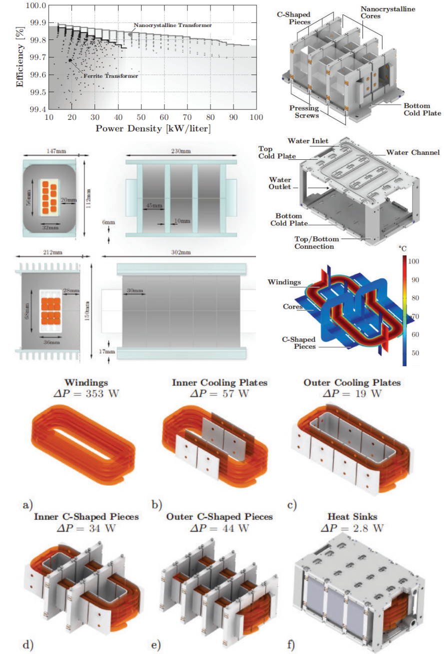

▲ Nanocrystalline MFT by ETHZ

ETHZ PES MFT - 2014 (CONT.)

Construction

- Shell Type
- for the use with TCM-DAB

Electrical Ratings

- Power: 166kW
- Frequency: 20kHz
- Input Voltage: ±750V
- Output Voltage: ±750V

Core Material

- Ferrite N87
- U-cores U96/76/30

Windings

- Square Litz Wire

Cooling

- Winding - Forced air
- Core - Heatsinks (Forced air)

Insulation

- PTFE (teflon)

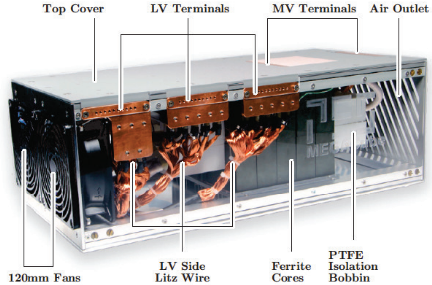

▲ 166kW MFT by ETH [51]

MFT dimensions

- Volume: ≈ 20 l
- V-Density: ≈ 8.21 kW/l
- Weight: not reported
- W-Density: not reported

Insulation Tests

- No details provided

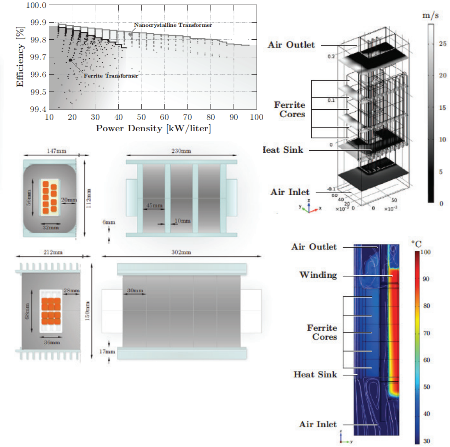

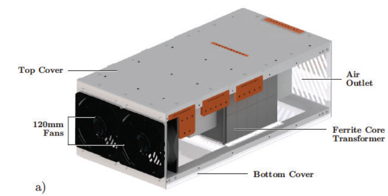

▲ Ferrite MFT by ETHZ

Construction

- Core Type

Electrical Ratings

- Power: 450kW
- Frequency: 8kHz
- Input Voltage: $\pm 1800V$
- Output Voltage: $\pm 1800V$

Core Material

- Nanocrystalline
- C cores

Windings

- Square Litz Wire

Cooling

- Winding - Oil
- Core - Air cooled

Insulation

- Solid combined with Oil
- Core in the air

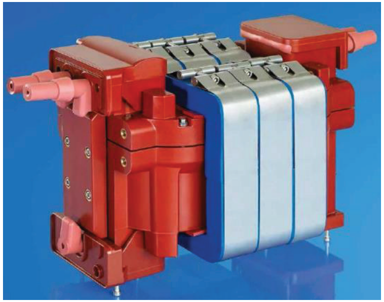

▲ 450kW MFT by STS

MFT dimensions

- Volume: ? l
- V-Density: ≈ ? kW/l
- Weight: 50 kg
- W-Density: ≈ 9 kW/kg

Insulation Tests

- PD: 37kV, 50Hz (PD < 5pC)
- BIL: not specified

▲ MFT by STS

ABB MFT - 2017

Construction

- Core Type

Electrical Ratings

- Power: 240kW
- Frequency: 10kHz
- Input Voltage: $\pm 600V$
- Output Voltage: $\pm 900V$

Core Material

- Nanocrystalline
- U cores (custom)

Windings

- Litz Wire (4 parallel)

Cooling

- Winding - Air
- Core - Air

Insulation

- Solid - Cast Resin
- Air

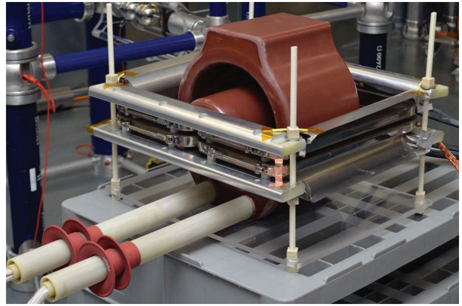

▲ 240kW MFT by ABB [54]

MFT dimensions

- Volume: ≈ 67.7 l
- V-Density: ≈ 3.6 kW/l
- Weight: ≈ 42 kg
- W-Density: ≈ 5.7 kW/kg

Insulation Tests

- PD: 53kV, 50Hz
- BIL: 150kV

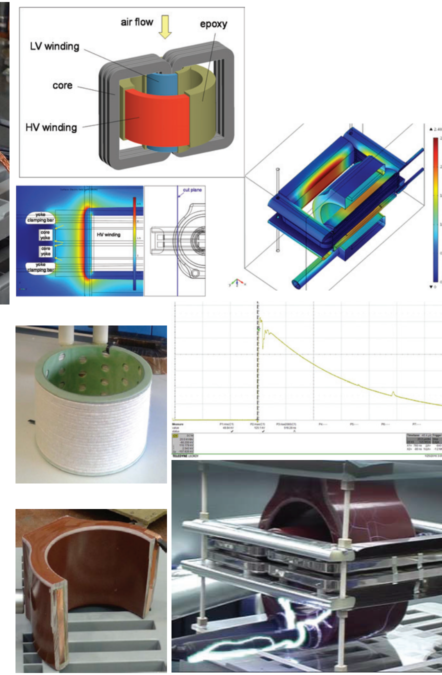

▲ MFT by ABB

ABB CERN MFT - 2017

Construction

- Core Type

Electrical Ratings

- Power: 100kW
- Frequency: 15kHz - 22kHz
- Input Voltage: $\pm 540V$
- Output Voltage: $\pm 540V$ x 24

Core Material

- Nanocrystalline
- U cores

Windings

- Litz Wire

Cooling

- Winding/Core - Oil Immersed
- MFT assembly - Air

Insulation

- Oil (Ester)

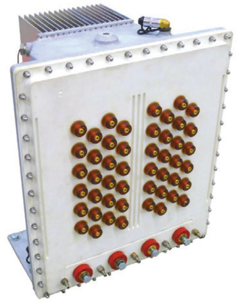

▲ 100kW MFT by ABB [55]

MFT dimensions

- Volume: ≈ 91 l (61 l without heatsink)
- V-Density: ≈ 1.1 kW/l
- Weight: ≈ 90 kg
- W-Density: ≈ 1.1 kW/kg

Insulation Tests

- PD: 30kV, 50Hz
- BIL: not reported

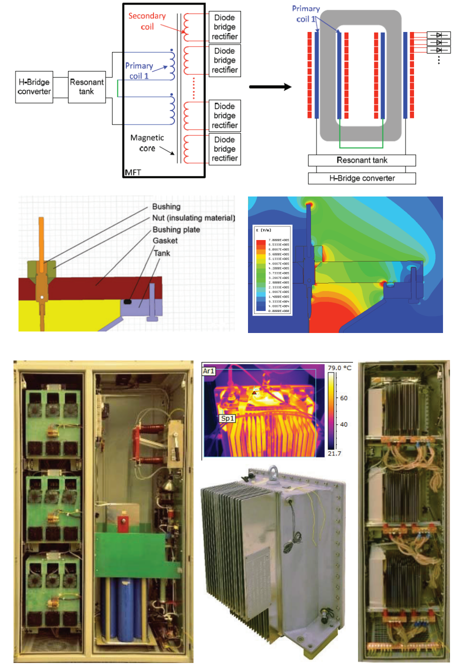

▲ MFT by ABB for CERN

EPFL PEL MFT - 2017

Construction
- Core Type

Electrical Ratings
- Power: 100kW
- Frequency: 10kHz
- Input Voltage: ±750*V*
- Output Voltage: ±750*V*

Core Material
- SiFerrite (UU9316 - CF139)
- U cores

Windings
- Square Litz Wire

Cooling
- Winding - Air
- Core - Air cooled heatsink

Insulation
- Air

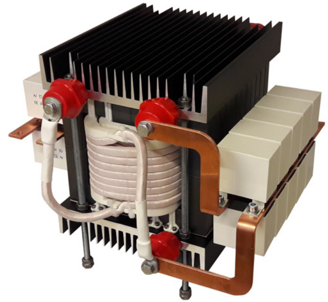

▲ 100kW MFT by EPFL [56], [57], [58]

MFT dimensions
- Volume: ≈ 12.2 l
- V-Density: ≈ 8.2 kW/l
- Weight: ≈ 28 kg
- W-Density: ≈ 3.6 kW/kg

Insulation Tests
- PD: 6kV, 50Hz
- BIL: not performed

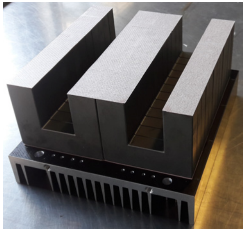

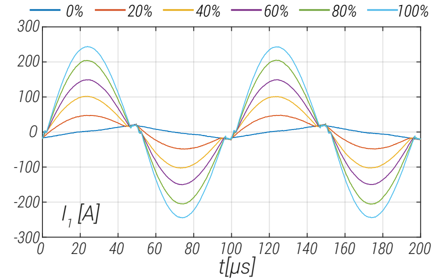

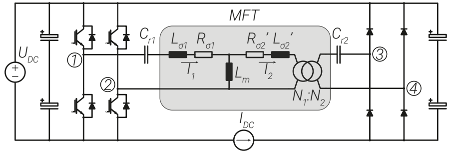

▲ MFT by EPFL

[58] Marko Mogorovic and Drazen Dujic. "100 kW, 10 kHz Medium-Frequency Transformer Design Optimization and Experimental Verification." *IEEE Transactions on Power Electronics* 34.2 (2019), pp. 1696–1708

Construction

- Shell Type
- for the use with DC-DC SRC

Electrical Ratings

- Power: 25kW
- Frequency: 48kHz
- Input Voltage: $\pm 3.5kV$
- Output Voltage: $\pm 400V$

Core Material

- Ferrite BFM8
- U-cores U96/60/30

Windings

- Square Litz Wire

Cooling

- Winding - Forced air
- Core - Forced air

Insulation

- Dry type - Vacuum poting (windings)

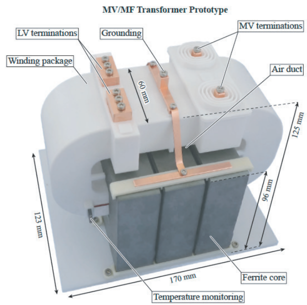

▲ 25kW MFT by ETH [59]

MFT dimensions

- Volume: ≈ 3.4 l
- V-Density: ≈ 7.4 kW/l
- Weight: ≈ 6.2 kg
- W-Density: ≈ 4 kW/kg

Insulation Tests

- 20kV

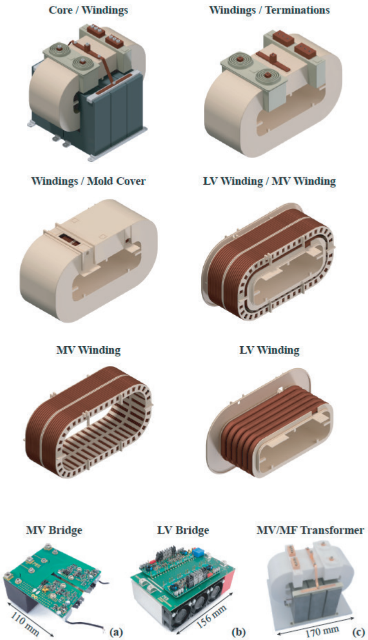

▲ Ferrite MFT by ETHZ

EPFL PEL MFT - 2019

Construction

- Planar type

Electrical ratings

- Power: 100kW
- Frequency: 10kHz
- Input Voltage: ±750*V*
- Output Voltage: ±750*V*

Core material

- Nanocrystalline VITROPERM 500F
- U cores

Windings

- Copper
- Litz wire

Cooling

- Winding - Forced air
- Core - Heatsinks (Forced air)

Insulation

- Solid - Cast resin

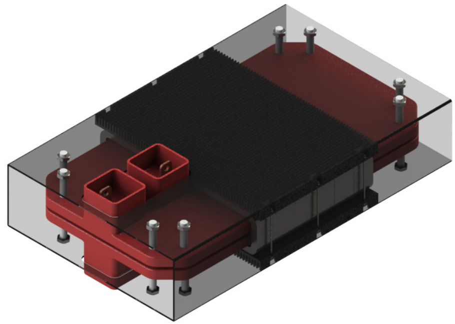

▲ 100kW Planar MFT by PEL.

MFT dimensions

- Volume: 18.5l
- V-Density: 5.4kW/l
- Weight: 26.3kg
- W-Density: 3.8kW/kg

Insulation tests

- PD: 5kV, 50Hz
- BIL: not reported

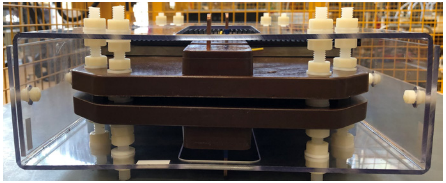

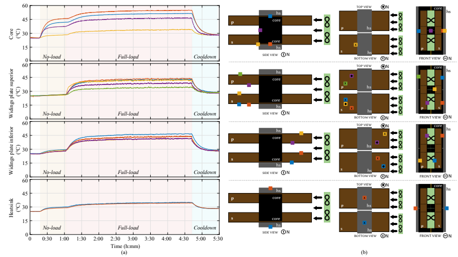

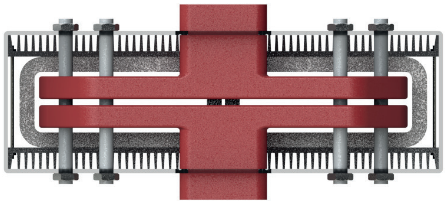

▲ MFT by PEL.

RWTH SCHAFFNER MFT - 2019

Construction

- 3-phase Core type

Electrical ratings

- Power: 5MW
- Frequency: 1kHz
- Input Voltage:
- Output Voltage:

Core material

- Grain oriented silicon steel
- U cores

Windings

- Copper
- Foil

Cooling

- Winding - Air
- Core - Air

Insulation

- Core in the air
- NOMEX/Mica tape?

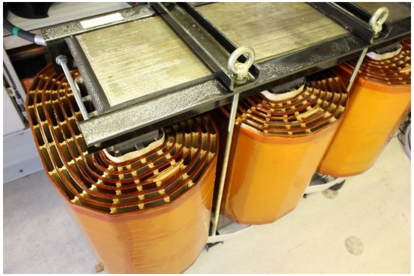

▲ 5MW 3-phase MFT by Schaffner [60].

MFT dimensions

- Volume: not reported
- V-Density: not reported
- Weight: less than 700kg
- W-Density: > 7.1kW/kg

Insulation tests

- PD, BIL: not reported

▲ MFT by Schaffner.

SUPERGRID INSTITUTE MFT - 2019

Construction
- Core type

Electrical ratings
- Power: 100kW
- Frequency: 20kHz
- Input Voltage: ± 1.2kV
- Output Voltage: ± 1.2kV

Core material
- Ferrite
- I cores

Windings
- Copper
- Litz wire

Cooling
- Winding - Forced air

Insulation
- Core in the air

▲ 100kW MFT by Supergrid Institute [61].

MFT dimensions
- Volume: not reported
- V-Density: not reported
- Weight: not reported
- W-Density: not reported

Insulation tests
- PD, BIL: not reported

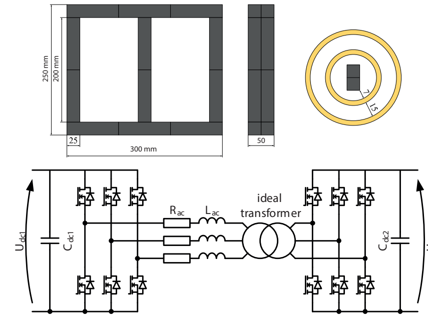

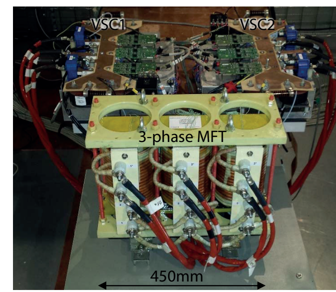

▲ MFT by Supergrid Institute.

Construction

- Core type

Electrical ratings

- Power: 300kW
- Frequency: 20kHz
- Input Voltage: ± 1.7kV
- Output Voltage: ± 4kV

Core material

- Nanocrystalline
- UU cores

Windings

- Copper
- Litz wire

Cooling

- Winding -Forced air
- Core - Forced air

Insulation

- Winding - Solid, cast resin
- Core - Air

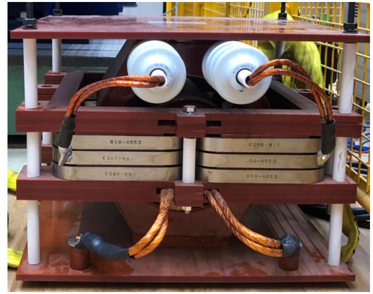

▲ 300kW Planar MFT by PEL and Hyosung.

MFT dimensions

- Volume: 62l
- V-Density: 4.8kW/l
- Weight: 39.7kg
- W-Density: 7.55kW/kg

Insulation tests

- PD: not reported
- BIL: not reported

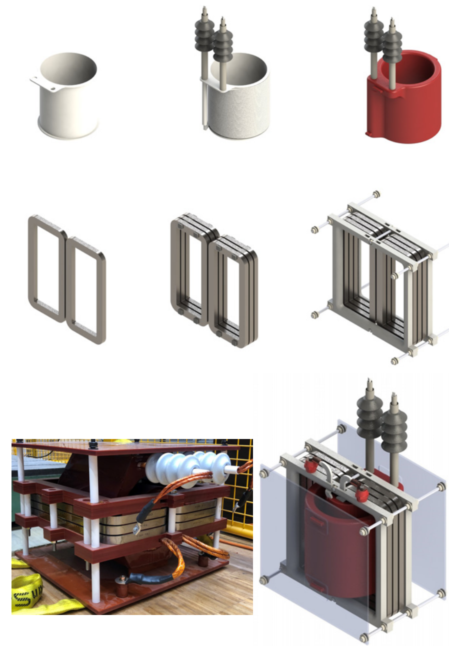

▲ MFT by PEL and Hyosung.

Construction

- Air core
- Aluminum conductive shielding

Electrical ratings

- Power: 166kW
- Frequency: 77.4kHz
- Input Voltage: ± 7kV
- Output Voltage: ± 7kV

Windings

- Copper
- Litz wire
- Cylindrical solenoids

Cooling

- Winding - Forced air

Insulation

- NOMEX pressboard

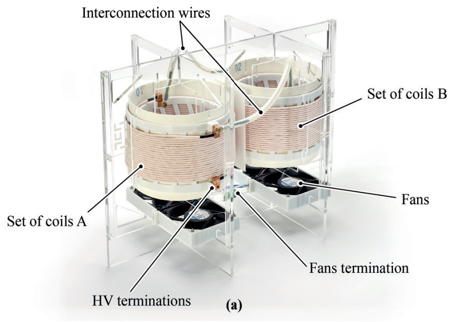

▲ 166kW MFT by ETH [62].

MFT dimensions

- Volume: not reported
- V-Density: not reported
- Weight: 10.1kg
- W-Density: 16.5kW/kg

Insulation tests

- PD, BIL: not reported

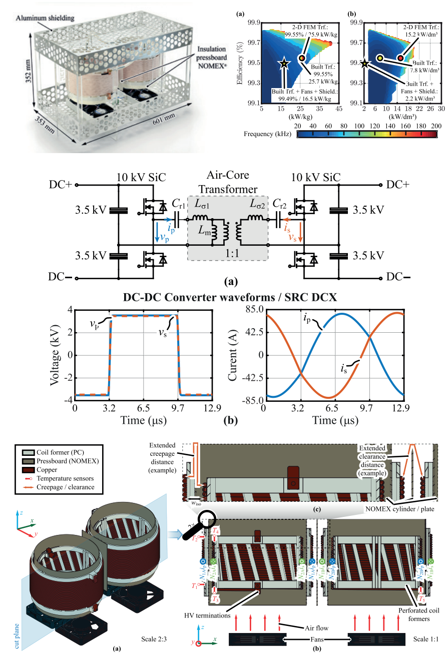

▲ MFT by ETH.

SUMMARY - MFT DESIGNS

Variety of MFT designs

- Shell Type, Core Type, C-Type
- Copper, Aluminum
- Solid wire, Hollow conductors, Litz wire, Foil
- SiFe, Nanocrystalline, Amorphous, Ferrite

Integration with Power Electronics

- Insulation coordination
- Cooling
- Electrical parameters
- Choice of core materials
- Form factor constraints
- Optimization at the system level

Custom designs prevail

There is no best design...

Limited commercial options. Example: STS ⇒

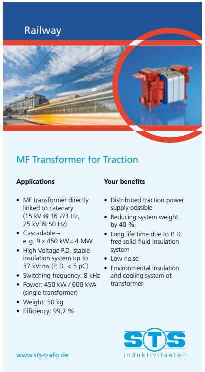

Source/ Type	P_n kVA	Freq. kHz	U_{iso} kV	Core mat.*	Cooling method	Tran. Power density†	Eff.⋆ %	Struct./ Wind.+
GE:1992[65] Dry	50	50	N/A	Ferr.	Air	12(wt)	$99.4^{a,c}$	Coaxial/ Cable
GE:2008[66] Dry	150	10	N/A	Amor.	Air	N/A	N/A	Core/ Ro. Litz
UWM:1995[67] Dry	120	20.4	N/A	Ferr.	Water	59.5(vol)	$99.6^{a,c}$	Coaxial/ Cable
ABB:2002[43] Dry	350	10	15	Nano.	Water	>7(wt)‡	N/A	Coaxial/ Cable
ABB:2007[47] Oil	75	0.4	15	Si-Fe	Oil	N/A	$>95^{b,c}$	So. Cu
ABB:2011[50, 52] Oil	150	1.75	15	Nano.	Oil	N/A	$\approx 96^{b,c}$	Ro. Litz
KTH:2009[68] Oil	170	4	30	Amor.	Water Oil	3.45(wt)	$99^{a,c}$	Shell/ Ro. Litz Foil
TUD:2005[69, 70] Dry	50	25	N/A	Nano.	Water	≈50(vol)	$>97^{b,c}$	Shell/ Foil
Bomb:2007[30] Dry	500	8	15	Nano.	Water	27.8(wt)	N/A	Shell/ Hol. Al
FAU:2011[71] Oil	450	5.6	25	Nano.	Water Oil	N/A	N/A	Core/ Hol. Al
NCSU:2010[72]◇ Dry	10	3	15	Amor.	Air	N/A	$96.76^{a,c}$ $97.3^{a,c}$ $97.16^{a,c}$	Core/ Ro. Litz
NCSU:2012[73] Dry	30	20	9.5	Nano.	Air	N/A	$99.5^{a,d}$	Coaxial/ Ro. Litz So. Cu
EPFL:2010[8] Dry	25	2	8	Amor.	Air	2.5(vol)	$99.13^{a,d}$	Shell/ Rec. Litz
IK4:2012[74]◇ Dry	400	<1 >5	18	Si-Fe Nano.	Air Fan	3.41(vol) 14.88(vol)	$99.36^{a,d}$ $99.76^{a,d}$	Shell Core
ETH:2013[14, 23]◇ Dry	166	20	N/A	Nano. Ferr.	Water Fan	32.7(vol) 8.21(vol)	$99.5^{a,c}$ $99.4^{a,c}$	Shell/ Rec. Litz
ETH:2015[75]◇ Dry	25	25 50 83	N/A	Ferr.	Air	8.2(vol) 13.3(vol) 15.9(vol)	N/A	Matrix/ Litz
Chalm:2016[76]◇ Dry	50	5	6	Nano. Ferr.	Air Air	15.1(vol) 11.5(vol)	$99.66^{a,c}$ $99.58^{a,c}$	Shell/ Rec. Litz
STS:2014[77] Oil/Dry∇	450	8	>30	N/A	Oil Air	9(wt)	$99.7^{a,c}$	Shell/ Litz

▲ Another overview of MFTs reported in literature [63]

MFT DESIGN OPTIMIZATION

Optimal design and realization of a 1MW MFT...

- Multi-objective optimization problem
- Multiple competing objectives
- Meeting converter parameters
- Respecting constraints
- Manufacturability

▼ Source: (https://formlabs.com/ch/)

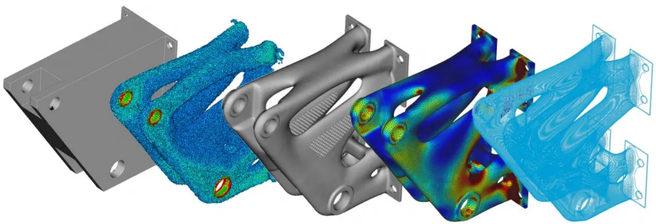

Genetic Algorithm

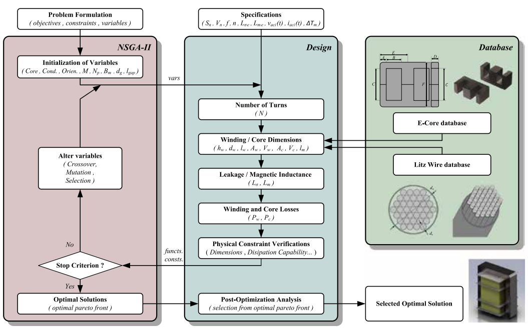

▲ Design flowchart using NSGA-II algorithm [64]

Neural Networks

- ANN must be trained somehow
- Measurements, simulations, FEM, datasheets

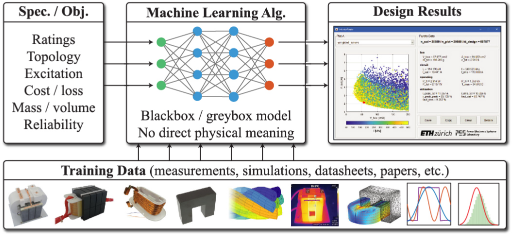

▲ Inductor design with the help of ANN [65]

Brute Force

- Exhaustive search concept
- All possible combinations
- Computationally intensive
- Easy to implement

▲ 10'000 combinations

MFT DESIGN OPTIMIZATION

Numerous variants of the brute force algorithm for MFT design exist:

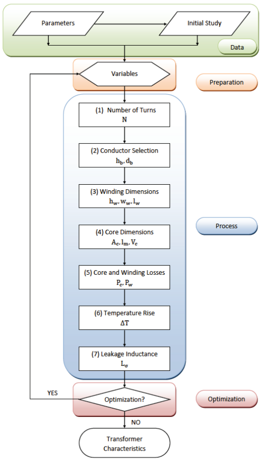

EPFL PhD: Villar [66]

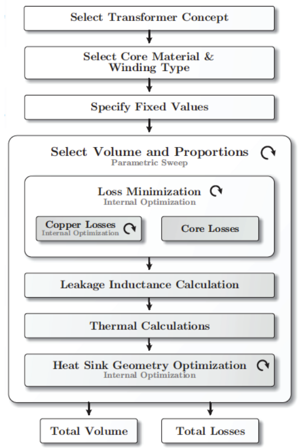

ETHZ PhD: Ortiz [51]

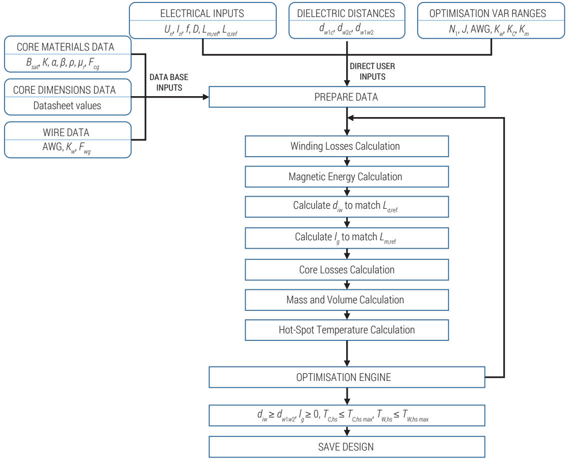

EPFL PhD: Mogorovic [67]

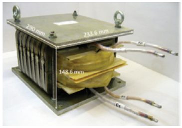

EPFL: 300kW, 2kHz

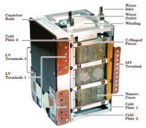

ETHZ: 166kW, 20kHz

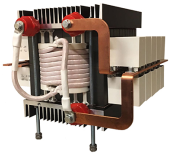

EPFL: 100kW, 10kHz

1 MW DC transformer for MVDC power distribution networks

- Resonant energy conversion, LLC converter
- Bulk power processing
- Reverse conducting IGCTs as switching devices, DI water cooling
- 10 kV (engineering samples) for the primary and 4.5 kV devices for the secondary converter side

Medium frequency transformer:

- Galvanic isolation, voltage adaptation
- Electrical MFT design requirements:

Characteristics	Unit	Value
Frequency	kHz	5
Nominal Power	MW	1
Turns Ratio	1	2 : 1
Primary Voltage	kV	±5
Secondary Voltage	kV	±2.5
Ref. magn. inductance	mH	25 – 40
Ref. leakage inductance	μH	25 – 50

- Compromise between multiple design criteria - **highest efficiency!**

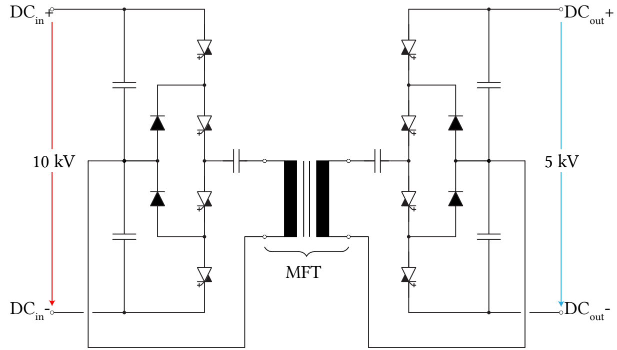

▲ DC transformer with 3-level NPC power stages, IGCT based.

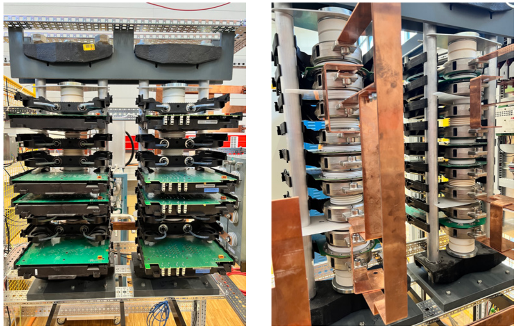
(a) (b)

▲ IGCT stacks used for the two power stages of the 1 MW DCT demonstrator.

Construction Choices:

- MFT Types

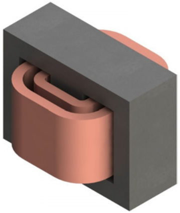

Shell Type

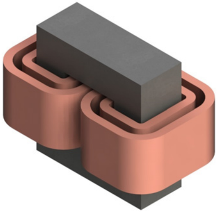

Core Type

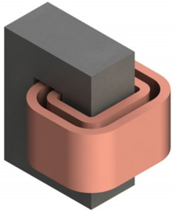

C-Type

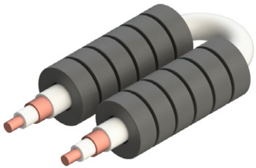

Coaxial Type

- Winding Types

Litz Wire

Foil

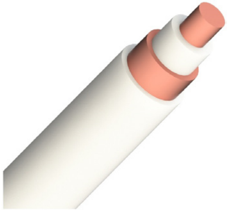

Coaxial

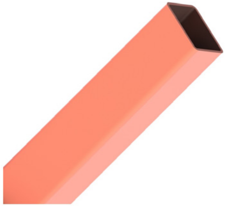

Hollow/Pipes

Materials:

- Magnetic Materials
  - **Silicon Steel**
  - **Amorphous**
  - **Nanocrystalline**
  - Ferrites
- Windings
  - **Copper**
  - Aluminum
- Insulation
  - **Air**
  - Solid
  - **Oil**
- Cooling
  - **Air natural**/forced
  - Oil natural/forced
  - **Water**

MFT WINDING ARRANGEMENTS

1-layer MFT structure:

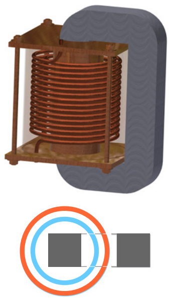

- Single oil vessel with 1 layer of PW and SW
- PW placed closer to the core limb to reduce its length, due to double number of turns
- Lower pressure drop on PW
- For optimal use of the core window area, different conductor's cross section profiles for PW and SW
- By design selection, PW and SW current densities kept equal
- Simple mechanical realization

2-vessel MFT structure:

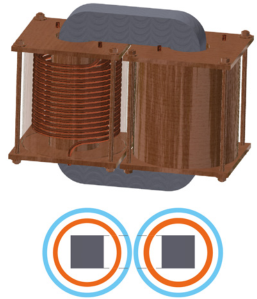

- Two oil vessels each with 1 layer of PW and SW
- One conductor type for both windings
- Correct turns ratio achieved by external electrical connection, PWs connected in series, SWs in parallel
- Equal current density in both windings
- More complicated realization, requires winding termination panel
- Number of windings doubled compared to 1-layer MFT

3-winding MFT structure:

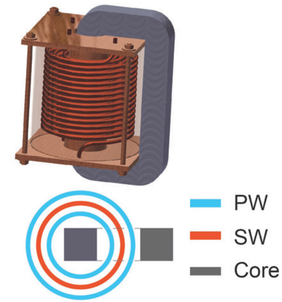

- Single oil vessel with PW interleaved around the SW
- Improved power density with 3 windings
- For optimal use of the core window area, the same conductor type used
- PW current density is 2 times smaller than the SW one
- Necessary turns ratio can be achieved inside or outside the oil vessel

MFT WINDING ARRANGEMENTS

1-layer MFT structure:

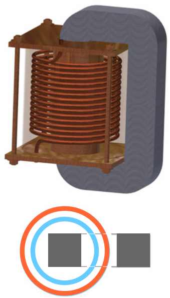

- Single oil vessel with 1 layer of PW and SW
- PW placed closer to the core limb to reduce its length, due to double number of turns
- Lower pressure drop on PW
- For optimal use of the core window area, different conductor's cross section profiles for PW and SW
- By design selection, PW and SW current densities kept equal
- Simple mechanical realization

2-vessel MFT structure:

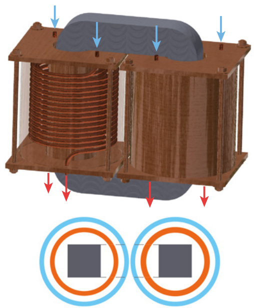

- Two oil vessels each with 1 layer of PW and SW
- One conductor type for both windings
- Correct turns ratio achieved by external electrical connection, PWs connected in series, SWs in parallel
- Equal current density in both windings
- More complicated realization, requires winding termination panel
- Number of windings doubled compared to 1-layer MFT

3-winding MFT structure:

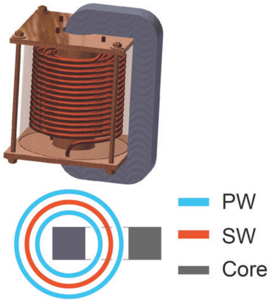

- Single oil vessel with PW interleaved around the SW
- Improved power density with 3 windings
- For optimal use of the core window area, the same conductor type used
- PW current density is 2 times smaller than the SW one
- Necessary turns ratio can be achieved inside or outside the oil vessel

Design optimization algorithm flowchart:

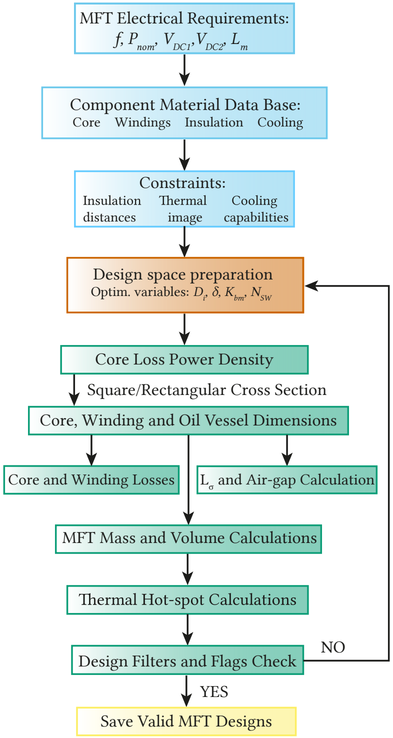

1) User-defined inputs:

- Electrical requirements
- Insulation, thermal, mechanical constraints (flags)
- Data sheets and material characteristics

2) Design optimization variables:

Var.	Min.	Max.	Res.	Description
D_i	3 mm	8 mm	16	Inner diameter
δ	$0.9\delta_{Cu}$	$2.2\delta_{Cu}$	14	Wall thickness
N_{SW}	10	45	36	SW turns number
K_{bm}	0.2	0.9	80	Flux density ratio

3) Design evaluation based on models, design filters and flags:

- Pipe winding loss model
- Thermal-hydraulic model of the oil
- Core to winding loss ratio (R_{WC})
- Minimal current and power density

4) Storing of valid MFT designs

Additional MFT models required!!

Optimal selection: 2-vessel core-type MFT with nanocrystalline material

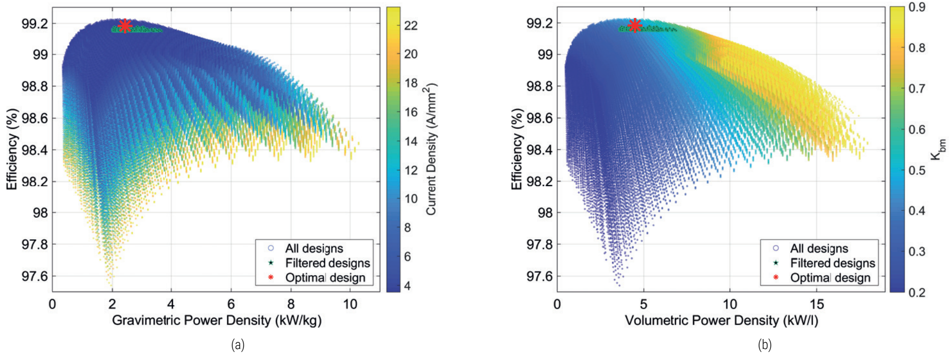

▲ (a) Efficiency vs. weight power density; (b) Efficiency vs. volume power density.

- **Applied design filters:**

R_{wc}	J	kW/kg
≤ 0.33	$\geq 6\,\mathrm{A\,mm^{-2}}$	≥ 2

- **Optimal MFT design specifications with the highest efficiency:**

D_i	δ	N_{PW}	N_{SW}	K_{bm}	$P_{loss,PW}$	$P_{loss,SW}$	P_{core}
7.6 mm	1.3 mm	34	17	0.475	2.87 kW	2.67 kW	2.67 kW
R_{wc}	J	kW/kg	kW/l	W	L	H	η
0.32	$6.1\,\mathrm{A\,mm^{-2}}$	2.36	3.47	494 mm	851 mm	685 mm	99.18%

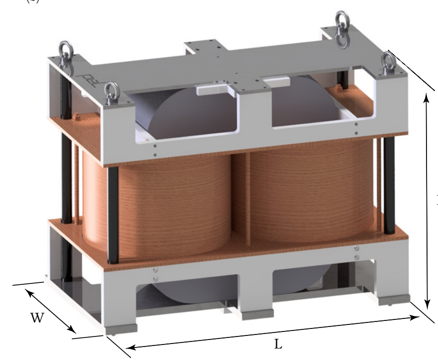

▲ 3D CAD render of the MFT prototype.

MFT PROTOTYPE ASSEMBLY (I)

Properties of the fully assembled MFT core: [68]

A	B	C	D	M_c
140 mm	256 mm	318 mm	232 mm	≈ 324 kg

- 4 sets put together to assemble the core
- Rectangular cross section
- Core supplied by Hitachi Metals [69]

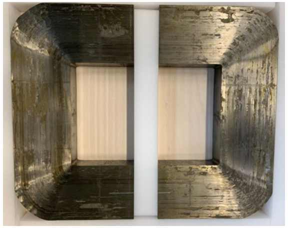

(a)

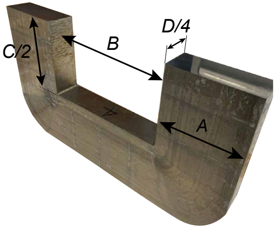

(b)

▲ Nanocrystalline material: (a) Set of two C-cut cores; (b) Single C-cut core.

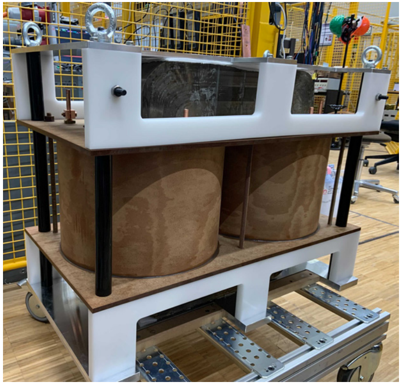

▲ Full-scale prototype of the 2-vessel MFT.

(c)

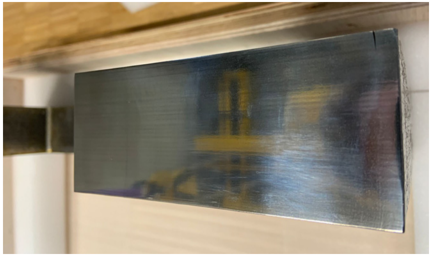

(d)

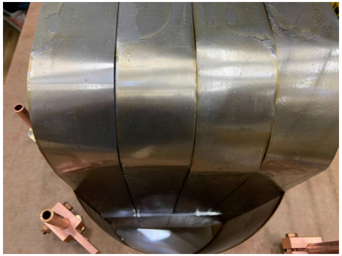

(e)

▲ (a) Side view of the MFT core; (b) Cross section surface of a single C-core; (c) Top view of the upper core half.

[68] Nikolina Djekanovic and Drazen Dujic. "Design Optimization of a MW-level Medium Frequency Transformer." *PCIM Europe 2022*. 2022, pp. 1–10

Pipe windings assembly:

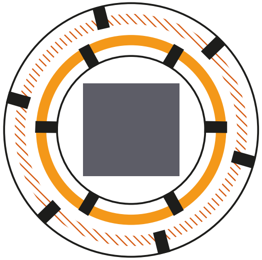
(a)


(b)

▲ (a) Spacer positioning inside the vessel; (b) Comb-alike spacers mounted every 60° on the SW from the inside.

- Soft temper copper, made by Luvata [70], used for winding realization
- Spacers made of thermoplastic POM material
- Oil vessels, made of phenolic paper composite material Etronit I and B66, produced by Elektro-Isola [71]
- Midel 7131 [72] insulation fluid used
- Instead of oil expansion vessel a sufficient air pocket is left in each vessel
- Air breathers filled with silica gel used to keep moisture and particles away


(c)


(d)


(e)

▲ (a) Mandrel bending approach; (b) Left vessel with oil, spacers and pair of windings; (c) In between the vessels.

MFT ELECTRICAL PARAMETER TESTING

Comparison of measured and modeled electrical parameters:

- Leakage inductance

L_σ(µH)	An.model	FEM	RLC	Bode 100
0 Hz	43.8	44.3	–	–
5 kHz	–	34	38.2	37.9

- Magnetizing inductance

L_m(mH)	Ref. value	RLC	Bode 100
5 kHz	35.77*	36.66	36.74

∗ - corresponds to 1 mm total air gap

Final MFT prototype dimensions:

M_{MFT}	kW/kg	kW/l	W^*	L^*	H^*
462 kg	2.17	1.59	778 mm	851 mm	950 mm

▲ 1 MW prototype of the 2-vessel MFT structure.

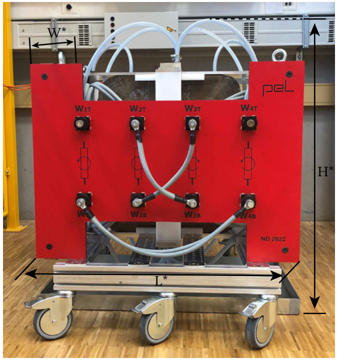

▲ Fully assembled prototype of the 2-vessel MFT.

DIRECT CURRENT TRANSFORMER

Operating principles, features, power reversal methods, and practical examples.

AC VS DC TRANSFORMER

AC Transformer

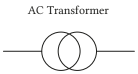

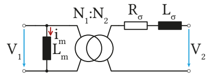

▲ Symbol and schematic

General considerations

- Simple
- Relatively cheap
- Very high efficiency

⇒ Essential for AC grids

DC Transformer

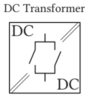

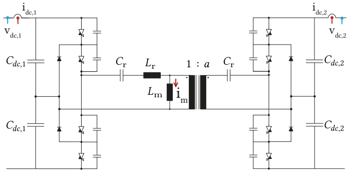

▲ Symbol and schematic

General considerations

- Complex
- Expensive
- Semiconductor losses

⇒ Essential for advanced DC grids

AC VS DC TRANSFORMER

AC Transformer

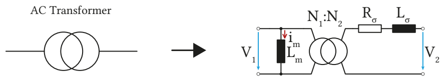

▲ Symbol and schematic

Features

- Naturally bidirectional
- Transient expected for 5-10x
- No-load losses

DC Transformer

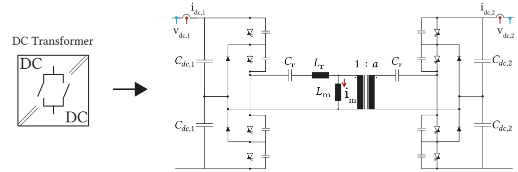

▲ Symbol and schematic

Features

- Power Reversal Algorithm
- Soft-Start
- Idle Mode
- Over-Load protection

AC VS DC TRANSFORMER

AC Transformer

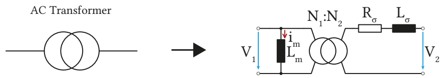

▲ Symbol and schematic

DC Transformer

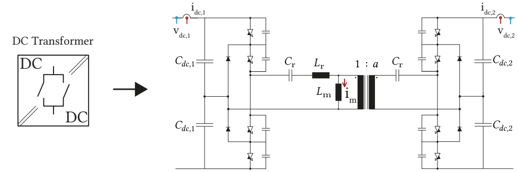

▲ Symbol and schematic

DCT and open-loop operation

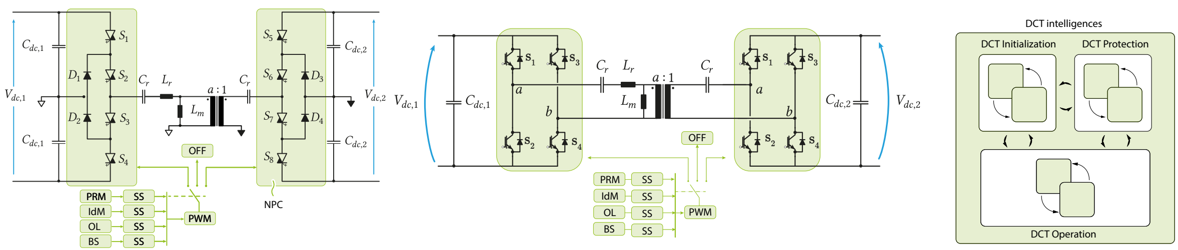

(a) MV DCT (b) LV DCT (c) Control

LVDC TRANSFORMERS (I)

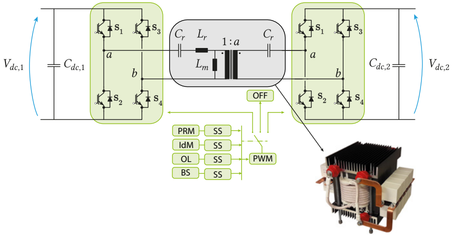

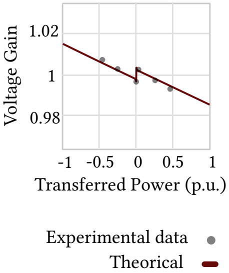

▲ DCT 1 with FB power stages

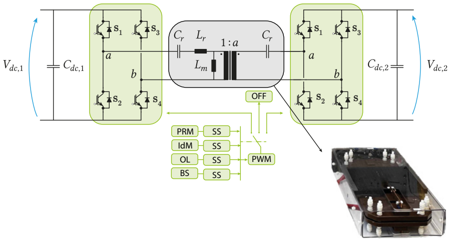

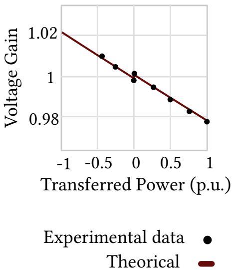

▲ DCT 2 with FB power stages

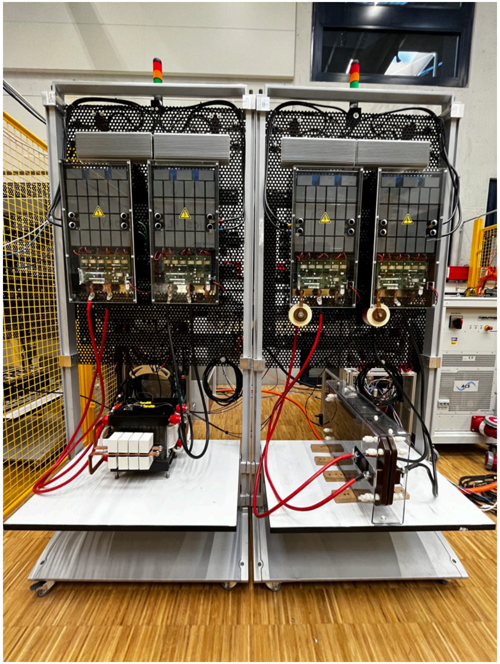

▲ Photo of the two low voltage DCTs of the Laboratory

DCT Operation - Example

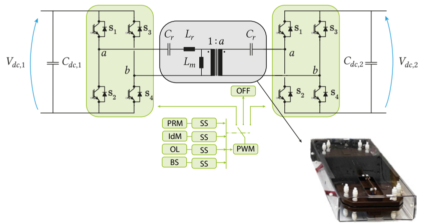

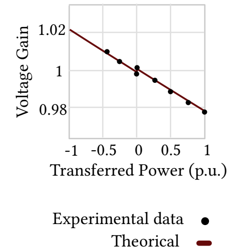

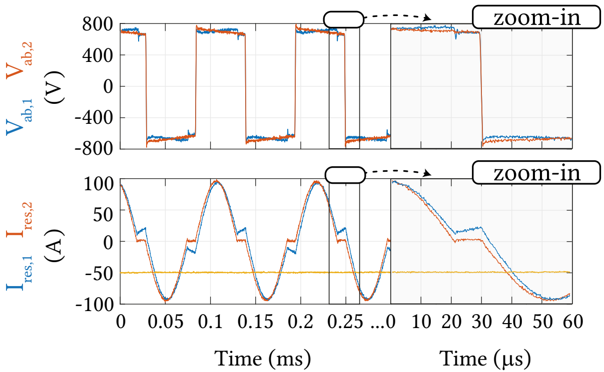

▲ Subresonant operation

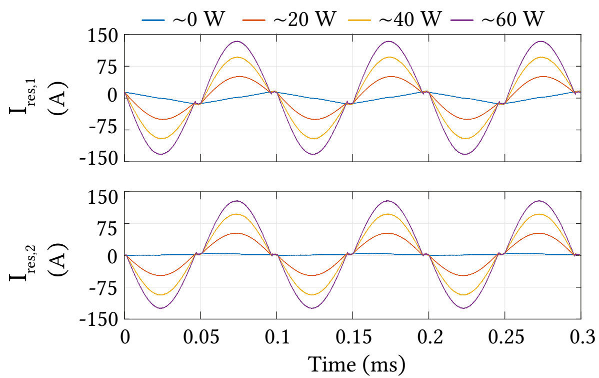

▲ Resonant Currents

Soft-start strategy

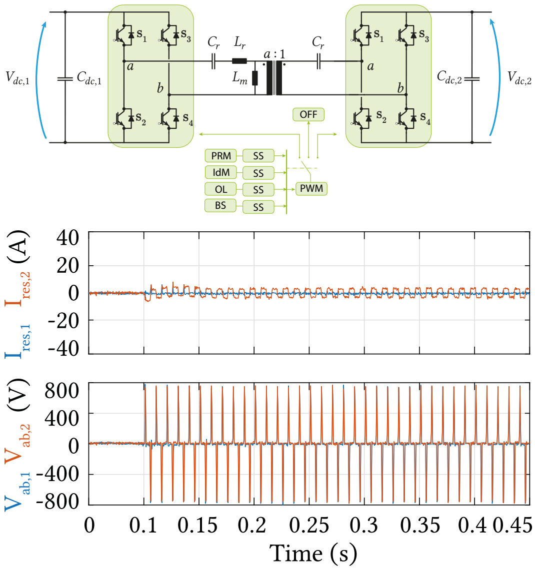

▲ Soft-start strategy

Soft-start with different speed

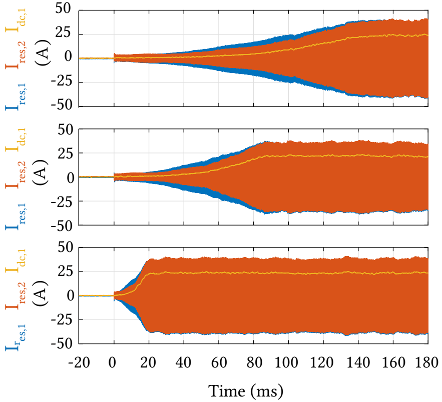

▲ Resonant currents and DC current

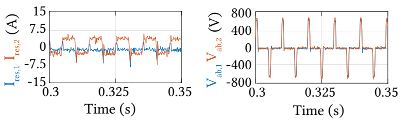

▲ Three-level waveform experiments

Power Reversal Algorithm (I)

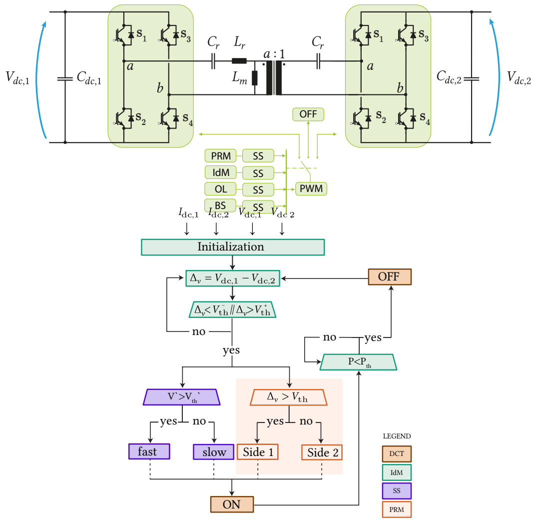

▲ Power Reversal Algorithm

Experimental results for a step change

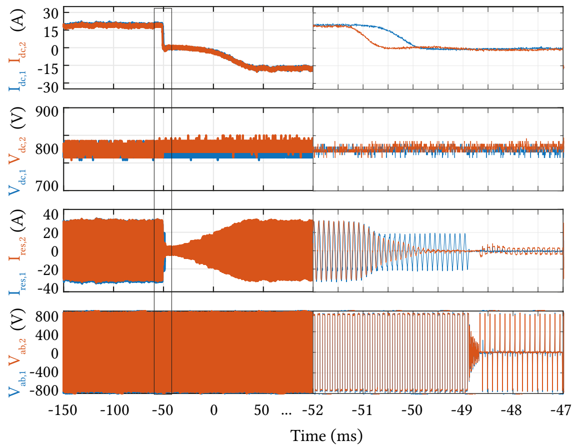

Power Reversal Algorithm (II)

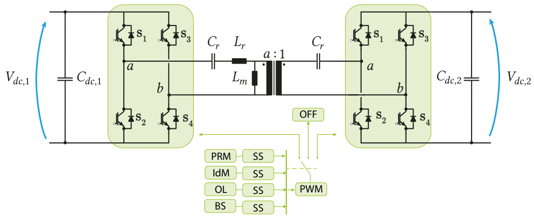

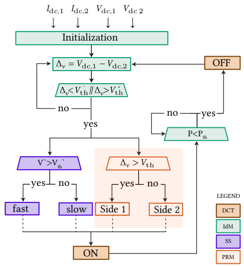

- Experimental results for ramp change and zoom in each stage

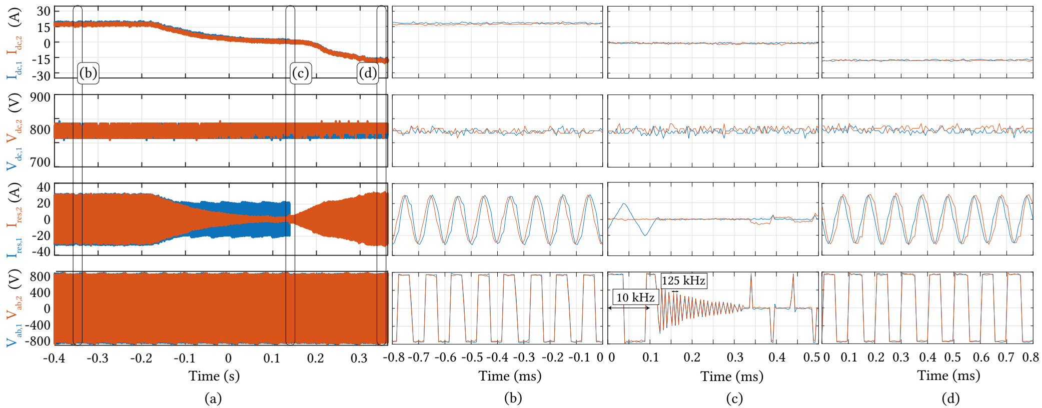

Idle Mode

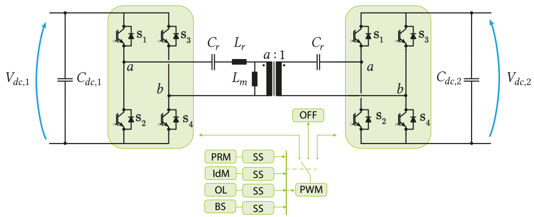

Idling Mode

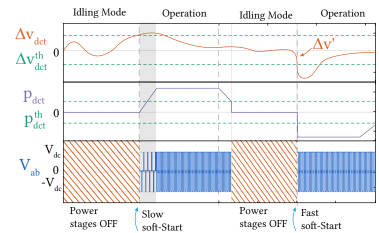

- Experimental results for Idle mode and zoom in each stage

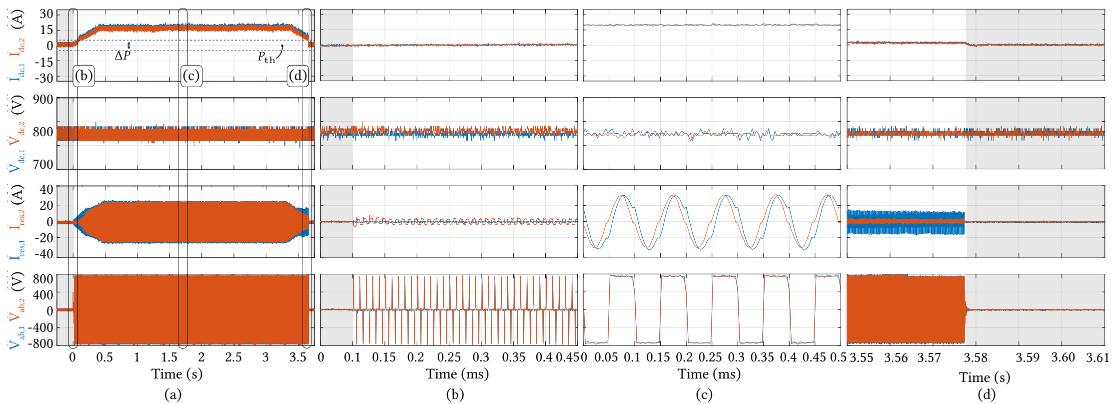

DCT - FEATURES AND EXPERIENCE (V)

Current limiting and Overload protection

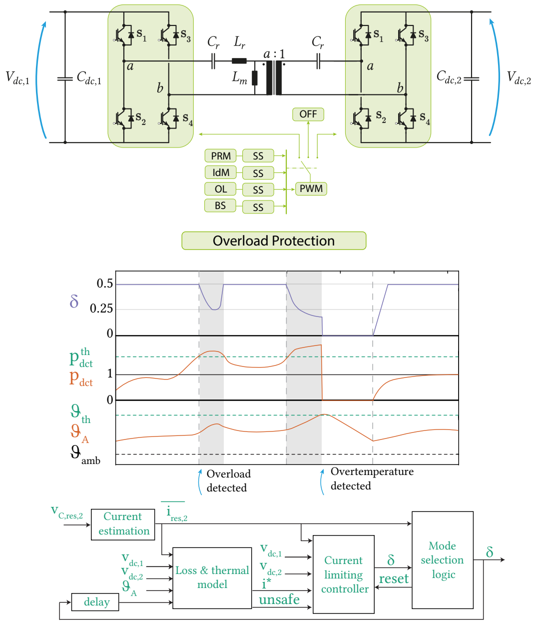

▲ Current limiting strategy

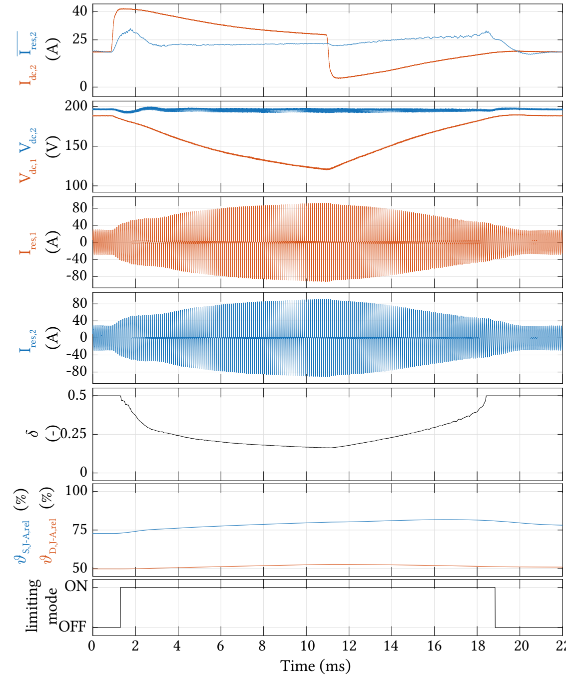

▲ Experimental results for current limiting strategy.

Parallel Operation

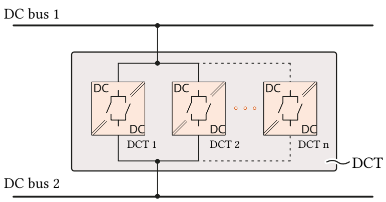

▲ Schematic for the parallel arrangement [73]

Input impedance

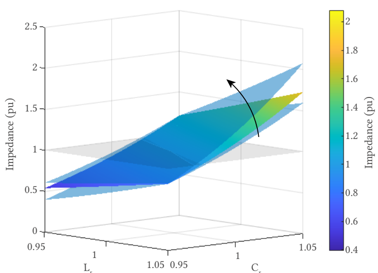

▲ Impact of switching frequency

At 10 kHz

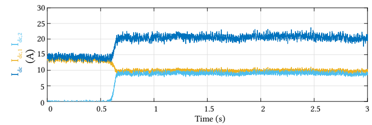

(a) DCT 1 = 10 kHz, DCT 2 = 10 kHz, $P_{dc} \approx 17$ kW

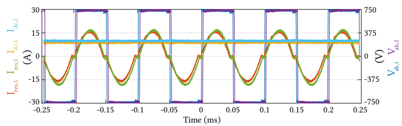

(b) DCT 1 = 10 kHz, DCT 2 = 10 kHz, $P_{dc} \approx 17$ kW

At 11 kHz

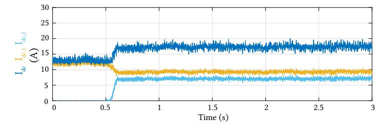

(c) DCT 1 = 10 kHz, DCT 2 = 11 kHz, $P_{dc} \approx 17$ kW

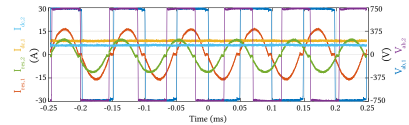

(d) DCT 1 = 10 kHz, DCT 2 = 11 kHz, $P_{dc} \approx 17$ kW

[73] Renan Pillon Barcelos and Drazen Dujic. "Scalability Assessment of the Parallel Operation of Direct Current Transformers." *CPSS Transactions on Power Electronics and Applications*. 2023

DCT in a DC Power Distribution Network

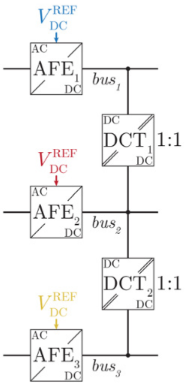

DCT Model:

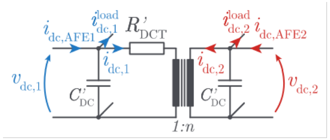

Experimental results

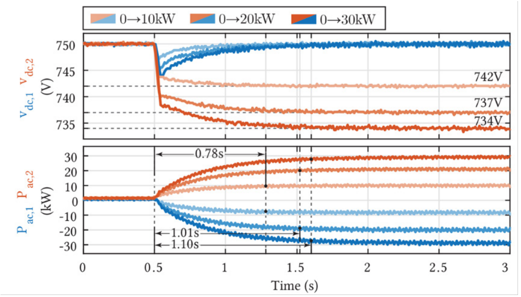

(a) VR-VR

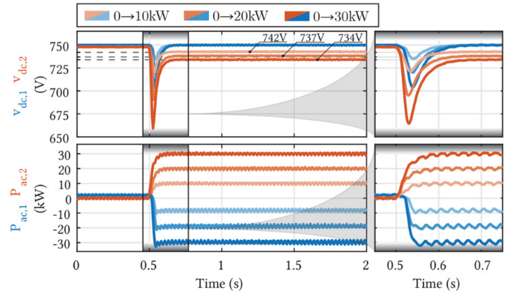

(b) VR-PR

SUMMARY AND CONCLUSIONS

Why DC? How DC? and When DC?

MVDC BULK POWER CONVERSION

MVDC Power Distribution Networks

- Feasibility
- Technology readiness
- Standards

Conversion

- Modular
- Bulk
- Performances

Applications

- Business Case - Owner
- Business Case - OEM
- Business Case - in general

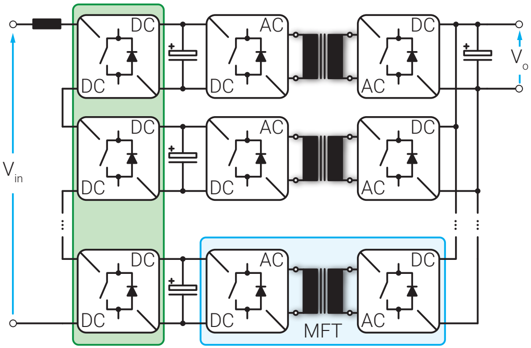

▲ Modular power processing

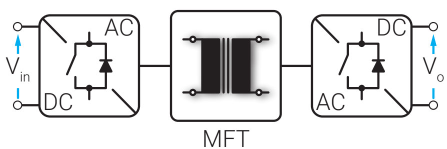

▲ Bulk power processing

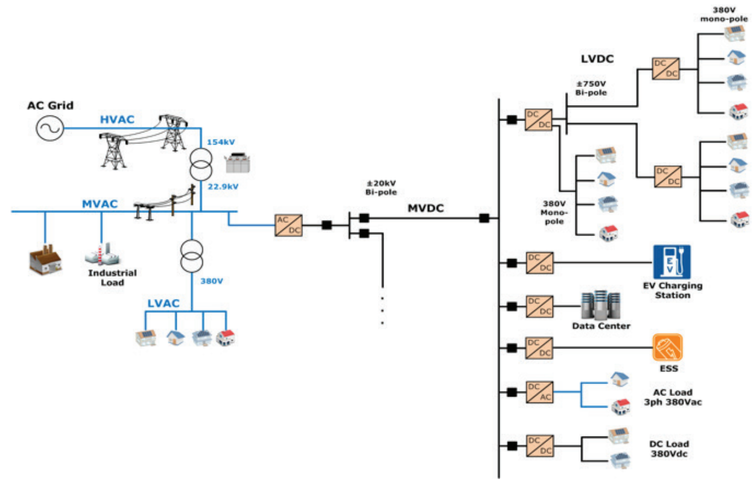

▲ Envisioned future MVDC grids and its links with existing grids

REFERENCES

[1] Uzair Javaid et al. “MVDC supply technologies for marine electrical distribution systems.” *CPSS Transactions on Power Electronics and Applications* 3.1 (2018), pp. 65–76.

[2] Alessandro Clerici, Luigi Paris, and Per Danfors. “HVDC conversion of HVAC lines to provide substantial power upgrading.” *IEEE transactions on Power Delivery* 6.1 (1991), pp. 324–333.

[3] Michael Häusler, Gernot Schlayer, and Gerd Fitterer. “Converting AC power lines to DC for higher transmission ratings.” *ABB review* (1997), pp. 4–11.

[4] D Marene Larruskain et al. “Conversion of AC distribution lines into DC lines to upgrade transmission capacity.” *Electric Power Systems Research* 81.7 (2011), pp. 1341–1348.

[5] D Marene Larruskain et al. “VSC-HVDC configurations for converting AC distribution lines into DC lines.” *International Journal of Electrical Power & Energy Systems* 54 (2014), pp. 589–597.

[6] ABB. *Tjæreborg*. `http://new.abb.com/systems/hvdc/references/tjaereborg`.

[7] Charles Bodel. *Paimpol-Bréhat tidal demonstrator project*. `http://eusew.eu/sites/default/files/programme-additional-docs/EUSEW1606160PresentationtoEUSEWbyEDF.pdf`. EDF.

[8] G. Bathurst, G. Hwang, and L. Tejwani. “MVDC - The New Technology for Distribution Networks.” *11th IET International Conference on AC and DC Power Transmission*. Feb. 2015, pp. 1–5.

[9] SP Energy Networks. *Angle dc*. `https://www.spenergynetworks.co.uk/pages/angle_dc.aspx`.

[10] S. Inoue and H. Akagi. “A Bidirectional Isolated DC-DC Converter as a Core Circuit of the Next-Generation Medium-Voltage Power Conversion System.” *IEEE Transactions on Power Electronics* 22.2 (Mar. 2007), pp. 535–542.

[11] Johann W Kolar and Gabriel Ortiz. “Solid-state-transformers: key components of future traction and smart grid systems.” *Proc. of the International Power Electronics Conference (IPEC), Hiroshima, Japan*. 2014.

[12] D. Dujic et al. “Power Electronic Traction Transformer-Low Voltage Prototype.” *IEEE Transactions on Power Electronics* 28.12 (Dec. 2013), pp. 5522–5534.

[13] C. Zhao et al. “Power Electronic Traction Transformer-Medium Voltage Prototype.” *IEEE Transactions on Industrial Electronics* 61.7 (July 2014), pp. 3257–3268.

[14] M. K. Das et al. “10 kV, 120 A SiC half H-bridge power MOSFET modules suitable for high frequency, medium voltage applications.” *2011 IEEE Energy Conversion Congress and Exposition*. Sept. 2011, pp. 2689–2692.

[15] A. Q. Huang. “Medium-Voltage Solid-State Transformer: Technology for a Smarter and Resilient Grid.” *IEEE Industrial Electronics Magazine* 10.3 (Sept. 2016), pp. 29–42.

[16] D. Wang et al. “A 10-kV/400-V 500-kVA Electronic Power Transformer.” *IEEE Transactions on Industrial Electronics* 63.11 (Nov. 2016), pp. 6653–6663.

[17] Xiaodong Zhao et al. “DC Solid State Transformer Based on Three-Level Power Module for Interconnecting MV and LV DC Distribution Systems.” *IEEE Transactions on Power Electronics* 36.2 (2021), pp. 1563–1577.

[18] R. W. A. A. De Doncker, D. M. Divan, and M. H. Kheraluwala. “A three-phase soft-switched high-power-density DC/DC converter for high-power applications.” *IEEE Transactions on Industry Applications* 27.1 (Jan. 1991), pp. 63–73.

[19] R. Withanage and N. Shammas. “Series Connection of Insulated Gate Bipolar Transistors (IGBTs).” *IEEE Transactions on Power Electronics* 27.4 (Apr. 2012), pp. 2204–2212.

[20] IA Gowaid et al. “Analysis and design of a modular multilevel converter with trapezoidal modulation for medium and high voltage DC-DC transformers.” *IEEE Transactions on Power Electronics* 30.10 (2015), pp. 5439–5457.

[21] IA Gowaid et al. “Quasi two-level operation of modular multilevel converter for use in a high-power DC transformer with DC fault isolation capability.” *IEEE Transactions on Power Electronics* 30.1 (2015), pp. 108–123.

[22] Stephan Kenzelmann et al. “Isolated DC/DC structure based on modular multilevel converter.” *IEEE Transactions on Power Electronics* 30.1 (2015), pp. 89–98.

[23] Stefan Milovanovic and Drazen Dujic. “Comprehensive analysis and design of a quasi two-level converter leg.” *CPSS Transactions on Power Electronics and Applications* 4.3 (2019), pp. 181–196.

[24] S. Milovanovic and D. Dujic. “MMC-Based High Power DC-DC Converter Employing Scott Transformer.” *PCIM Europe 2018*. June 2018, pp. 1–7.

[25] Jakub Kucka and Drazen Dujic. “Smooth Power Direction Transition of a Bidirectional LLC Resonant Converter for DC Transformer Applications.” *IEEE Transactions on Power Electronics* 36.6 (2021), pp. 6265–6275.

[26] Umamaheswara Vemulapati et al. “Recent advancements in IGCT technologies for high power electronics applications.” *2015 17th European Conference on Power Electronics and Applications (EPE’15 ECCE-Europe)*. 2015, pp. 1–10.

[27] Dragan Stamenkovic et al. “Soft Switching Behavior of IGCT for Resonant Conversion.” *2019 IEEE Applied Power Electronics Conference and Exposition (APEC)*. 2019, pp. 2714–2719.

[28] Dragan Stamenković et al. “IGCT Low-Current Switching—TCAD and Experimental Characterization.” *IEEE Transactions on Industrial Electronics* 67.8 (2020), pp. 6302–6311.

[29] Gabriele Ulissi et al. "High-Frequency Operation of Series-Connected IGCTs for Resonant Converters." *IEEE Transactions on Power Electronics* 37.5 (2022), pp. 5664–5674.

[30] ABB. "Applying IGCT Gate Units." *Application Note 5SYA 2031-05* (2017).

[31] Zhengyu Chen et al. "Stray Impedance Measurement and Improvement of High-Power IGCT Gate Driver Units." *IEEE Transactions on Power Electronics* 34.7 (2019), pp. 6639–6647.

[32] H. Gruening et al. "6 kV 5 kA RCGCT with advanced gate drive unit." *Proceedings of the 13th International Symposium on Power Semiconductor Devices and ICs. IPSD01*. 2001, pp. 133–136.

[33] Luyao Xie, Xinmin Jin, and Yibin Tong. "The design of IGCT Gate-Unit equipped in the three-level NPC converter." *2011 International Conference on Electrical Machines and Systems*. 2011, pp. 1–6.

[34] H.E. Gruening and K. Koyanagi. "A modern low loss, high turn-off capability GCT gate drive concept." *2005 European Conference on Power Electronics and Applications*. 2005, 10 pp.–P.10.

[35] Jakub Kucka and Drazen Dujic. "SOFTGATE – An IGCT Gate Unit for Soft Switching." *PCIM Europe 2022; International Exhibition and Conference for Power Electronics, Intelligent Motion, Renewable Energy and Energy Management*. 2022, pp. 1–9.

[36] Jakub Kucka and Drazen Dujic. "IGCT Gate Unit for Zero-Voltage-Switching Resonant DC Transformer Applications." *IEEE Transactions on Industrial Electronics* 69.12 (2022), pp. 13799–13807.

[37] Jakub Kucka and Drazen Dujic. "Shoot-Through Protection for an IGCT-Based ZVS Resonant DC Transformer." *IEEE Transactions on Industrial Electronics* (2022), pp. 1–1.

[38] Dragan Stamenkovic. "IGCT Based Solid State Resonant Conversion." PhD thesis. EPFL, 2020.

[39] Gabriele Ulissi et al. "Resonant IGCT Soft-Switching: Zero-Voltage Switching or Zero-Current Switching?" *IEEE Transactions on Power Electronics* 37.9 (2022), pp. 10775–10783.

[40] Drazen Dujic et al. "Characterization of 6.5 kV IGBTs for High-Power Medium-Frequency Soft-Switched Applications." *IEEE Transactions on Power Electronics* 29.2 (2014), pp. 906–919.

[41] G. Ortiz et al. "Soft-switching techniques for medium-voltage isolated bidirectional DC/DC converters in solid state transformers." *IECON 2012 - 38th Annual Conference on IEEE Industrial Electronics Society*. 2012, pp. 5233–5240.

[42] A. Nagel et al. "Characterization of IGCTs for series connected operation." *Conference Record of the 2000 IEEE Industry Applications Conference. Thirty-Fifth IAS Annual Meeting and World Conference on Industrial Applications of Electrical Energy (Cat. No.00CH37129)*. Vol. 3. 2000, 1923–1929 vol.3.

[43] L. Heinemann. "An actively cooled high power, high frequency transformer with high insulation capability." *APEC. Seventeenth Annual IEEE Applied Power Electronics Conference and Exposition (Cat. No.02CH37335)*. Vol. 1. Mar. 2002, 352–357 vol.1.

[44] B Engel et al. "15kV/16.7Hz energy supply system with medium frequency transformer and 6.5kV IGBTs in resonant operation." *Proceedings of the 10th European Conference on Power Electronics and Applications (EPE 2003), Toulouse*. 2003.

[45] J. Taufiq. "Power Electronics Technologies for Railway Vehicles." *2007 Power Conversion Conference - Nagoya*. Apr. 2007, pp. 1388–1393.

[46] N. Hugo et al. "Power electronics traction transformer." *2007 European Conference on Power Electronics and Applications*. Sept. 2007, pp. 1–10.

[47] M. Steiner and H. Reinold. "Medium frequency topology in railway applications." *2007 European Conference on Power Electronics and Applications*. Sept. 2007, pp. 1–10.

[48] H. Hoffmann and B. Piepenbreier. "Medium frequency transformer in resonant switching dc/dc-converters for railway applications." *Proceedings of the 2011 14th European Conference on Power Electronics and Applications*. Aug. 2011, pp. 1–8.

[49] H. Hoffmann and B. Piepenbreier. "High voltage IGBTs and medium frequency transformer in DC-DC converters for railway applications." *SPEEDAM 2010*. June 2010, pp. 744–749.

[50] H. Hoffmann and B. Piepenbreier. "Medium frequency transformer for rail application using new materials." *2011 1st International Electric Drives Production Conference*. Sept. 2011, pp. 192–197.

[51] Gabriel Ortiz. "High-Power DC-DC Converter Technologies for Smart Grid and Traction Applications." PhD thesis. ETHZ, 2014.

[52] M. Leibl, G. Ortiz, and J. W. Kolar. "Design and Experimental Analysis of a Medium-Frequency Transformer for Solid-State Transformer Applications." *IEEE Journal of Emerging and Selected Topics in Power Electronics* 5.1 (Mar. 2017), pp. 110–123.

[53] G. Ortiz et al. "Design and Experimental Testing of a Resonant DC-DC Converter for Solid-State Transformers." *IEEE Transactions on Power Electronics* 32.10 (Oct. 2017), pp. 7534–7542.

[54] T Gradinger, U Drofenik, and S Alvarez. "Novel Insulation Concept for an MV Dry-Cast Medium-Frequency Transformer." *Proceedings of the 19th European Conference on Power Electronics and Applications (EPE 2017 - ECCE Europe), Warsaw, Poland*. 2017.

[55] S Isler et al. "Development of a 100 kW, 12.5 kV, 22 kHz and 30 kV Insulated Medium Frequency Transformer for Compact and Reliable Medium Voltage Power Conversion." *Proceedings of the 19th European Conference on Power Electronics and Applications (EPE 2017 - ECCE Europe), Warsaw, Poland*. 2017.

REFERENCES

[56] M. Mogorovic and D. Dujic. “Medium Frequency Transformer Design and Optimization.” *PCIM Europe 2017; International Exhibition and Conference for Power Electronics, Intelligent Motion, Renewable Energy and Energy Management*. May 2017, pp. 1–8.

[57] M Mogorovic and D Dujic. “Thermal Modeling and Experimental Verification of an Air Cooled Medium Frequency Transformer.” *Proceedings of the 19th European Conference on Power Electronics and Applications (EPE 2017 - ECCE Europe), Warsaw, Poland*. 2017.

[58] Marko Mogorovic and Drazen Dujic. “100 kW, 10 kHz Medium-Frequency Transformer Design Optimization and Experimental Verification.” *IEEE Transactions on Power Electronics* 34.2 (2019), pp. 1696–1708.

[59] Thomas Guillod. “Modeling and Design of Medium-Frequency Transformers for Future Medium-Voltage Power Electronics Interfaces.” PhD thesis. ETHZ, 2018.

[60] Group Schaffner. *World’s first 5 MW-DC converter*. Accessed 2020.02.13. 2020. URL: `https://impulse.schaffner.com/en/worlds-first-5-mw-dc-converter`.

[61] Piotr Dworakowski et al. “3-phase medium frequency transformer for a 100kW 1.2 kV 20kHz Dual Active Bridge converter.” *IECON 2019-45th Annual Conference of the IEEE Industrial Electronics Society*. Vol. 1. IEEE. 2019, pp. 4071–4076.

[62] Piotr Czyz et al. “Design and experimental analysis of 166 kW medium-voltage medium-frequency air-core transformer for 1: 1-DCX applications.” *IEEE Journal of Emerging and Selected Topics in Power Electronics* (2021).

[63] Peng Shuai. “Optimal Design of Highly Efficient, Compact and Silent Medium Frequency Transformers for Future Solid State Transformers.” PhD thesis. ETHZ, 2017.

[64] Asier Garcia-Bediaga et al. “Multiobjective Optimization of Medium-Frequency Transformers for Isolated Soft-Switching Converters Using a Genetic Algorithm.” *IEEE Transactions on Power Electronics* 32.4 (2017), pp. 2995–3006.

[65] Thomas Guillod, Panteleimon Papamanolis, and Johann W. Kolar. “Artificial Neural Network (ANN) Based Fast and Accurate Inductor Modeling and Design.” *IEEE Open Journal of Power Electronics* 1 (2020), pp. 284–299.

[66] Irma Villar. “Multiphysical Characterization of Medium-Frequency Power Electronic Transformers.” PhD thesis. EPFL, 2010.

[67] Marko Mogorovic. “Modeling and Design Optimization of Medium Frequency Transformers for Medium-Voltage High-Power Converters.” PhD thesis. EPFL, 2019.

[68] Nikolina Djekanovic and Drazen Dujic. “Design Optimization of a MW-level Medium Frequency Transformer.” *PCIM Europe 2022*. 2022, pp. 1–10.

[69] *Hitachi Metals Ltd. Japan*. `https://www.hitachi-metals.co.jp/e/`. URL: `https://www.hitachi-metals.co.jp/e/`.

[70] *Luvata Pori Oy, Finland*. `https://www.luvata.com/`. URL: `https://www.luvata.com/`.

[71] *Elektro-Isola A/S, Denmark*. `https://www.elektro-isola.com/`. URL: `https://www.elektro-isola.com/`.

[72] *Midel 7131*. `https://www.midel.com/`. URL: `https://www.midel.com/`.

[73] Renan Pillon Barcelos and Drazen Dujic. “Scalability Assessment of the Parallel Operation of Direct Current Transformers.” *CPSS Transactions on Power Electronics and Applications*. 2023.

THANK YOU FOR YOUR ATTENTION

Tutorial pdf can be downloaded from:

- `https://www.epfl.ch/labs/pel/publications-2/publications-talks/`